

MATHEMATICAL ANALYSIS OF HEMODYNAMIC PULSE WAVE IN
HUMAN FLUID-STRUCTURE INTERACTION

BY

NZEREM FRANCIS EGENTI

B.Sc (NIGERIA), M.Sc. (FUT, OWERRI)

PG/Ph.D/07/43744

DEPARTMENT OF MATHEMATICS
UNIVERSITY OF NIGERIA
NSUKKA

A THESIS SUBMITTED IN PARTIAL FULFILLMENT OF THE
REQUIREMENTS FOR THE AWARD OF THE DEGREE OF DOCTOR OF
PHILOSOPHY (Ph.D) IN MATHEMATICS OF THE
UNIVERSITY OF NIGERIA, NSUKKA

AUGUST, 2014

CERTIFICATE OF APPROVAL

We the undersigned hereby certify that this thesis by Nzerem Francis Egenti meets the requirement for the award of the degree of Doctor of Philosophy in Mathematics and this thesis has not, to the best of our knowledge, been previously submitted for award of any certificate or degree in any institution.

Prof.M.O.Oyesanya
(Supervisor)

Date

Prof. G.C.E Mbah
(Supervisor)

Date

Prof. M.O.Oyesanya
(H.O.D. Mathematics)

Date

Prof. Okoya S.S.
(External Examiner)

Date

ACKNOWLEDGMENT

If there was anything to circumvent in this work, it was me having to write this acknowledgement! It was a rather demanding but less intriguing venture. I am yet to know why I should take anybody for granted while reeling off the names of those whom I owed a great debt of gratitude for my success in this work. Maybe I had been obtrusive by telling many a student who had worked under my watch to avoid the penchant for profuse use of God in academic works. I always believe that having to include HIM in acknowledgements and dedications involving academic exercises is by no means effectual; I would rather reserve my doxologies for a medium other than this. Yet again, another member of mine wondered how sublime such a medium other than this would be.

It was a privilege to work under the watch of Professors M.O. Oyesanya and G.C.E. Mbah. I knew Professor Oyesanya as one of our lecturers during my undergraduate studies at the University of Nigeria. He changes not! The greatest mistake would be to assume his soft-spoken disposition for compromise; He is soft-spoken but adroit! He is a mathematician *par excellence*. Neither Oyesanya nor Mbah has sympathy for suppositions and perfunctory effort. Bio-Mathematics is quite enigmatic; Pundits in that domain are, by extension, enigmatic. Professor Mbah is a panacea for the huddles that make this field of Mathematics a *will-o'-the-wisp*. It is better to encounter these erudite gentlemen in their natural element than only to hear about them.

I had ever sought an opportunity to appreciate my mentor who supervised my first research work at University of Nigeria, Professor F.I. Ochor. He therefore has the honour that behoove his mentoring.

I owe a great deal of my success to Professors emeritus J.C. Amazigo, G.C Chukwumah (blessed memory), U.B.C.O Ejike (blessed memory) among a plethora of academics. I am grateful to all the staff of Department of Mathematics, University of Nigeria, Nsukka for their immense contributions to the success of this work. I would not be fair to Professor E.C. Nduka of Department of Mathematics and Statistics, University of Port Harcourt if I did not recognize his contributions to my success. He might not know that I remember him for two things for now: When he did not know me, he called me on phone and told me to appear for an interview in his institution, even as he was not in an official position to do so. While I served in the institution and worked on this thesis, he kept encouraging me and requesting for updates on my work.

Myriad of friends and relations provided me with the inspirational *compact support* that could not be easy to forget. In a finite medium like this, it was difficult to catalog their names. Moreover I asked myself: How could I write on paper all I felt in my mind about them? (Apologies to Jim Reeves, of blessed memory.) Mr Joseph Eze (Joe Hitman) is a fine gentleman. Ever since the turbulent time I encountered him, during the year of my national youthsø service in Kano, my joy has known no bounds. He was largely instrumental in my disposition to the career in academics. I was mindful of the stoical stance of my wife, Ijeoma, during those discommodious times I made the computer my *companion*. I am especially grateful to my daughter, Nakita, for her neonatal understanding, even when she needed a fatherø attention. But for Ndidi Alozie, my niece, this work would have suffered some technical setback. She kept scanning this work for errors. Oftentimes I disagreed with myself while on this work; I battled with the work and all its concomitant spondylosis; a member of me would ask: Why not

rest? Another member would ask: Would rest solve your problem? I said to myself, *I must rest when I must rest*. To you, who read and appraised this work, I owe my appreciation.

F.E. NZEREM

DEDICATION

To

Nze Bartholomew Nzeribe & Lolo Salome Okuakanwa Achara,

my late parents.

Abstract

Mathematical study of human pulse wave was studied with the view to gaining an insight into physiological situations. Fluid-Structure interaction (FSI) in blood flow is associated with pressure pulse wave arising from ventricular ejection. Solution of the coupled system of non-linear PDEs that arose from the FSI was sought in order to determine pressure. Further study on pressure pulse waves showed that the Korteweg-de Vries (KdV) equations hold well for the propagation of nonlinear arterial pulse wave. Solutions of the KdV equation by means of the hyperbolic tangent (**tanh**) method and the bilinear method each yielded solitons. The solitons describe the peaking and steepening characteristics of solitary wave phenomena.

The morphologies of the waves were studied in relation to the length occupied by the waves (which corresponds to length of arterial segment and stature) and the left ventricular ejection time (LVET). The study showed that both stature and LVET are independent descriptors of cardio-vascular state.

Table of Contents

Title page	
Certificate of Approval	i
Acknowledgement	ii
Dedication	v
Abstract	vi
Chapter One	
Overview of Fluid-Structure Interaction Problem	1
1.0 Introduction	1
1.1 Body vessels	1
1.2 Arteries and their structure	4
1.3 Blood	6
1.4 Blood Pressure (BP)	7
1.5 Arterial Pulse	8
1.6 Pulse Pressure	9
1.7 Fluid-Structure Interaction	10
1.8 Pulse Wave	11
1.9 Resonance	12
1.10 Aim and objectives of the study	12
1.11 Scope and limitations of the study	13
1.12 Methodology	13
1.13 Significance of the study	14
Chapter Two	
Literature Review	15

Chapter Three

Fluid-Wall interaction and non-linear pulse wave models in blood flow	21
3.1.0 Generalized equation of motion of viscous fluid	21
3.1.1 Action of fluid on the wall	26
3.1.2 Fluid óStructure interaction model: Problem presentation	29
3.1.3 Fluid óStructure coupling	36
3.2.0 Model of non-linear arterial pulse: Problem presentation	39
3.2.1 Linear superposition of forward and backward ABP waves	41

Chapter Four

Solutions to model problems	44
4.1.0 Solution of fluid-wall interaction problem	44
4.1.1 Weak Formulation and Variational Form	45
4.1.2 Rescaled Problem and asymptotic expansion	50
4.1.3 Weak Formulation	51
4.1.4 Energy estimates after rescaling	52
4.1.5 Asymptotic Expansions	53
4.1.6 Justification for asymptotic expansions	54
4.1.7 Reduced problem using Expansion I	55
4.1.8. Reduced problem using Expansion II	58
4.2.0. Nonlinear arterial pulse model	62
4.2.1 Methods of Solution of non-Linear Wave model problem	67
4.2.2 The Tanh (hyperbolic tangent) Method of Solution	68
4.3.0 Bilinear Method	73
4.3.1 Solitons by bilinear method	75
4.4 Systolic and Diastolic PW Representation	80

Chapter Five

Results and discussions	83
5.1.0 Features of:	84

5.1.1 Tanh method	84
5.1.2 Bilinear Method	84
5.2.0 Physiological Analysis using solitary waveform	85
5.2.1 Distance effect	85
5.2.2 Short and tall statures	86
5.2.3 Time effects	91
5.2.4 Harmonic Components of Arterial Pulse Waves	94
5.2.5 Heart-Organ Resonance	95
5.2.6 Hypertension and vaso-active Agents	96
5.2.6 Dying Process	98
5.3.0 Summary and Conclusion	99
5.4.0 Recommendation(s) for further studies	101
References	102
Appendices	112

CHAPTER ONE

OVERVIEW OF FLUID-STRUCTURE INTERACTION

1.0 Introduction:

In this work we analyzed hemodynamic pulse waves (PW) in human fluid-structure interaction problems. The work engaged mathematical models to show, among other things, that arterial pressure which has systolic and diastolic components generates PW which are enough to determine the physiological state of each of the internal organs, especially of the heart. The understanding of some of the terms used in this work may be necessary. In subsection 1.1 below some of such terms are explained.

1.1 Body vessels

In anatomy, a vessel is a tubular structure that conducts body fluid: a duct that carries fluid, especially blood or lymph to parts of the body. Thus, blood vessels are blood-carrying ducts. Blood vessels are in three varieties: *arteries*, *veins* and *capillaries*.

Arteries

The main arteries are:

Pulmonary arteries: Carry deoxygenated blood from the body to the lungs where it is oxygenated and freed of carbon dioxide.

Systemic arteries: They deliver blood to the arterioles, then to the capillaries where gases and nutrients are exchanged.

Aorta: This artery is supplied with blood from the left ventricle of the heart via the aortic valve. It is the root systemic artery, and it branches to daughter arteries. It carries blood away from the heart.

Arterioles: These are the smallest of the true arteries. They regulate blood pressure and deliver blood to the capillaries.

Carotid, subclavian, mesenteric, renal, iliac arteries and the celiac trunk are branches of the aorta

Venules are the small blood vessels that transfer blood from the capillaries to the veins.

Veins

- They are large collecting vessels, such as the subclavian, jugular, renal, and iliac veins. They carry blood at low pressures.
- Venae cavae are the largest veins, which they carry blood into the heart.

Capillaries

These are the smallest blood vessels (about 5-10 μ m in diameter). They form part of microcirculation. Arteries divide into arterioles and continue to narrow, and as they reach the muscles they become capillaries. Capillaries do not transport blood. They are specially designed for the passage of substances, mainly oxygen and carbon dioxide. They are thin-walled and are composed only of endothelial cells, which allow easy passage of substances. A notable feature of capillary beds is their control of blood flow through auto regulation. This helps an organ to maintain constant flow despite changes in central blood pressure. New capillaries can be formed by pre-existing capillaries in a process called *angiogenesis*. Fig.1.1 shows the location of various arteries in the body.

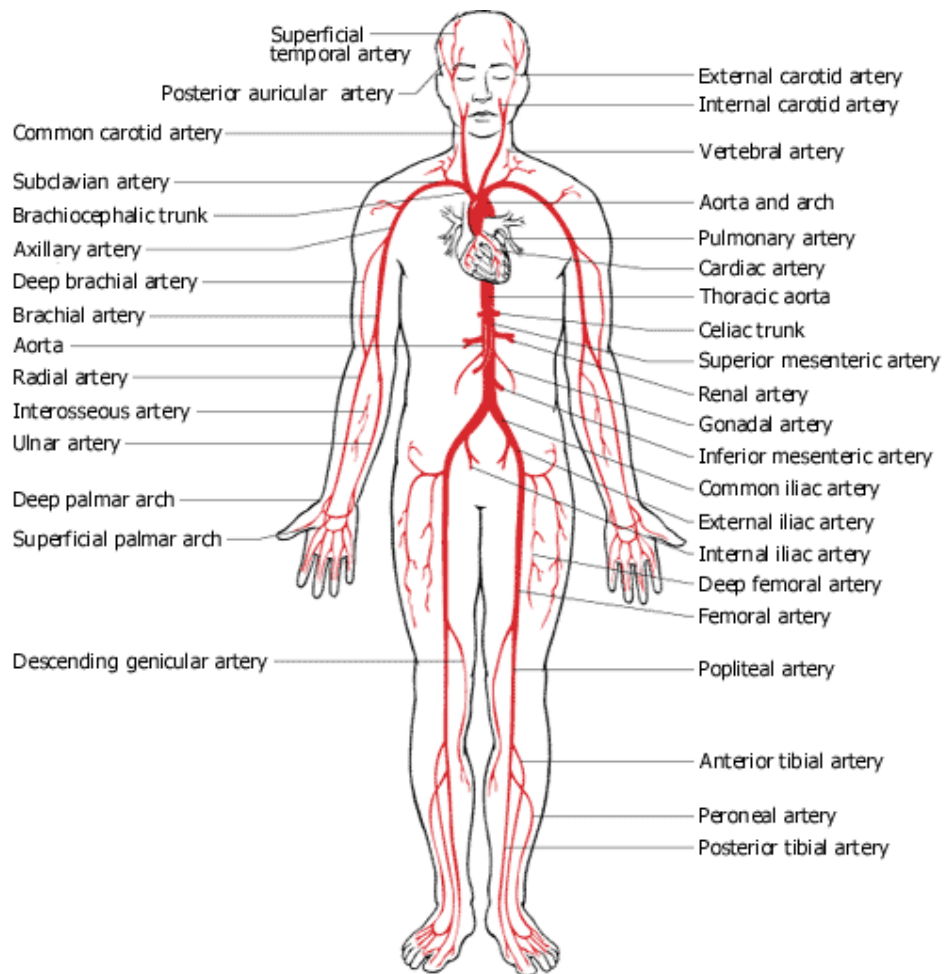


Fig1.1 Human arterial system. (Available at www.chakras.org.uk/chakra_yoga_health_holistic_arterial.gif)

#	Artery Name	Function
0	Arterial system	Canals that carry blood from the heart to the organs
1	Posterior	Vessel that carries blood to the head.
3	External carotid	Neck vessel that carries blood to the face
4	Internal carotid	Neck vessel that carries blood to the brain
5	Common carotid (left)	Carries blood to the left side of the neck
6	Brachio- cephalic	Main vessel of the arm
7	Left subclavian	Carries blood beneath the left clavicle
8	Right coronary artery	Feeds the tissues of the right side of the heart with blood
9	Thoracic aorta	Main artery of the thorax
10	Celiac trunk	Carries blood to the thoracic cavity
11	Renal	Carries blood to the kidneys
12	Superior mesenteric	Carries blood to the upper part of the abdomen
13	Abdominal aorta	Main artery in the abdominal area
14	Inferior mesenteric	Carries blood to the lower part of the abdomen.
15	Common iliac	Principal artery of the human lower limb
16	Internal iliac	Internal branch of the iliac artery
17	External iliac	External branch of the iliac artery
18	Profunda femoris	Carries blood towards the inside of the thigh
19	Peroneal	Carries blood to the lower leg
20	Lateral planter	Carries blood to the side of the sole of the foot
21	Dorsalis pedis	Carries blood to the dorsal part of the foot
22	Plantar arc	Carries blood to the instep area
23	Medial plantar	Carries blood to the median of the sole of the foot
24	Anterior tibial	Carries blood to the front part of the lower leg
25	Posterior tibial	Carries blood to the back part of the lower leg
26	Popliteal	Carries blood to the back of the foot
27	Femoral	Carries blood to the thigh
28	Superficial palmar arch	Situated beneath the skin of the palmar arc of the hand
29	Ulnar	Situated in the area of the ulnar
30	Common interosseous	Situated between the two bones of the forearm
31	Gonadal (Genital)	Carries blood to the genital organs
32	Radial	Situated in the area of the radius
33	Brachial	Carries blood to the arm
34	Profunda brachial	Carries blood towards the interior of the arm
35	Axillary	Carries blood to the armpit
36	Right subclavian	Carries blood beneath the right clavicle
37	Right vertebral	Situated on the right, carries blood to the vertebrae
38	Common carotid (right)	Carries blood to the right of the neck
39	Superior thyroid	Carries blood to the thyroid
40	Lingual	Carries blood to the tongue
41	Facial	Carries blood to the face
42	Maxillary	Carries blood to the maxillae
43	Superficial temporal	Carries blood to the surface of the skin, in the area of the temples

Table 1.1 The 43 human main arteries and related function (Almanasreh (2007))

1.2 Arteries and their structure

All relatively large arteries have similar basic structure. The artery consists of the outermost layer known as the *tunica adventitia*. This layer is composed of connective tissue. The inner

layer is known as the *tunica media*, and is made of smooth muscle cells and elastic tissues. The innermost layer is known as the *tunica intima*. This layer is in direct contact with the flowing blood. The *lumen* is the hollow internal cavity in which the blood flows (as seen in Fig. 1.2).

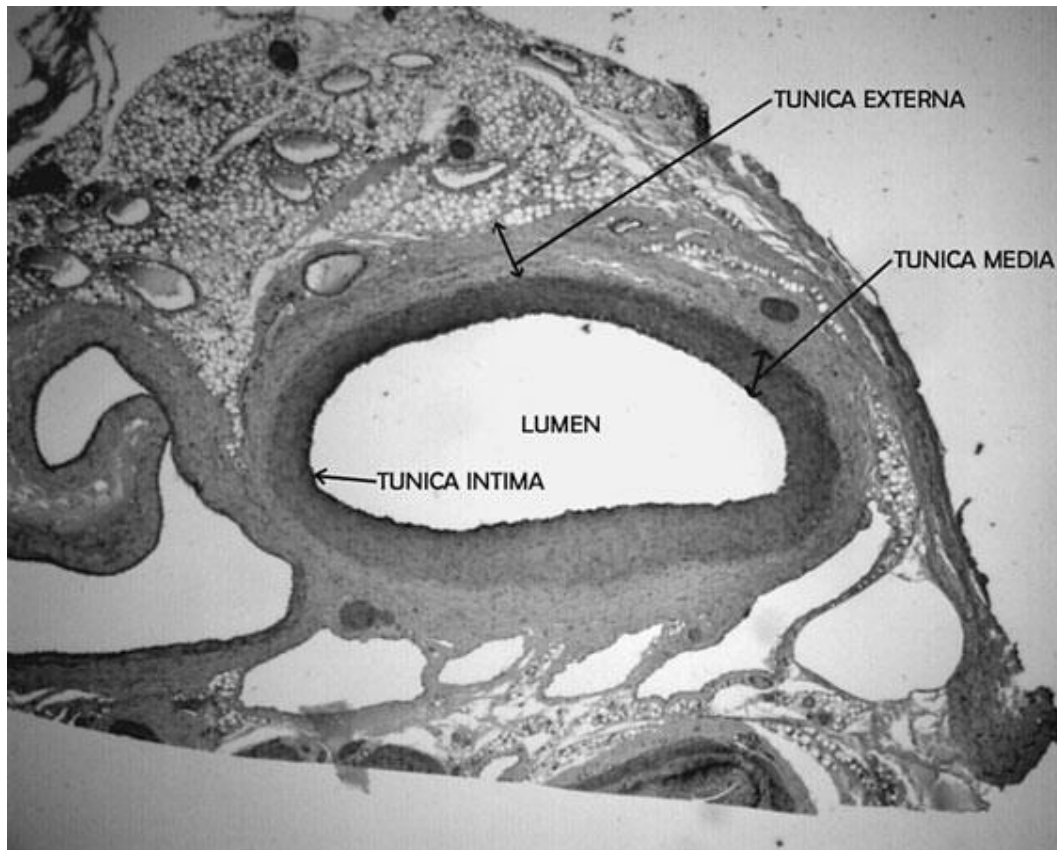


Fig 1.2 Photomicrograph of the cross section of an artery showing the tunica intima, tunica media, and tunica externa. Available at <http://www.mhprofessional.com/product.php?isbn=0071472177>

The endothelium of the *intima* is surrounded by sub-endothelial connected tissue. Around this there exists a layer of vascular smooth muscle, which is developed in arteries. There is a further layer of connective tissue known as the *adventitia*, which contains nerves that supply blood to the muscular layer as well as nutrient to the capillaries in the larger blood vessels.

Blood vessels do connect and form *anastomosis* (a region of diffuse vascular supply). In event of blockages anastomoses provide critical alternative route for the flow of blood.

In course of blood circulation arteries mainly carry blood away from the heart. The capillaries link the arteries to the veins, and the veins carry the blood back to the heart. Besides blood circulation, arteries (and blood vessels as a whole) help to measure vital health statistics such as pulse and blood pressure. We can measure heart rate, or pulse, by touching an artery. The rhythmic contraction of the artery as the heart beats keeps pace with the pulse. The proximity of the artery to the surface of the skin enhances the accurate measurement of the heart's pulse by touching the artery. The heart itself is deeply protected.

1.3 Blood

Talking about whole blood, we think of the formed elements that are suspended in plasma. The red blood cells (RBCs) constitute major part of the formed elements. The ratio of this part to the other constituents of whole blood is known as *hematocrit*.

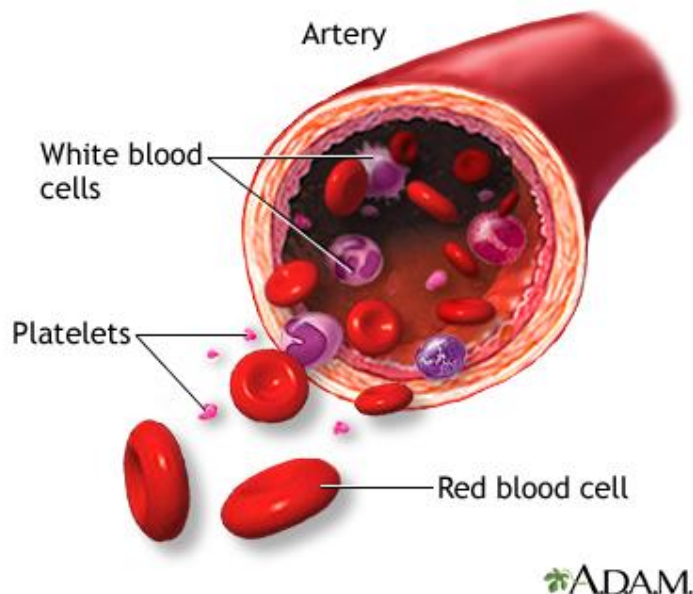


Fig1.3 Formed elements of blood, Dugdale (2010)

It is the preponderance of the RBCs in the whole blood composition that make them very important in determining the flow characteristics of blood. RBCs aggregate at low shear rates (values $< 100 \text{ dyn s}^{-1}$) and form rouleaux. This has the effect of increasing the viscosity of blood. Rouleaux disaggregation occurs as shear rate increases, resulting in the shear-thinning characteristics that cause the non-Newtonian behavior of blood. In effect, blood viscosity decreases. We consider blood as Newtonian when its shear-thinning characteristic disappears as a result of increase in shear rate beyond the low shear rate region (Ku (1999), Kang (2002)).

1.4 Blood Pressure (BP)

Blood pressure is the force being exerted on the walls of the arteries in the event of blood being transported to parts of the body. It is customary to use the blood flowing from the arteries to measure blood pressure because it is transported at a higher pressure than the blood in the veins. BP is measured using two numbers (see Blood pressure chart in Appendix A). The first number, which is usually higher, is taken when the heart beats during *systole* (the contraction of the heart during which blood is pumped into the arteries), as the heart rests between cycles. The *systolic pressure* is the peak pressure during heart contraction while the second number is taken when the heart relaxes during *diastole* (rhythmic expansion of the heart's chambers at each heartbeat during which they fill with blood). The *diastolic pressure* is the minimum pressure between contractions. Each of the numbers is recorded in millimeters column of mercury (*mmHg*). It is normal for BP to increase in course of exercise and to decrease when asleep. If BP stays too high or too low, there may be the risk of heart disease.

The heart pumps blood out through a main artery known as the dorsal aorta. This main aorta divides and branches out into several smaller arteries so that each region of the body has a system of arteries that supply it with fresh oxygenated blood.

When the heart beats (during systole) the artery is filled with blood and it expands. When the heart relaxes (during diastole) the artery contracts and exerts force that would push the blood along. The integrity of blood flow and efficient circulation is the synergy between the heart and the artery.

1.5 Arterial pulse

Pulse may be explained in terms of regular beat of blood flow as the regular expansion of an artery, caused by the heart pumping blood through the body, or in terms of single beat of blood flow as a single expansion and contraction of an artery, caused by a beat of the heart. Usually, in medicine, pulse is the tactile arterial palpation by trained fingertips. Such palpation may be in any place where an artery can be compressed against a bone. Such places include neck (carotid artery), the wrist (radial artery), behind the knee (popliteal artery), on the inside of the elbow (brachial artery), and near the ankle joint (posterior tibial artery), as shown in Fig.1.4.

Pulse may be used in expediency as a tactile method of determination of systolic blood pressure to a trained observer, but this cannot be said about diastolic blood pressure. Below are the physiological pulse rates at rest (the resting heart rate (HR_{rest}) is a person's heart rate when they are at rest, that is lying down but awake, and not having recently exerted themselves http://en.wikipedia.org/wiki/Heart_rate#At_rest).

newborn (0-3 months old)	infants (3 — 6 months)	infants (6 — 12 months)	children (1 — 10 years)	children over 10 years & adults, including seniors	well- trained adult athletes
100-150	90-120	80-120	70-130	60-100	40-60

Table 1.2 Normal pulse rates at rest, in beats per minute (BPM):^{US(20)}

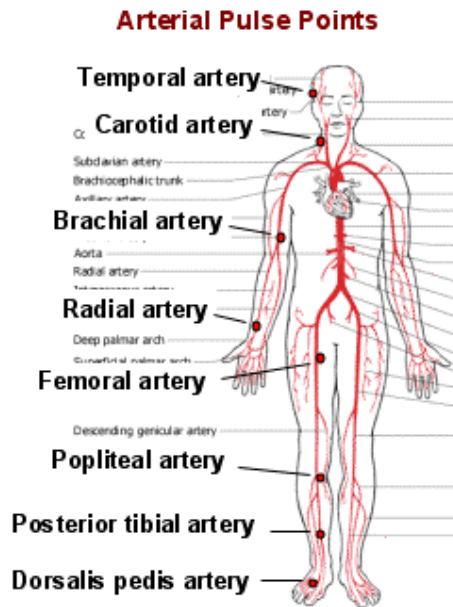


Fig1.4 Arterial pulse points (at: http://www.nakedscience.org/mrg/AnatomyLectureNotesUnit7CirculatorySystem-TheBloodVessels_files/image006.gif)

1.6 Pulse Pressure (PP)

This is the amount of pressure that is required to create the feeling of a pulse. The variation of pressure within the artery produces pulse which is transmitted through the artery; hence the name arterial pressure pulse. When the heart's left ventricle contracts, systemic arterial pressures are generated. PP is most easily defined as being the amount of pressure required to create the feeling of a pulse. The amount of pulse is created is measured (in mmHg) by the Systolic versus Diastolic difference of blood pressures. It is mainly related to the amount of blood ejected by each heart beat, stroke volume and the elasticity of the major arteries. If you

have a resting blood pressure is (systolic/diastolic) 120/80 mmHg, then your PP is 40, which is a healthy PP. A consistent high resting PP is very harmful, and is most likely to quicken the normal ageing of the heart, brain and kidney. In recent times researches have been carried out to determine the relationship between pulse pressure and hypertension (Martin *et al* (1995)). There is the possibility that resistance vessel structural adaptation in hypertension may be closely related to pulse pressure than to other blood pressure parameters. Studies show that the widening of PP is seen as a consequence of a loss of compliance in the large conduit arteries and increased wave reflections from the periphery, and less to increased resistance in peripheral arteries (Safar (1993)). It is most likely to be evident in, and prognostic of, cardiovascular abnormally.

1.7 Fluid-Structure Interaction (FSI)

The notion of fluids-structure interaction with regard to human dynamical structure is the interplay of blood flow and the arterial conduit. The flow of blood via the arterial conduit induces concomitant motion of the arterial wall, and thus there exists some interfacial region within which fluid-structure interaction (FSI) is felt. Flow usually occurs in radial, angular and axial directions. The arterial wall is expected to be compliant in order to sustain the integrity of the flow. In compliant arteries flow in radial direction induces radial dilatation, whilst axial flow induces longitudinal (axial) stretch.

In the main, the circulatory system of animated life owes its integrity to FSI. Within reasonable expectation this interaction would present some mixed blessing to human physiological state. Within physiological range of flow and pressure, the body would be held at normal cardio-vascular state. On the unpleasant version, there could be incipient pathology in the physiological state when the interaction fails to yield the desired goal. Beside various hemodynamic parameters we take exceptions at arterial pressure pulse wave. We shall give

attention to details on the nonlinear waves generated by the pulse. The injection of blood from the left ventricle into the aorta generates far more than traveling waves in the arterial system, otherwise forced stationary oscillations of the entire arterial system would be untenable; thus pressure pulse would not likely reveal details about the resonance conditions of the whole body in a defined manner. It is against this background that we are attracted to the mathematical analysis of pulse waves and the resonance conditions there from, in a bid to furnish medics with some contribution to wave-related issues in physiology. As we attest to the solitary nature of the pulse waves, Wang *et al* (2010) reminds us in more physiological terms that the resonance conditions of the whole body, sequel to the wave train must be a benchmark for normal conditions of organs. This reminder is worthwhile in treating the waveforms alongside their harmonic components. With this treatment, salient information could be supplied regarding organ patho-physiology and hypertension. In this regard medics could be availed of the benefits derivable from this work.

1.8 Pulse Wave (PW)

Pulse wave is a very complex physiological phenomenon observable, and detectable in blood circulation. Any segment of blood ejected and transported through the artery in event of heart systole is transformed between kinetic and potential energy. There are three observable coherent phenomena on each artery or venous segment affected by pulse wave: blood flow (flow pulse), the change in BP (pressure pulse) and the extension in transverse profile (volume pulse). PPW is generated from the combination of the incident wave (i.e. the pressure wave generated by the left ventricle in systole) and waves reflected back from the periphery.

The shape of PW changes as moves to the distal arteries. This change could be largely due to the pulse wave reflection and arterial tapering.

Pulse waveform varies in different vessels in the same individual. It depends on the (visco-elastic) properties of the artery (inducing wave amplification as it travels from more elastic central to stiffer peripheral arteries), the viscosity of the blood, wave reflection and wave dispersion.

1.9 Resonance

The term resonance as used here is in association with mechanical systems. In this regard it is used to describe large oscillation at natural frequency. In the event of physiological arterial flow, there is increased amplitude of oscillation of the organs (the mechanical system), when they are subjected to vibration arising from the PW. The wave transmits through the artery (source) proximal to the organ in question. Each of the organs (specifically the heart, liver, lungs, kidney and spleen) has its own natural frequency. Each of the organs is influenced by both the input pulsatile blood and by the harmonic driving force, both of which are proportional to the PP and the connecting site of the local main artery. PP is good enough to reveal information about the resonance conditions of the whole body. Wang *et al* (1990), therefore was of the view that periodic injection of blood from the left ventricle would not generate only traveling waves, but would also induce forced stationary oscillation of the arterial system. This work buys this view, and would use the organ specific harmonics to analyze the patho-physiological state of the body.

1.10 Aim and objectives of the study

The aim of this work is to determine whether stature (height) and LVET each can be implicated in cardiac-vascular events.

The objectives of this work are:

- To carry out a study of hemodynamic pressure pulse wave due to left ventricular ejection.
- To use pulse waveforms to analyze the human physiological state.
- To extend the frontiers of existing knowledge of the subject under consideration.

1.11 Scope and limitations of the study

This work studied hemodynamic pulse waves arising from the heart's left ventricular ejection and the FSI. It studied the effect of stature on pulse waveforms and analyzed the physiological implications of the waveforms.

The study was non-invasive (as applicable in most medical practice). However, the work relied on some experimental findings where necessary. We must agree, without prejudice, that it takes maturity to know that models *should be used, not believed* (Henry (2012)).

1.12 Methodology

A set of nonlinear partial differential equations was used to describe the pressure-induced viscous flow of the fluid. Another set of nonlinear partial differential equations was used to describe the motion of the arterial wall. We expressed the FSI as a coupled system and the equation of the radial contact force was obtained. The model of arterial pulse was built on the system of equations governing the FSI. Analytic method was used to get the solutions of the FSI problem which yielded the desired equation of arterial pressure. In a similar way, the solution of the arterial pulse was sought. We used a combination of the hyperbolic tangent (tanh) and the bilinear methods of solution to get the solutions of the arterial pulse problem. We obtained solitary wave (soliton-) solutions. We therefore described pulse waves as solitons. Matlab Software was used for the processing and plotting of graphs of our solutions and our analysis. We went further to analyze the physiology underlying the pulse waves. Stature and the LV

ejection time were the parameters used for clinical purposes. In each of the cases the values of the parameters were varied in order to study the (patho-) physiology underlying arterial pulse waveforms.

1.13 Significance of the study

This work is important in many respects:

- (i) It would underscore the importance of arterial pulse waveforms in determining patho-physiological state of humans.
- (ii) It would help medics to decide the course of their treatment to related pathologies.

CHAPTER TWO

LITERATURE REVIEW

This work is *Mathematical Analysis of Hemodynamic Pulse Wave in Human Fluid – Structure Interaction*.

Analysis of hemodynamic pulse waves poses new challenges in the world of emerging pathophysiology. It is technically difficult to undertake the analysis of nonlinearities in arterial morphology, and thus nonlinear pulse waves and the resulting resonance conditions of the body become rather intriguing. In this work we shall resolve the gap between treating arterial pulse waves as mere progressive waves whose solutions are sought, and the harmonic analysis that actually supplies details relating to organ morphology.

Hemodynamics was proposed by McDonald (1974), to be defined as the physical study of flowing *blood*, and all the *solid structures* through which it flows. It is therefore, the science of forces that maintain the integrity of blood flow through the arteries.

In hemodynamics flow phenomena are treated from the standpoints of fluid motion and the motion of the arterial wall. Any wall-free model such as those proposed by Rappitch and Perktold (1996), Wada and Karino (1999) do not consider the motion of the arterial wall in relation to fluid flow. In such cases the arterial wall may be treated only as a boundary condition. The arteries, together with blood play a vital role in blood circulatory system, which enhance physiological balance.

The study of hemodynamics involves some mechanical parameters such as *pulse*, *pressure*, wall shear stress (WSS), oscillatory shear index (OSI) wall circumferential stress (WCS), among other parameters. A good study of the constituents of blood aids the knowledge of the mechanical properties of blood. Shibeshi and Collins (2005) treated the constituents of blood, in which the red blood cells (RBCs) are adjudged crucial in determining flow characteristics. The behavior of blood may be Newtonian or non-Newtonian, depending on shear rate (McDonald (1974), Shibeshi and Collins (2005)). It is believed (Fung (1996)) that hematocrit (the RBCs proportion in the whole blood) determines blood viscosity, a major factor in Newtonian/non Newtonian behavior of blood. As usual with flow models, continuity and momentum equations govern the flow of blood. These equations of flow were utilized judiciously in this work. The modeling of arterial adaptation to flow engaged the attention of Atabek (1968), Fung (1996) and Rachev (2000). In dealing with arterial properties, it is customary to assume incompressibility, elasticity and compliance. Although arterial incompressibility is assumed, arteries are, to all intents and purposes, conditionally compressible (Choung and Fung, (1984), Carew et al. (1968)). It was shown by Boutouyrie et al. (2001) that compression can be generated by large interstitial proteoglycans (heavily glycosylated proteins that are involved in binding cations (such as sodium, potassium and calcium), and water and also regulate the movement of molecules through animal extracellular matrix). The stroke change in the wall cross-sectional area can be calculated to approach volumetric strain; an index of compressibility (Choung and Fung (1984)).The assumption of pure arterial elasticity does not foreclose the viscoelastic property of arterial wall. The works of Warriner et al. (2008) suggested that viscoelasticity is vital in arterial wave propagation, whereas it was suggested that viscoelastic effects of arteries are negligible within physiological range of flow and pressure (Olufsen (1998)).The arterial adaptation to flow is partly by means of wall movement. The viscosity of blood has a drag

effect on the arterial wall in the longitudinal direction. The viscous drag induces a shearing force, which prevails on the inside of the wall. The notion of wall tethering in longitudinal direction almost killed the thought of longitudinal motion (see McDonald (1974)). It was observed by Lawton and Greene (1956) that systolic pressure induces variation in arterial length. Moreover Hai-Chao et al. (1994) suggested the existence of longitudinal stretch in arteries due to any of, or a combination of ageing, pregnancy, vascular diseases and reconstructive vascular surgery.

Beside longitudinal motion, arteries are subject to radial movement. Any radial dilatation is related to velocity of fluid flow, but not to pressure (Atabek (1968) Mbah (2010(b))). Acceleration in pulsatile flow in any short section of an artery is the prime cause of distension of the segment. This is so because more fluid enters than leaves the region.

The question is: Is there any form of interaction between blood and the vessel's wall? The answer is, to all reasonableness, yes. At the plasma phase and at the deformable solid phase of blood cells there exists an interface where the two phase blood interact (Fung (1996)). The level set method was used by Kavouklis *et al* (2011) in locating the interface shared by the two fluids. The action of the fluid on the vessel's wall may better be explained by a theorem due to Becker (Milne-Thomson (1974)). It was shown therein that normal pressure, together with an accompanying shear are incident on the wall. The elastic property of the wall determines flow characteristics to a large extent. Maoyeri and Zendchbudi (2003) and the work by Mbah (2010(b)) showed the effect of elastic property of the wall to such flow characteristics through arterial stenosis. We stated earlier that this work would deal extensively on hemodynamic arterial *pulse*, and its physiological implications. Flow owes its integrity to pressure gradient. Blood pressure (BP) is a periodic phenomenon, which consists of two components: a steady and a pulsatile component. The steady component is determined

exclusively by two hemodynamic measurements: cardiac output and vascular resistance, while the pulsatile component is influenced by ventricular ejection, large artery compliance and timing of reflected waves (Darne *et al* (1989)). When blood is ejected into the aorta, a high pressure wave is propagated to other arteries throughout the body. The forward-traveling pressure wave may be reflected at all points of structural and/or functional discontinuity of the arterial tree (Safar (2003)). This work has special interest on pulse wave propagated through arteries by ejected blood, since it formed the basis of our mathematical theory.

Nonlinear terms are evident in pulse waves with large amplitudes, and non-linearities exist, since the modulus of elasticity of the vessel varies quite strongly with pressure. Our work on pulse wave shows that the Korteweg óde Vrie (KdV) equation, which describes non-linear shallow water waves satisfies the equations of arterial pressure waves. The works by Zebusky and Porter (2010), Drazin and Johnson (1989), Monteanu and Donescu (2004) depict nonlinear waves which may be linked to shallow waves. In the mathematical formulations here, the decomposition of pulse waves into a travelling wave representing fast transmission phenomena during systolic phase and a windkessel term representing slow transmission phenomena during diastolic phase (Wang *et al.* (2002), Parker and tyberg (2002)) was proposed.

A major issue that physical problems contend with is the form in which a partial differential equation (PDE) appears. In many cases we suffer the sight of hideous PDEs that arise from physical problems. Such PDEs appear in some form that defies mathematical analysis. Lamentably, understandable solution is imperative if physiological exigencies must have mathematical analysis. We should note that solutions may not be approximated by plane wave solution in physiological cases; instead they may require exponentially decaying solutions. Many conditions that do not apply to physiological phenomena may hold well for

other similar physical phenomena. To this end, it would be customary to talk of *physiological wave* to stress the divorce between such wave and a group of other physical waves. In general, two major wave phenomena are the *peaking* and *steepening* morphologies. Solitons are isolated waves that travel without dissipating energy. They are a product of wave phenomena. Many studies on waves show that physiological waves are known to behave like solitons (rather than sinusoid). Arterial pulse waves are physiological waves that decompose into a travelling wave representing fast transmission phenomena during systolic phase and a windkessel term representing slow transmission phenomena during diastolic phase. Solitons are evident at the systolic phase and the diastolic phase is marked by slow flow waves. In this regard, it was indicated (Babin, and Figotin, 2006) that soliton-based signal processing, together with a windkessel model may be used to compute blood pressure wave in large proximal arteries. By simple theories, linear waves are subject to superposition. Interestingly, non-linear waves are amenable to superposition. The suitability of constructing soliton solutions derives from linear superposition of non-linear waveform so obtained from a given problem. The solution of the emerging KdV equation yielded solutions which are bell-shaped *sech* solutions that characterize arterial pulse wave. Those bell-shaped solutions are enough to describe the arterial pulse peaking and steepening wave phenomena (Laleg *et al* (2006)). Before now, Nwachukwu and Ifidon (1991) had considered the KdV equation under consideration as a symmetric group of equations. The hyperbolic tangent (*tanh*) method of solution of partial differential equations advanced by Malfliet (1992), (see also Wazwaz (2002)) provides a veritable tool in obtaining solitons besides Hirota's method (Hirota (1980), Curry(2008)). We utilized both methods in the quest for solutions of the KdV equation.

Beside what these solutions may offer, we saw the position of O'Rourke and Pauca (2001) that "other uses for pulse wave analysis are certain to be encountered in the future" as challenging! Motivated by this, we went further to analyze our solution with the view to

gaining an insight into the etiology of pulse wave associated pathologies. Specifically, Nzerem and Alozie (2013) in their analysis of pulse wave, showed how stature is remarkable in determining cardiovascular state. In another related study, Nzerem and Ugorji (2014) showed that the duration (time) of left ventricular ejection may bring to bear on the cardiovascular state of subjects. As much as we know, there is the paucity of mathematical details in this direction. Moreover, such analysis would be more precise in furnishing details that are clinically usable.

Finally, we find resonance as a missing link; we therefore undertook an enquiry into the resonance conditions of the body resulting from arterial pulse waves. The resolution of pressure waves into their harmonic frequency components is a *sine-qua-non* to having some clue to the application of the wave contour to internal organs's specific harmonics. Wang *et al* (2004, 2010, 1991) and Kuo *et al* (2004, 2006, 2005) had insisted on the use of organ specific harmonics as a means of furnishing the physiological state of the body's organs. We reasoned in that direction and discussed how such impact on hypertension and the process of dying.

CHAPTER THREE
FLUID-WALL INTERACTION AND NONLINEAR PULSE WAVE
MODELS IN BLOOD FLOW

Issues regarding flow inside deformable domains (arteries) and the resulting motion of the domains are here considered. The flow is governed by a time dependent pressure head difference and modeled by the Navier-Stokes equations for an incompressible viscous fluid, and the Navier's equations for an elastic membrane describe the behaviour of the elastic tube. Here we advanced from the inadequacies of the one-dimensional models to more effective equations that meet physiological conditions. The flow is driven by pulsatile inlet and outlet dynamic pressure condition. The inherent hyperbolic-parabolic equations, with memory effects are considered. The memory effects explain the wave-like phenomena in the model (Suncica *et al* (2005)). The derivation of a set of useful equations is achieved by recourse to asymptotic techniques which are compatible with thin domains (Saloua (2007), Delfour and Zolesco (1995)).

As stated earlier, and as would be expected, fluid flow through mediums has associated nonlinear wave phenomena, which may be analyzed according as the viscosity or otherwise of the flowing fluid and/or the smoothness or otherwise of the medium. It is against this background that we developed models of fluid-wall (blood-arterial) interaction and the inherent pulse waves. We derived the governing equations, and sought the solutions in the next chapter.

3.1.0 Generalized equation of motion of viscous fluid

Here we showed that in a given momentum transport equation, the pressure term is absorbed in the surface stress term. In the case where the pressure component is implicitly expressed

by surface stress we could rely on the relationship between pressure and the rate of strain in the fluid body to obtain the required pressure component. The need to have an explicit pressure term is borne out of the requirement of the pressure gradient in the flow momentum equation. The momentum equations which contain pressure gradient are the so called Navier-Stokes equations. The derivation of Navier-Stokes equations for a general viscous flow is shown below.

We shall assumed homogeneous fluid (of whole blood), for the moment, among other assumptions. Consider an idealized cubical small region of fluid whose sides have normal parallel to the coordinate axes OX_1, OX_2, OX_3 , (as shown in Fig 3.1, John (1975)).

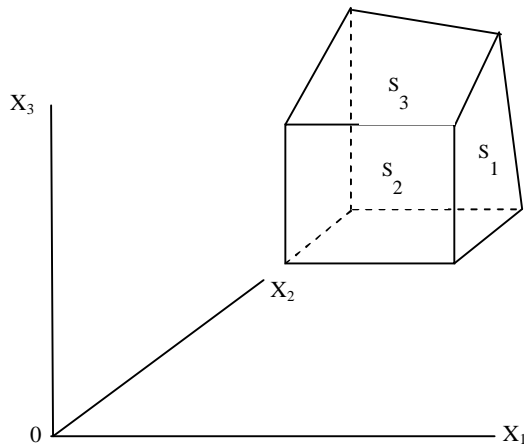


Fig 3.1 Idealized cubical fluid region

Let the surface area and the volume of the cube be S and V respectively, and let dS_j be a small element of the surface whose normal is in the direction of OX_j axis. Suppose ϕ is the fluid characteristic. The flux of ϕ across this elemental surface due to fluid velocity, u_j is $\phi u_j dS_j$. The total flux over the surface S is

$$\int_S \phi u_j dS_j \quad (3.1)$$

The measure of ϕ which is contained within the volume V is given by

$$\int_V \phi dV \quad (3.2)$$

The rate of change of ϕ contained within V is

$$\frac{\partial}{\partial t} \left[\int_V \phi dV \right] = \int_V \frac{\partial \phi}{\partial t} dV \quad (3.3)$$

It is assumed that ϕ is continuous and differentiable within V . If we make an allowance for bulk surface flux, then the rate of change of ϕ becomes

$$\int_V \left(\frac{\partial \phi}{\partial t} \right) dV + \int \phi u_j dS_j = \int_V \left[\frac{\partial \phi}{\partial t} + \frac{\partial(\phi u_j)}{\partial x_j} \right] dV \quad (\text{by divergence theorem}) \quad (3.4)$$

In application, John (1975) stated that some processes other than bulk surface flux can cause changes in ϕ within. These processes create four effects:

- (i) Radiative effects R_a , which act directly on the mass elements within V and independently of surface interaction. Some of such effects are gravitational and radiation phenomena.
- (ii) Surface effects S_j , which are associated directly with the surfaces, such as shear stress, thermal conduction, mass diffusion. Those effects exclude the effects due to bulk surface flux by fluid velocity.
- (iii) Productions P_r of ϕ within, such as production of entropy, turbulent energy, and mass energy, etc.
- (iv) Dissipation D_s of ϕ within V , such as dissipation of turbulent energy by viscosity.

If we add these effects and equate the sum to the rate of change of ϕ within V we get

$$\int_V \left[\frac{\partial \phi}{\partial t} + \frac{\partial}{\partial x_j} (\phi u_j) \right] dV + \int_V R_a dV + \int_S S_j dS_j + \int_V D_s dV + \int_V P_r dV = 0 \quad (3.5)$$

By Greenø's theorem we get

$$\int_V \left[\frac{\partial \phi}{\partial t} + \frac{\partial}{\partial x_j} (\phi u_j) + R_a + \frac{\partial S_j}{\partial x_j} + D_s + P_r \right] dV = 0 \quad (3.6)$$

Since volume is arbitrary, the quantities within the integral sign must vanish, and we get

$$\frac{\partial \phi}{\partial t} + \frac{\partial}{\partial x_j} (\phi u_j) + R_a + \frac{\partial S_j}{\partial x_j} + D_s + P_r = 0 \quad (3.7)$$

We had presupposed fluid homogeneity, and thus a single component flow. We replace ϕ in equation (3.7) by the fluid density ρ . If there are no dissipation and production effects, then $D_s = P_r = 0$. Similarly R_a must be zero since the fluid is a single component one; there is no surface flux effect other than that due to fluid velocity u_j . Thus $S_j = 0$. We have the continuity equation

$$\frac{\partial \rho}{\partial t} + \frac{\partial}{\partial x_j} (\rho u_j) = 0 \quad (3.8)$$

Or

$$\frac{D\rho}{Dt} + \rho \frac{\partial u_j}{\partial x_j} = 0 \quad (3.9)$$

Where D/Dt is the total differential coefficient defined by

$$\frac{D}{Dt} = \frac{\partial}{\partial t} + u_j \frac{\partial}{\partial x_j}$$

[Note that the continuity equation of a constant density flow is $\frac{\partial \rho}{\partial t} = 0$, since neither

expansion nor contraction takes place.]

The radiation effect due to gravitational field is given by John (1975)

$$R_{ai} = \rho \frac{\partial \Phi}{\partial x_i} \quad (3.10)$$

where Φ is the gravitational potential.

Since the surface forces cause a change in momentum of the fluid contained within the surface, their effects are accommodated in the flow equation (3.7) by replacing the tensor S_j by the negative stress tensor, $-\sigma$. Thus the components of S and σ are related by

$$S_{ij} = -\sigma_{ij} \quad (3.11)$$

On replacing ϕ by ρu_i and substituting (3.10) and (3.11) in (3.7), with $D_s = P_r = 0$ we get

$$\frac{\partial}{\partial t}(\rho u_i) + \frac{\partial}{\partial x_j}(\rho u_i u_j) + \rho \frac{\partial \Phi}{\partial x_j} - \frac{\partial \sigma_{ij}}{\partial x_j} = 0 \quad (3.12)$$

Or

$$u_i \frac{\partial \rho}{\partial t} + \rho \frac{\partial u_i}{\partial t} + u_i \frac{\partial}{\partial x_j}(\rho u_j) + \rho u_j \frac{\partial u_i}{\partial x_j} + \rho \frac{\partial \Phi}{\partial x_i} - \frac{\partial \sigma_{ij}}{\partial x_j} = 0 \quad (3.13)$$

Using the equation of continuity (3.8) together with equation (3.12) the momentum transport equation becomes

$$\frac{\partial u_i}{\partial t} = -\left[u_j \frac{\partial u_i}{\partial x_j} - \frac{1}{\rho} \frac{\partial \sigma_{ij}}{\partial x_j} + \frac{\partial \Phi}{\partial x_i} \right] \quad (3.14)$$

The term $\frac{1}{\rho} \frac{\partial \sigma_{ij}}{\partial x_j}$ is the surface stress term. The pressure term p can be determined via the

relationship between pressure and the rate of strain in the fluid given by John (1975),

$$\sigma_{ij} = -p \delta_{ij} + \lambda \delta_{ij} \frac{\partial u_k}{\partial x_k} + \mu \left[\frac{\partial u_i}{\partial x_j} + \frac{\partial u_j}{\partial x_i} \right] \quad (3.15)$$

where λ and μ are the bulk and shear coefficients of viscosity and δ_{ij} is the Kronecker delta.

When we substitute equation (3.15) into the momentum equation (3.14) we obtain momentum equations which contain pressure gradient that induces flow. Thus we have the Navier óStokes equations for viscous pipe-flow, given by

$$\frac{\partial u_i}{\partial t} + u_j \frac{\partial u_i}{\partial x_j} = \frac{1}{\rho} \frac{\partial p}{\partial x_i} + \frac{\partial}{\partial x_i} \left[\lambda \frac{\partial u_k}{\partial x_k} \right] + \frac{1}{\rho} \frac{\partial}{\partial x_j} \mu \left[\frac{\partial u_i}{\partial x_j} + \frac{\partial u_j}{\partial x_i} \right] - \frac{\partial \Phi}{\partial x_i} = 0 \quad (3.16)$$

The above equation (3.16) has shown that the surface stress term $\frac{1}{\rho} \frac{\partial \sigma_{ij}}{\partial x_j}$ would reduce to pressure gradient and viscosity gradient terms.

3.1.1 Action of fluid on the wall

In the previous section we derived an equation that holds good for a generalized viscous pipe-flow, in which the resulting motion of the elastic wall was not considered. In our arterial flow, the motion of the elastic arterial wall due mainly to blood flow shall be considered.

The interaction of blood with the vessel wall has dual effects. Blood cells deform as a consequence; in fact the distribution of the red cells in arteries is affected by the vessel wall (Fung (1996)). On the other hand, the fluid flow impacts on the wall. The action of the fluid on the wall may be explained better by Becker as contained in Milne-Thomson (1974). We apply his principle using the theorem below.

Theorem 3.1: Draw a unit normal \mathbf{n} into the vessel wall at X (Fig.3.2). The action of the fluid on the wall is given by the stress vector

$$\mathbf{t} = \left(p - \frac{4}{3\mu} \nabla \cdot \mathbf{T} \right) \mathbf{n} + \nabla \mathbf{T} \cdot \mathbf{n} \quad (3.17)$$

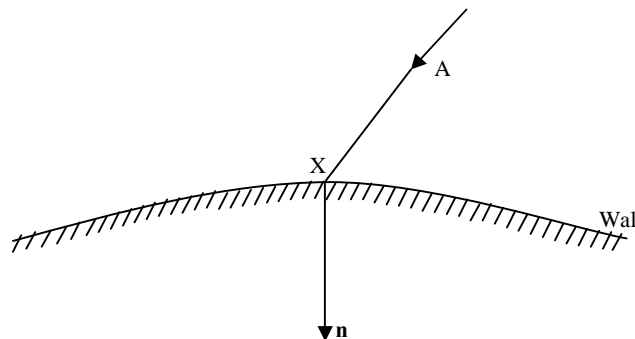


Fig 3.2 Unit normal to the vessel wall

where in (3.17) above, p is pressure, μ is the coefficient of fluid viscosity, \mathbf{q} is the fluid velocity at X and $\boldsymbol{\zeta}$ is the vorticity (in the case of non-vortex flow, $\boldsymbol{\zeta} = 0$).

Proof: Draw a closed circuit round the point P of the wall to enclose the area S of the wall. On the wall the velocity $\mathbf{q} = 0$ (Milne-Thomson (1974)). As a consequence of Stokes theorem, we have

$$(\boldsymbol{\zeta} \wedge \nabla) \wedge \boldsymbol{\tau} - \boldsymbol{\zeta} \wedge (\nabla \wedge \boldsymbol{\tau}) = (\nabla \cdot \boldsymbol{\tau}) - (\nabla \cdot \boldsymbol{\tau}) \quad (3.18)$$

And thus

$$\int_S dS \boldsymbol{\tau} = \int_S \boldsymbol{\zeta} \wedge \nabla \boldsymbol{\tau} dS = \int_S [\boldsymbol{\zeta} \wedge \nabla \mathbf{q} - (\nabla \mathbf{q}) \wedge \boldsymbol{\zeta}] dS \quad (3.19)$$

where $\boldsymbol{\zeta} = \nabla \times \boldsymbol{\tau}$ is the vorticity.

Since S is arbitrary, we have from equation (3.19)

$$(\mathbf{n} \cdot \nabla) \mathbf{q} - \mathbf{n} (\nabla \cdot \mathbf{q}) + \mathbf{n} \wedge \boldsymbol{\zeta} = 0 \text{ on the wall} \quad (3.20)$$

We extend to viscosity hypothesis (Milne-Thomson (1974)). In a viscous fluid the stress on element dS of the surface of the fluid particle is not necessarily normal to dS . We therefore express the stress tensor in the form

$$= -p \mathbf{I} + \boldsymbol{\tau} \quad (3.21)$$

where the tensor $-p \mathbf{I}$, has all-round symmetry as in a non-viscous case, while the tensor depends directly on viscosity. The stress on dS is

$$\mathbf{n} \cdot \boldsymbol{\tau} = -p \mathbf{n} + \mathbf{n} \cdot \boldsymbol{\tau} \quad (3.22)$$

Fluid particle motion is like a rigid body motion, with an accompanying rate of pure strain, whereby the direction of motion of each point of the particle is normal to a certain quadric. Rigid body motion causes no relative motion and thus, has no effect in producing forces of a frictional character and thus viscosity is not regarded as exhibiting its influence through friction on the surface of the fluid particle surrounding the fluid. Thus, by hypothesis we associate the stress $\mathbf{n} \cdot \boldsymbol{\tau}$ of (3.22) solely to pure strain.

Consider a spherical particle; centre X , of infinite-seminal radius r (see Fig. 3.3)

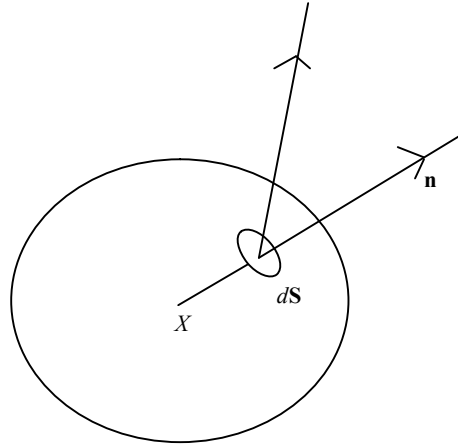


Fig 3.3 Idealized spherical particle

Let \mathbf{n} be the outward normal at the area of dS of the particle. A pure strain induces a motion of dS relative to the centre of the sphere with velocity

$$f(\mathbf{rn}) = \mathbf{rn}\mathcal{D}$$

where $\mathcal{D} = \left(\frac{1}{2}(\nabla\mathbf{v} + \mathbf{v}\nabla; \nabla) \right)$ is the rate of deformation tensor.

By viscosity hypothesis we suggest that $\mathbf{n}\mathcal{D}$ is proportional to $f(\mathbf{n})$; precisely

$$\mathbf{n}\mathcal{D} = 2\mu f(\mathbf{n}) = 2\mu\mathbf{n}\mathcal{D} \quad (3.23)$$

where μ is the coefficient of viscosity. Thus equation (3.21) becomes

$$= -p\mathbf{I} + \mu(\nabla; \mathbf{q} + \mathbf{q}; \nabla) \quad , \quad (3.24)$$

where the semi-colon (;) represents dyadic multiplication. The pressure defined by the invariant scalar of Ψ is, Milne-Thomson (1974)

$$-3p = \Psi_I = -3p' + 2\mu(\nabla\mathbf{q}) \quad (3.25)$$

Thus, we get the symmetrical tensor given by

$$\Psi = -p\mathbf{I} - \frac{2}{3}\mu(\mathbf{v}\nabla) + \mu(\nabla\mathbf{v} + \mathbf{v}\nabla; \nabla) \quad ,$$

and thus the stress on dS is

$$\mathbf{T} = -p \mathbf{n} - \frac{2}{3} \mu (\nabla \cdot \mathbf{v}) \mathbf{n} + 2\mu \nabla \mathbf{v} \cdot \mathbf{n} \quad (3.26)$$

where $\boldsymbol{\zeta} = \nabla \wedge \mathbf{q}$ is the vorticity. From (3.18) we get

$$\mathbf{T} = -p \mathbf{n} - \frac{2}{3} \mu (\nabla \cdot \mathbf{v}) \mathbf{n} + 2\mu \nabla \mathbf{v} \cdot \mathbf{n} \quad (3.27)$$

When $(\nabla \cdot \mathbf{v})$ is substituted from (3.27) then (3.17) follows ■

From the foregoing we see that the action of the fluid on the wall consists of a normal pressure, $p - \frac{4}{3} \mu \nabla q$ and an accompanying shear, of magnitude $\mu \boldsymbol{\zeta}$ in the sense of vorticity, which is tangential to the wall, oriented at right-angle in the clockwise sense of rotation about \mathbf{n} (where \mathbf{n} is directed into the wall), (Fig.3.4)

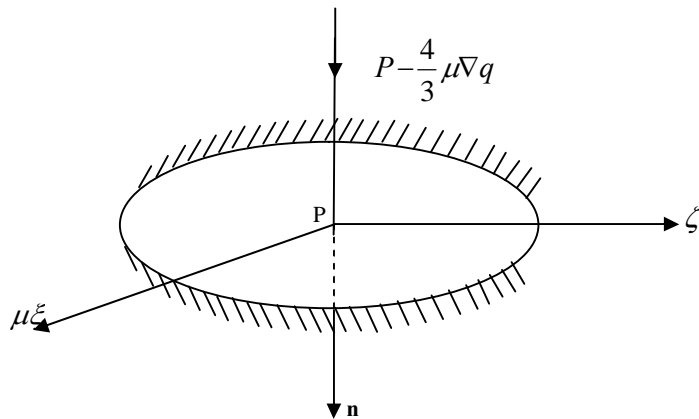


Fig 3.4 Action of fluid on the wall

3.1.2 Fluid-Structure interaction model: Problem presentation

The first model, which we shall present here, describes the interaction of fluid (blood) with the structure (elastic wall).

Assumptions:

- (i) The fluid is Newtonian, viscous and incompressible
- (ii) The flow is axisymmetric

(iii)The artery is thin-walled (i.e.with small wall thickness and with negligible radial stress) and elastic

(iv)The artery is a homogeneous, isotropic membrane shell (i.e with negligible bending stress)

We now describe the equations of fluid flow, the membrane equation and the fluid-wall dynamic coupling equations. This work considered unsteady axisymmetric flow of a Newtonian incompressible fluid in a thin elastic right cylinder whose radius is small with respect to its length. We define an aspect ratio (the ratio between the radius R and the length L of the cylinder) by $\varepsilon := R/L$ and for each fixed $\varepsilon > 0$, we define the reference domain (Figure 3.5) by

$$\Omega_\varepsilon(t) = \{x \in \mathbb{R}^3 : x = (r \cos \theta, r \sin \theta, z), r < R + \eta^\varepsilon(z, t), 0 < z < L\} \quad (3.28)$$

Define the lateral boundary by

$$\Sigma = \{x = (R(z) \cos \theta, R(z) \sin \theta, z) \in \mathbb{R}^3 : \theta \in (0, 2\pi), z \in (0, L)\} \quad (3.29)$$

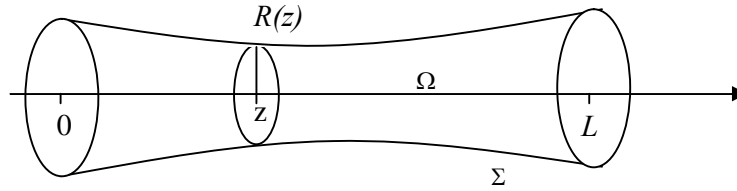


Fig 3.5 Reference domain diagram

This lateral boundary behaves as a homogeneous, isotropic, linearly elastic membrane shell, with thickness h (Ciarlet and Lods (1996)) and at the reference configuration the shell is prestressed by $\sigma_{\theta\theta}^0 = p_{ref} R_{max}/h$, where p_{ref} is the pressure at the reference state, and $\sigma_{\theta\theta}^0$ is the θ, θ component of the stress tensor (see Luchini *et al* (1991), Ma (1992)).

The flow in the Eulerian formulation of $\Omega_\varepsilon(t) \times R_+$ in cylindrical co-ordinates we consider here is premised on the following:

- (i) The domain $\Omega_\varepsilon(t)$ contains a fully developed flow.
- (ii) The flow is axisymmetric.
- (iii) The flow in the angular direction is negligible (and so the equation of flow in that direction is neglected).

We, therefore, have the following equations of flow, (Pedrizzetti and Dominichini (2003), Atabek (1968)):

$$\rho \left\{ \frac{\partial v_r^\varepsilon}{\partial t} + v_r^\varepsilon \frac{\partial v_r^\varepsilon}{\partial r} + v_z^\varepsilon \frac{\partial v_r^\varepsilon}{\partial z} \right\} - \mu \left(\frac{\partial^2 v_r^\varepsilon}{\partial r^2} + \frac{\partial^2 v_r^\varepsilon}{\partial z^2} + \frac{1}{r} \frac{\partial v_r^\varepsilon}{\partial r} - \frac{v_r^\varepsilon}{r^2} \right) + \frac{\partial p^\varepsilon}{\partial r} = 0 \quad (3.30)$$

$$\rho \left\{ \frac{\partial v_z^\varepsilon}{\partial t} + v_r^\varepsilon \frac{\partial v_z^\varepsilon}{\partial r} + v_z^\varepsilon \frac{\partial v_z^\varepsilon}{\partial z} \right\} - \mu \left(\frac{\partial^2 v_z^\varepsilon}{\partial r^2} + \frac{\partial^2 v_z^\varepsilon}{\partial z^2} + \frac{1}{r} \frac{\partial v_z^\varepsilon}{\partial r} \right) + \frac{\partial p^\varepsilon}{\partial z} = 0 \quad (3.31)$$

and the continuity equation (Panton, (1996))

$$\frac{\partial v_r^\varepsilon}{\partial r} + \frac{\partial v_z^\varepsilon}{\partial z} + \frac{v_r^\varepsilon}{r} = 0 \quad \text{in } \times R_+ \quad (3.32)$$

In the equation above v_r , v_z are the radial and longitudinal components of the fluid respectively, μ is the viscosity of the fluid p is the pressure and ρ is the density. The equation (3.32) represents the incompressibility condition, $div v = 0$. We shall now consider the equations of tube in the radial and lateral directions. A healthy human has a systolic blood pressure (SBP) about 120mm Hg, and the diastolic blood pressure around 80mm Hg. This suggest a mean arterial blood pressure (MAP) $P_0 = 100$ mm Hg. In event of flow there is a dynamical pressure increment $\Delta p = \pm 20$ mm Hg added in the initial pressure field.

Arteries are usually subjected to an axial pre-stretch λ_z (Fung (1996)). Thus, a dynamic pressure (or a radial displacement) is superimposed on the initial static deformation both in

the radial and axial direction. The external tethering in the axial direction depletes the effect of axial displacement (McDonald, (1974)). The assumption of arterial longitudinal tethering precludes the treatment of the behaviour of artery with variable radius. However, since systolic pressure induces variations in arterial length, (Lawton and Greene (1956)) and since age, pregnancy, vascular diseases among other factors cause longitudinal stretch (Hai-Chao *et al* (1994)) it is safe to treat flow through artery with variable radius.

We consider a thin and long tube of circular cross-section with initial reference radius R_0 in the cylindrical polar coordinates (R^*, θ, Z^*) . In line with Demiray (1976) we described the position vector of a point on the tube by

$$\mathbf{R} = R_0 \mathbf{e}_r + Z^* \mathbf{e}_z \quad (3.33)$$

where \mathbf{e}_r , \mathbf{e}_θ and \mathbf{e}_z are the unit base vectors in the cylindrical polar coordinates and Z^* is the axial coordinates of a material point in the natural state. Along the meridional and circumferential curves the arc lengths are given by (Bakirtas and Demiray (2004))

$$dS_Z = dZ^*, \quad dS_\theta = R_0 d\theta \quad (3.34)$$

Assuming the elastic tube is subjected to an axial stretch ratio λ_z and a static pressure $P_0^*(Z^*)$ (see Fung (1981), then the deformation is described by

$$\mathbf{r}_\theta = [r_0 - f^*(z^*)] \mathbf{e}_r + z^* \mathbf{e}_z, \quad z^* = \lambda_z Z \quad (3.35)$$

where z^* is the axial coordinate at the intermediate configuration, r_0 is the deformed end radius at the origin, and $f(z^*)$ is the stenosis function after deformation. The deformation induces an arc along the meridional and circumferential directions given by (Demiray (1976))

$$ds_z^0 = [1 + (-f^{*'})^2]^{1/2} dz^*, \quad ds_\theta = [r_0 - f^*(z^*)] d\theta, \quad (3.36)$$

where a prime denotes the differentiation of the corresponding field variable with respect to z^* . Assume a negligible axial displacement and let $v^*(z^*, t^*)$ be a finite dynamical

displacement superimposed on the initial static deformation. The position vector \mathbf{r} of a generic point on the tube is

$$\mathbf{r} = [r_0 \phi f^*(z^*) + v^*(z^*, t^*)] \mathbf{e}_r + z^* \mathbf{e}_z \quad (3.37)$$

This time, the dynamic deformation induces the following meridional and circumferential arc lengths respectively:

$$ds_z = \left[1 + \left(-f^{*'} + \frac{\partial v^*}{\partial z^*} \right)^2 \right]^{\frac{1}{2}} dz^*, \quad ds_\theta = [r_0 \phi f^*(z^*) + v^*(z^*, t^*)] d\theta \quad (3.38)$$

The meridional and circumferential curves in this final configuration have the respective stretch ratios,

$$\lambda_1 = \lambda_2 \left[1 + \left(-f^{*'} + \frac{\partial v^*}{\partial z^*} \right)^2 \right]^{\frac{1}{2}}, \quad \lambda_2 = \frac{1}{R_0} [r_0 \phi f^*(z^*) + v^*(z^*, t^*)] \quad (3.39)$$

The unit tangent \mathbf{W} along the deformed meridional curve and the unit exterior normal \mathbf{n} to the deformed membrane are given by

$$\mathbf{W} = \frac{\left(-f^{*'} + \frac{\partial v^*}{\partial z^*} \right) \mathbf{e}_r + \mathbf{e}_z}{\beta}, \quad \mathbf{n} = \frac{\mathbf{e}_r - \left(-f^{*'} + \frac{\partial v^*}{\partial z^*} \right) \mathbf{e}_z}{\beta}, \quad (3.40)$$

where the function β is defined by

$$\beta = \left[1 + \left(-f^{*'} + \frac{\partial v^*}{\partial z^*} \right)^2 \right]^{\frac{1}{2}}$$

By the assumption of incompressibility of material, the thickness H and h , before and after final deformation respectively would satisfy

$$h = \frac{H}{\lambda_1 \lambda_2} \quad (3.41)$$

Suppose M_1 and M_2 are the membrane forces along the meridional and circumferential curves respectively. A small tube element situated between the planes $z^* = \text{constant}$ and $z^* + dz^* =$

constant, $\theta = \text{constant}$ and $\theta + d\theta = \text{constant}$ may have equation of radial motion described by

$$\frac{\partial}{\partial z^*} \left[\frac{M_1}{\beta} (r_0 - f^{*+v^*}) \left(-f^{*'} + \frac{\partial v^*}{\partial t^*} \right) \right] - M_2 \beta + \beta (r_0 - f^{*+v^*}) F_r = \rho_w \frac{H}{\lambda_z} R_0 \frac{\partial^2 v^*}{\partial t^{*2}} \quad (3.42)$$

where ρ_w is the mass of density of the membrane material, and F_r is the radial fluid reaction force on the inner surface of tube, to be expressed mathematically later.

Let \mathcal{W}^* be the strain energy density function of the tube material where \mathcal{W} is the shear modulus. Then the membrane forces M_1 and M_2 can be expressed in terms of the stretch ratios as

$$M_1 = \frac{\pi H}{\lambda_2} \frac{\partial \Sigma^*}{\partial \lambda_1}, \quad M_2 = \frac{\pi H}{\lambda_1} \frac{\partial \Sigma^*}{\partial \lambda_2} \quad (3.43)$$

When equation (3.43) is introduced into equation (3.42) we get the equation of the tube in radial direction given by

$$\pi R_0 \frac{\partial}{\partial z^*} \left\{ \frac{(-f^{*'} + \frac{\partial v^*}{\partial t^*}) \partial \Sigma^*}{\beta \partial \lambda_1} \right\} - \frac{\tau}{\lambda_z} \frac{\partial \Sigma^*}{\partial \lambda_2} + \frac{\beta \mathbf{F}_r}{H} (r_0 - f^{*+v^*}) - \rho_w \frac{R_0}{\lambda_z} \frac{\partial^2 v^*}{\partial t^{*2}} = 0 \quad (3.44)$$

With this we describe the evolution of the response of the lateral boundary to the fluid flow by the Naviers equations (Quartaroni *et al* (2000)) in the form

$$\rho_w h \frac{\partial^2 v_z}{\partial t^2} = \frac{Eh}{1-\sigma^2} \left(\frac{\sigma}{R} \frac{\partial v_r}{\partial z} + \frac{\partial^2 v_z}{\partial z^2} \right) + \chi_z \quad \text{in } \Sigma \times (0, L) \quad (3.45)$$

where, h is the arterial wall thickness, E is the Young modulus of elasticity, R is the arterial reference radius at rest, ρ_w is the arterial volumetric mass, χ is the forcing term due to the external forces, including the stress from the fluid. It is noteworthy that this model is based on a Lagrangian description of the motion of the elastic wall, referred to a material domain $\mathcal{Q}(0)$, corresponding to the rest state, where $v_r = v_z = 0$.

The cylinder together with its boundary deform as a result of the fluid-wall interaction between the fluid occupying the domain and the cylinder's boundary (Figure 3.6).

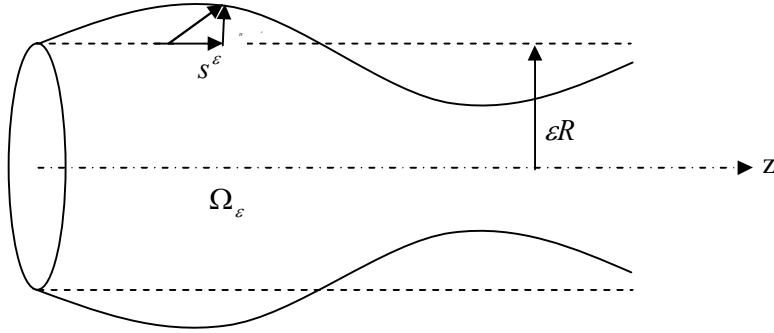


Fig 3.6 Wall displacement

For this lateral wall which allows presumably, only radial displacements, $\Sigma_\varepsilon(t) = \{r = R + \eta^\varepsilon(z, t)\} \times (0, L)$, we have the radial contact force given by

$$F_r = \frac{-h(\varepsilon)E(\varepsilon)}{1-\sigma^2} \frac{\eta^\varepsilon}{R^2} + h(\varepsilon)G(\varepsilon)\kappa(\varepsilon) \frac{\partial^2 \eta^\varepsilon}{\partial z^2} - \rho_w h(\varepsilon) \frac{\partial^2 \eta^\varepsilon}{\partial t^2} \quad (3.46)$$

where η^ε is the radial displacement from the reference state, $E(\varepsilon)$ is the Young's modulus of elasticity, $h(\varepsilon)$ is the wall thickness, κ is the Timoshenko shear correction factor (see Reismann (1988) and Nobile (2001)), G is the shear modulus, σ ($= 0.5$ for an incompressible material) is the Poisson ratio

In the equation (3.46) the right-hand members are described as follows: the first term is the *elastic response function*, the second term is related to the *radial pre-stress state* of the vessel and the third term is the *inertia* term that is proportional to the radial acceleration of the vessel wall.

Further Assumptions:

The Young's modulus $E(\varepsilon)$, the wall thickness $h(\varepsilon)$ and the shear modulus $G(\varepsilon)$ satisfy

$$h(\varepsilon) E(\varepsilon) > \varepsilon \quad (3.47)$$

$$\lim_{\varepsilon \rightarrow 0} \frac{h(\varepsilon)E(\varepsilon)}{\varepsilon} = E_0 \in (0, +\infty) \quad (3.48)$$

$$\lim_{\varepsilon \rightarrow 0} \varepsilon h(\varepsilon)G(\varepsilon)\kappa(\varepsilon) = G_0 \in [0, +\infty) \quad (3.49)$$

3.1.3 Fluid-Structure Coupling

The fluid and the wall form a coupled system at the interface. The lateral boundary conditions require continuity of velocity and continuity of forces. This is the basis of the coupling of the fluid equations with the membrane equations. We consider the coupling at the deformed interface in the Lagrangean framework with respect to the reference configuration Σ_ε^0 (Pedrizzetti and Perktold (2003)). The fluid velocity at the deformed interface $(R+\eta^\varepsilon, z, t)$ must be equal to the Lagrangean velocity of the membrane. Since only the radial displacements are non-zero we have (Surulescu (2008), Pedrizzetti and Domenichini (2003)).

$$v_r^\varepsilon(R+\eta^\varepsilon, z, t) = \frac{\partial \eta^\varepsilon}{\partial t}(z, t) \text{ on } (0, L) \times \mathbb{R}_+ \quad (3.50)$$

$$v_z^\varepsilon(R+\eta^\varepsilon, z, t) = \frac{\partial S^\varepsilon}{\partial t} = 0 \text{ on } (0, L) \times \mathbb{R}_+ \quad (3.51)$$

Equation (3.51) comes from the continuity of velocity along the longitudinal displacement S ,

which is assumed zero, and thus $\frac{\partial S^\varepsilon}{\partial t} = 0$. We set the radial force in (3.46) equal to the radial

displacement component of the stress exerted by the fluid to the membrane

$$-F_r = [(p^\varepsilon - p_{ref})\mathbf{I} - 2\mu\mathbf{D}(\mathbf{v}^\varepsilon)] \mathbf{n} \cdot \mathbf{e}_r = (p^\varepsilon - p_{ref}) - 2\mu \frac{\partial v_r^\varepsilon}{\partial r}, \quad (3.52)$$

where:

\mathbf{I} : is the *idemfactor* (Milne ó Thomson (1974)). The idemfactor is such that: for any vector \mathbf{x} ,

$$\mathbf{I}\mathbf{x} = \mathbf{x}\mathbf{I} = \mathbf{x}$$

$D(v^\varepsilon)$: is the deviatoric part of an axially symmetric vector (tensor) valued function

$v^\varepsilon = v_r^\varepsilon e_r + v_z^\varepsilon e_z$ such that

$$\square (v^\varepsilon) = \begin{pmatrix} \frac{\partial v_r^\varepsilon}{\partial r} & 0 & \frac{1}{2} \left(\frac{\partial v_r^\varepsilon}{\partial z} + \frac{\partial v_z^\varepsilon}{\partial r} \right) \\ 0 & \frac{v_r^\varepsilon}{r} & 0 \\ \frac{1}{2} \left(\frac{\partial v_r^\varepsilon}{\partial z} + \frac{\partial v_z^\varepsilon}{\partial r} \right) & 0 & \frac{\partial v_z^\varepsilon}{\partial z} \end{pmatrix}$$

n : the unit normal at the deformed structure given by

$$n = \frac{-R' + \eta^{\varepsilon'}}{\sqrt{1 + (R' + \eta')^2}} e_z + \frac{1}{\sqrt{1 + (R' + \eta^{\varepsilon'})^2}} e_r$$

We recall that fluid flow is defined in the Eulerian formulation, whereas the reference, pressure and the contact force (3.46) is given in Lagrangean co-ordinates. For compatibility of coordinates, we transform from Eulerian to Lagrangean coordinates (This pre-coupling transformation is the reverse form of the one obtainable in Pedrizzetti and Domenichini (2003)). We now consider for this transformation the Jacobean of the Transformation from Eulerian to Lagrangean coordinates

$$J := \sqrt{\det(\nabla\Theta)^T \nabla\Theta} = \sqrt{(R + \eta^\varepsilon)^2 (1 + (\partial_z \eta^\varepsilon)^2)} \quad (3.53)$$

where $\Theta : (z, \theta) \rightarrow (x, y, z)$, whose gradient $\nabla\Theta$ is such that if

$$x = (R + \eta^\varepsilon) \cos \theta, y = (R + \eta^\varepsilon) \sin \theta, z = z,$$

$$\nabla\Theta = \begin{pmatrix} \frac{\partial x}{\partial z} & \frac{\partial x}{\partial \theta} \\ \frac{\partial y}{\partial z} & \frac{\partial y}{\partial \theta} \\ 1 & 0 \end{pmatrix} = \begin{pmatrix} \left(\frac{\partial \eta^\varepsilon}{\partial z} \right) \cos \theta & -(R + \eta^\varepsilon) \sin \theta \\ \left(\frac{\partial \eta^\varepsilon}{\partial z} \right) \sin \theta & (R + \eta^\varepsilon) \cos \theta \\ 1 & 0 \end{pmatrix}$$

We consider the generic points on the lateral boundary, where coupling occurs. We now consider the fluid-structure coupling. This requires that for each subset (see Kechris (1995), Dudley (1989)) of the lateral boundary Σ_ε , the contact force (3.46) exerted by the fluid on the wall equals the opposite of the contact force exerted by the wall to the fluid; thus

$$\int_B [(p^\varepsilon - p_{ref})I - 2\mu D(v^\varepsilon)] \cdot \nu_r J d\theta dz = \int_B F_r R d\theta dz.$$

Thus we get, at each point, the dynamic coupling condition

$$[(p^\varepsilon - p_{ref})I - 2\mu D(v^\varepsilon)] \cdot \nu_r \left(1 + \frac{\eta^\varepsilon}{R}\right) \sqrt{(1 + \partial_z \eta^\varepsilon)^2} = F_r \text{ on } \Sigma_\varepsilon \times \mathbb{R}^+, \quad (3.54)$$

where F_r is given by (3.46). The cylinder's initial condition when filled with fluid, under reference pressure p_{ref} is such that

$$\eta^\varepsilon = s^\varepsilon = \frac{\partial \eta^\varepsilon}{\partial t} = \frac{\partial s^\varepsilon}{\partial t} = 0, \text{ and } v^\varepsilon = 0 \text{ on } \Sigma_\varepsilon \times \{0\} \quad (3.55)$$

Here s^ε is the longitudinal displacement from the reference state.

Since we assume that the integrity of flow is the temporal dynamic pressure prescribed at both ends of the cylinder, we have the following boundary (inlet/outlet) conditions

$$v_r^\varepsilon = 0, \quad p^\varepsilon + \frac{\rho(v_z^\varepsilon)^2}{2} = p_0(t) + p_{ref} \quad \text{on } (\partial\Omega_\varepsilon \cap \{z=0\}) \times \mathbb{R}_+, \quad (3.56)$$

$$v_r^\varepsilon = 0, \quad p^\varepsilon + \frac{\rho(v_z^\varepsilon)^2}{2} = p_L(t) + p_{ref} \quad \text{on } (\partial\Omega_\varepsilon \cap \{z=L\}) \times \mathbb{R}_+, \quad (3.57)$$

$$\frac{\partial s^\varepsilon}{\partial z} = \eta^\varepsilon = 0 \text{ for } z = 0, \quad s^\varepsilon = \eta^\varepsilon = 0 \text{ for } z = L \text{ and } \forall t \in \mathbb{R}_+, \quad (3.58)$$

where pressure drop is assumed to be $A(t) = p_L(t) - p_0(t) \in C_0^\infty(0, +\infty)$. We note that an assumption of zero longitudinal displacement of the structure reduces the application of the model for tube with variable cross-sectional radius. If we assume that there is a small change

in radius, then the model is reasonable. Now we summarize for eventual solution of the fluid-structure interaction problem as follows:

$$\left. \begin{array}{ll}
 \text{Equations (3.30), (3.31), (3.32)} & \text{in } \Omega_\epsilon \\
 \text{Equations (3.50), (3.51)} & \text{on } \times R_+ \\
 \text{Equation (3.52)} & \text{on } \times R_+ \\
 \text{Equations (3.56), (3.57)} & \text{on } (\dot{U} \quad \{z = 0, L\} \times R_+ \\
 \text{Equation (3.58)} & \text{for } z = 0, L \quad \forall t \in R_+
 \end{array} \right\} \quad (3.58)^*$$

The solution to the problem (3.58)* is sought in the next chapter.

3.2.0. Model of arterial pulse: Problem presentation

A remarkable feature of arterial blood flow is its pulsatile character. Blood which is ejected into the aorta from the left ventricle (LV) of the heart produces pulse in the arterial tree. The pulse wave is a physiological phenomenon, which is observable and measurable in the arterial system during blood circulation. A certain blood volume is expelled during one heart systole. This volume of blood propagates through the arteries due to the reciprocal transformation between kinetic energy of a segment of such blood volume and the potential energy of a stretched segment of the vascular wall. The whole pulse manifests the changes in pressure, blood flow, velocity and profile. In essence, it could be used for classification of arterial elasticity. A very essential physiological index is the pulse wave velocity (PWV). The aortic index is determined largely by PWV. The propagation of arterial pulse wave is as follows (http://criticalcareassessment.com/PWV_Analysis.html):

S_w (starting point): Arterial pulse-wave starts. The aortic valve opens and blood is expelled from the LV.

P_w (Percussion Waves): Wave caused by LV ejection that increases the arterial wall elasticity.

T_w (Tidal Wave): Reflected wave from the small artery

I (Incisura): Endpoint of systolic phase, the aortic valve closes.

D_w (Dicrotic Wave): Reflective oscillatory wave resulting from the blood crash into aortic valve by blood pressure of aorta.

The transmission of pressure pulse is usually accompanied by an increase in amplitude (peaking) and a decrease in pulse width (steepening). Going through many works on linearized models of blood flow and waves ((Pedley (1980)), (Westerhorf *et al* (1972)), (Berger *et al* (1993)), (Olufsen (1998))), we find that one of the assumptions underlying the linear model is the neglect of the non-linear convective terms in the equation of fluid motion. The convective terms are considered small since the mean flow velocity is usually less than 10% of the wave velocity. Secondly, linearized theories assume that the distortion of the vessel wall is a small percentage of the radius of the vessel. Thirdly, the vessel walls are assumed to be linearly elastic.

The non-linear model contends that:

- (i) The condition that justifies neglecting the nonlinear terms would not hold good in the case of arterial pulse waves with large amplitude.
- (ii) Although in systemic arteries, the change in radius during one cardiac cycle is less than 4% (Wen-Shan *et al*(1997)) the accompanying change in cross-sectional area may not be negligible .
- (iii) The modulus of elasticity of the vessels varies quite strongly with pressure.

These three contentions considered against the underlying assumptions of the respective linear models are a basis for nonlinearity of waves in arteries. We shall, therefore consider

the dynamical nonlinear equation of pressure wave. In event of the δ peakingö and δ steepeningö phenomena that are associated with pulse waves , we compare the behaviour of the waves to *solitons* generated by a Korteweg-deVries (KdV) non-linear wave)model ((Zebusky and Porter (2010))

3.2.1 Linear superposition of forward and backward ABP waves

When the heart beats, pressure and flow waves are created. The waves are propagated through the aorta and the major arteries to the periphery with a certain wave speed. In event of the waves encountering some shock, as in bifurcations or stenosis (or both), some eddies and reflections result. These eddies and reflections continuously modify the magnitude and morphology of the waves (McDonald (1974)). The pressure and wave therefore consist of incident and backward components propagating away and towards the heart. The extent to which the backward wave approaches the heart (but would not reach to the heart, as a rule) depends on the pulse wave velocity.

Suppose as usual, that z is a spatial position, on the arterial tree and t is a time variable, then the description of pressure $P(z, t)$ and flow $Q(z, t)$ is a linear superposition of forward and backward waves (Westerhof *et al* (1972)) given by

$$P(z, t) = P_f(z - c_o t) + P_b(z + c_o t) \quad (3.59)$$

$$Q(z, t) = Q_f(z - c_o t) + Q_b(z + c_o t) \quad (3.60)$$

where the subscripts f and b refer respectively to the forward and backward components of the waves; c_o is a parameter that represents the MoensóKorteweg sound wave velocity in the vessel filled with blood of density , given by

$$c_o = \sqrt{\frac{Eh_o}{2\rho R_o}} , \quad (3.61)$$

with the underlying assumption that the vessel thickness h_o is much smaller than the vessel radius R_o , E is the wall elasticity. If the vessel's compressibility is taken into account the true speed c_t is slightly higher than c_o . (In such a case $c_t = 1.15c_o$, Oates (2001)).

Determining the forward and reflected components of flow and pressure by input impedance method is a relation between the BP and flow with linearity assumption. In frequency domain the ratio of time Fourier transforms of pressure and flow at the position z and frequency is given by

$$Z(z, \omega) = \frac{\dot{P}(z, \omega)}{\dot{Q}(z, \omega)} = \frac{\dot{P}_f(z, \omega) + \dot{P}_b(z, \omega)}{\dot{Q}_f(z, \omega) + \dot{Q}_b(z, \omega)}. \quad (3.62)$$

If $\Omega(z, \omega)$ is the global reflection coefficient, then it can be expressed in terms of pressure and flow transform and the characteristic impedance Z_c .

This global reflection coefficient Ω is defined by (Westerhof *et al* (1972))

$$\Omega(z, \omega) = \frac{Z(z, \omega) - Z_c}{Z(z, \omega) + Z_c} \quad (3.63)$$

where the characteristic impedance Z_c can be estimated by several methods (for a reflectionless tube $Z_c = Z$). The forward and backward components of the pressure and flow are given by:

$$\dot{P}_f = \frac{\dot{P}}{1 + \Omega}, \quad \dot{Q}_f = \frac{\dot{Q}}{1 - \Omega} \quad (3.64)$$

$$\dot{P}_b = \Omega \dot{P}_f, \quad \dot{Q}_b = -\Omega \dot{Q}_f \quad (3.65)$$

The adequacy of this method is on grounds that pressure and flow are measured at only one location, but it only assumes a linear model. We have stated the salient equations of the vascular input impedance concept without derivation. The idea is to create an impression of

what obtain in a linear superposition of forward and backward wave transmission. In the next chapter, we shall present a mathematical framework for nonlinear wave models.

CHAPTER FOUR

SOLUTIONS TO MODEL PROBLEMS

The previous chapter presented the *fluid-structure interaction* and the *non-linear arterial pulse wave* model problems, whose solutions shall be sought in this chapter. In the first model, the fluid-wall interaction was a coupled system that yielded the momentum conservation equations, together with the continuity equation in a prescribed domain, subject to the stipulated conditions. In the second model we deduced that non-linear arterial pulse wave model can be satisfied by the Korteweg-de Vrieø equation that describes shallow water wave. The Korteweg de-Vrieø equation is amenable to some methods of solution that we shall consider.

4.1.0 Solution of fluid-wall interaction problem

For each fixed $\varepsilon > 0$, we seek a solution to (3.30), (3.31) and (3.32) in $\Omega_\varepsilon(t)$ defined by (3.28), with an elastic boundary $\Sigma_\varepsilon(t)$ whose conditions are given by the continuity of velocity (3.50) and (3.51), and the continuity of radial forces (3.46), in which the left hand member is replaced by (3.52). We prescribe the boundary conditions at the inlet and outlet as (3.56), (3.57) and the behaviour of the elastic wall is given by (3.58). The initial data are specified by (3.55).

In the face of enormous difficulties inherent in the solution of the fluid-structure problem of this magnitude, we shall invite some aspects of existence of solution theorems and weak formulation theorems (Surulescu (2008), Nobile (2001) Boulakia (2003), Barbu *et al* (2008), among others). We shall as well be mindful of some strong solutions for well posed fluid-structure interaction problems treated in Kukavica *et al* (2009), (2010). It is necessary to explore the existence of solutions, which is invaluable in our enquiry into a solution.

A solution that yields pressure in the light of the fluid-structure prescriptions shall be sought. A prelude to the rescaling of the equations for a tractable solution is the energy estimate of the velocity field (see Surulescu (2008)). We shall supply some of the vital energy estimates due to Suncica *et al* (2005). The energy of the fluid-structure interaction (FSI) problem consists of the membrane's elastic energy, fluids viscous elastic energy, and the energy of the outside forcing term.

4.1.1 Weak Formulation and Variational Form

Let V^ε be a test function space and let V^ε be a solution space. We define:

Definition 4.1 The space $V^\varepsilon \subset H^1(\Omega_\varepsilon)^3$ consists of axially symmetric functions φ such that $\varphi_r|_{\Sigma_\varepsilon} = \varphi_z|_{\Sigma_\varepsilon} = 0$, $\varphi_r(0,r) = \varphi_r(L,r) = 0$, $\varphi_z(L, \varepsilon R) = 0$ for $r \leq \varepsilon R$ and $\text{div} \varphi = 0$ in Ω_ε

Definition 4.2: The space V consists of all functions $(w_r, w_z, d_r, d_z) \in H^1((0,T); V) \times (H^1((0,L) \times (0,T))^2 \cap H^2((0,T); L^2(0,L))^2)$ such that:

1. $\frac{\partial w_r}{\partial r} + \frac{\partial w_z}{\partial z} + \frac{w_r}{r} = 0$ in $\times \mathbb{R}_+$
2. $r^{-1} w_r \in L^2((0,T) \times \Omega_\varepsilon)$
3. $d_r(t,0) = d_z(t,L) = d_r(t,L) = 0$ on \mathbb{R}_+
4. $w_r = 0$ on $(\partial\Omega_\varepsilon \cap \{z=0\}) \times \mathbb{R}_+$
5. $w_r = 0$ on $(\partial\Omega_\varepsilon \cap \{z=L\}) \times \mathbb{R}_+$
6. $w_r = \frac{\partial d_r}{\partial t}$ and $w_z = \frac{\partial d_z}{\partial t}$ on $\Sigma_\varepsilon \times \mathbb{R}_+$.

For an axially symmetric vector-valued function, $\psi = \psi_r \vec{e}_r + \psi_z \vec{e}_z$. To obtain the variational formulation we multiply equations (3.30) and (3.31) by test functions φ_r and φ_z respectively, and integrate over the domain Ω .

In this variational form, equation (3.30) becomes:

$$\int_{\Omega} \left(\rho \frac{\partial v_r^\varepsilon}{\partial t} - \mu \left(\frac{\partial^2 v_r^\varepsilon}{\partial r^2} + \frac{\partial^2 v_r^\varepsilon}{\partial z^2} + \frac{1}{r} \frac{\partial v_r^\varepsilon}{\partial r} - \frac{v_r^\varepsilon}{r^2} \right) + \frac{\partial p^\varepsilon}{\partial r} \right) \varphi_r r dr dz = 0 \quad (4.1)$$

A term by term expression of equation (4.1) yields:

$$\begin{aligned} * \int_{\Omega} \rho \frac{\partial v_r^\varepsilon}{\partial t} \varphi_r r dr dz &= \rho \int_{\Omega} \frac{\partial v_r^\varepsilon}{\partial t} \varphi_r r dr dz \\ * - \mu \int_{\Omega} \frac{\partial^2 v_r^\varepsilon}{\partial r^2} \varphi_r r dr dz &= \\ &- \mu \int_{\partial\Omega} \frac{\partial v_r^\varepsilon}{\partial r} \varphi_r r dS_{\Omega} + \mu \int_{\Omega} \frac{\partial v_r^\varepsilon}{\partial r} \frac{\partial}{\partial r} [\varphi_r r] dr dz \\ &- \mu \int_0^L \frac{\partial v_r^\varepsilon}{\partial r} (-1) \varphi_z(0) dz - \mu \int_0^R \frac{\partial v_r^\varepsilon}{\partial r} (0) \varphi_z(r) dr - \mu \int_0^L \frac{\partial v_r^\varepsilon}{\partial r} (1) \varphi_r(R) dz \\ &- \mu \int_0^R \frac{\partial v_r^\varepsilon}{\partial r} (0) \varphi_r(r) dr + \mu \int_{\Omega} \frac{\partial v_r^\varepsilon}{\partial r} \frac{\partial \varphi_r}{\partial r} r dr dz + \mu \int_{\Omega} \frac{\partial v_r^\varepsilon}{\partial r} \varphi_r dr dz \\ &= -R\mu \int_0^L \frac{\partial v_r^\varepsilon}{\partial r} \varphi_r dz + \mu \int_{\Omega} \frac{\partial v_r^\varepsilon}{\partial r} \frac{\partial \varphi_r}{\partial r} r dr dz + \mu \int_{\Omega} \frac{\partial v_r^\varepsilon}{\partial r} \varphi_r dr dz \\ - \mu \int_{\Omega} \frac{\partial^2 v_r^\varepsilon}{\partial z^2} \varphi_r r dr dz &= - \mu \int_{\partial\Omega} \frac{\partial v_r^\varepsilon}{\partial z} \varphi_r r dS_{\Omega} + \mu \int_{\Omega} \frac{\partial v_r^\varepsilon}{\partial r} \frac{\partial}{\partial z} [\varphi_r r] dr dz \\ &= - \mu \int_0^L \frac{\partial v_r^\varepsilon}{\partial z} (0) \varphi_r(0) dz - \mu \int_0^R \frac{\partial v_r^\varepsilon}{\partial z} (1) \varphi_r(r) dr \Big|_{at z=L \Rightarrow \varphi_r=0} - \mu \int_0^L \frac{\partial v_r^\varepsilon}{\partial z} (0) \varphi_r(R) dz \\ &- \mu \int_0^R \frac{\partial v_r^\varepsilon}{\partial z} (-1) \varphi_r(r) dr \Big|_{at z=0 \Rightarrow \varphi_r=0} + \mu \int_{\Omega} \frac{\partial v_r^\varepsilon}{\partial z} \frac{\partial \varphi_r}{\partial z} r dr dz \\ &= \mu \int_{\Omega} \frac{\partial v_r^\varepsilon}{\partial z} \frac{\partial \varphi_r}{\partial z} r dr dz \\ * - \mu \int_{\Omega} \frac{1}{r} \frac{\partial v_r^\varepsilon}{\partial r} \varphi_r r dr dz &= - \mu \int_{\Omega} \frac{\partial v_r^\varepsilon}{\partial r} \varphi_r dr dz \end{aligned}$$

$$* \mu \int_{\Omega} \frac{v_r^\varepsilon}{r^2} \varphi_r r dr dz = \mu \int_{\Omega} \frac{v_r^\varepsilon}{r} \varphi_r dr dz$$

$$\begin{aligned} * \int_{\Omega} \frac{\partial p^\varepsilon}{\partial r} \varphi_r r dr dz &= \int_{\partial\Omega} p^\varepsilon \varphi_r dS_\Omega - \int_{\Omega} p^\varepsilon \frac{\partial}{\partial r} [\varphi_r r] dr dz \\ &= \int_0^L p(-1) \varphi_r(0) dz + \int_0^R p(0) \varphi_r(r) dr + \int_0^L p(1) \varphi_r(R) dz + \int_0^R p(0) \varphi_r(r) dr + \int_{\Omega} p^\varepsilon \frac{\partial}{\partial r} [\varphi_r r] dr dz \\ &= R \int_0^L p \varphi_r dz - \int_{\Omega} p \frac{\partial \varphi_r}{\partial r} r dr dz - \int_{\Omega} p \varphi_r dr dz \end{aligned}$$

Now we apply similar procedure on equation (3.31), by multiplying the indicated equation by the test function φ_z and integrating over the whole domain Ω_ε .

$$\int_{\Omega} \left(\rho \frac{\partial v_z^\varepsilon}{\partial t} - \mu \left(\frac{\partial^2 v_z^\varepsilon}{\partial r^2} + \frac{\partial^2 v_z^\varepsilon}{\partial z^2} + \frac{1}{r} \frac{\partial v_z^\varepsilon}{\partial r} \right) + \frac{\partial p^\varepsilon}{\partial z} \right) \varphi_z r dr dz = 0 \quad (4.2)$$

We integrate term by term to get:

$$(\#) \int_{\Omega} \rho \frac{\partial v_z^\varepsilon}{\partial t} \varphi_z r dr dz = \rho \int_{\Omega} \frac{\partial v_z^\varepsilon}{\partial t} \varphi_z r dr dz$$

$$\begin{aligned} (\#) \int_{\Omega} \frac{\partial p^\varepsilon}{\partial z} \varphi_z r dr dz &= \int_{\partial\Omega} p^\varepsilon \varphi_z dS_\Omega - \int_{\Omega} p^\varepsilon \frac{\partial}{\partial z} [\varphi_z r] dr dz \\ &= \int_0^L p(0) \varphi_z(0) dz + \int_0^R p(1) \varphi_z(r) dr \Big|_{z=L \Rightarrow \varphi_z=A(t)} + \int_0^L p(0) \varphi_z(R) dz + \int_0^R p(-1) \varphi_z(r) dr \Big|_{z=0 \Rightarrow \varphi_z=0} \\ &\quad + \int_{\Omega} p^\varepsilon \frac{\partial}{\partial z} [\varphi_z r] dr dz \\ &= \int_0^L A(t) \varphi_z r dr - \int_{\Omega} p \frac{\partial \varphi_z}{\partial r} r dr dz \end{aligned}$$

Collect all terms of the kinds (*) and (#) of equation (4.1) and (4.2), and use equation (3.32), with the property $\text{div}(\cdot) = 0$:

$$\begin{aligned}
& \rho \int_{\Omega} \frac{\partial v_r^\varepsilon}{\partial t} \varphi_r r dr dz - R \mu \int_0^L \frac{\partial v_r^\varepsilon}{\partial r} \varphi_r dz + \mu \int_{\Omega} \frac{\partial v_r^\varepsilon}{\partial r} \frac{\partial \varphi_r}{\partial r} r dr dz + \mu \int_{\Omega} \frac{\partial v_r^\varepsilon}{\partial r} \varphi_r dr dz^{(2)} \\
& + \mu \int_{\Omega} \frac{\partial v_r^\varepsilon}{\partial z} \frac{\partial \varphi_r}{\partial z} r dr dz^{(4)} - \mu \int_{\Omega} \frac{\partial v_r^\varepsilon}{\partial r} \varphi_r dr dz^{(2)} + \mu \int_{\Omega} \frac{v_r^\varepsilon}{r} \varphi_r dr dz + R \int_0^L p \varphi_r dz - \int_{\Omega} p \frac{\partial \varphi_r}{\partial r} r dr dz^{(1)} - \int_{\Omega} p \varphi_r dr dz^{(1)} \\
& + \rho \int_{\Omega} \frac{\partial v_z^\varepsilon}{\partial t} \varphi_z r dr dz - R \mu \int_0^L \frac{\partial v_z^\varepsilon}{\partial r} \varphi_z dz^{(4)} + \mu \int_{\Omega} \frac{\partial v_z^\varepsilon}{\partial r} \frac{\partial \varphi_z}{\partial r} r dr dz^{(4)} + \mu \int_{\Omega} \frac{\partial v_z^\varepsilon}{\partial r} \varphi_z dr dz^{(3)} + \mu \int_{\Omega} \frac{\partial v_z^\varepsilon}{\partial z} \frac{\partial \varphi_z}{\partial z} r dr dz \\
& - \mu \int_{\Omega} \frac{\partial v_z^\varepsilon}{\partial r} \varphi_z dr dz^{(3)} + \int_0^L A(t) \varphi_z r dr - \int_{\Omega} p \frac{\partial \varphi_z}{\partial r} r dr dz^{(1)} = 0
\end{aligned}$$

where the subscripted term:

(1) is equal to zero by divergence of

(2) cancel each other and so do (3)

(4) vanish by definition of v_r and v_z as functions of r and z respectively.

Thus we get

$$\begin{aligned}
& \rho \int_{\Omega} \frac{\partial v_r^\varepsilon}{\partial t} \varphi_r r dr dz + \mu \int_{\Omega} \frac{\partial v_r^\varepsilon}{\partial r} \frac{\partial \varphi_r}{\partial r} r dr dz + \mu \int_{\Omega} \frac{\partial v_z^\varepsilon}{\partial z} \frac{\partial \varphi_z}{\partial z} r dr dz + \mu \int_{\Omega} \frac{v_r^\varepsilon}{r} \varphi_r dr dz \\
& + R \int_0^L \left(p - \mu \frac{\partial v_r^\varepsilon}{\partial r} \right) \varphi_r dz + \int_0^R A(t) \varphi_z r dr = 0
\end{aligned}$$

Now we use equation (3.52) and end up the variational formulation of the given problem. We

say that $(v_r^\varepsilon, v_z^\varepsilon, \eta^\varepsilon) \in V^\varepsilon$ is a weak solution of equation (3.58*) if the following variational formulation is satisfied:

$$\begin{aligned}
& \rho \int_{\Omega} \frac{\partial v_r^\varepsilon}{\partial t} \varphi_r r dr dz + 2\mu \int_{\Omega_\varepsilon} D(v^\varepsilon) : D(\varphi) r dr dz + \varepsilon R \rho_w h(\varepsilon) \frac{d^2}{dt^2} \int_0^L \eta^\varepsilon \varphi_r \Big|_{r=\varepsilon R} dz \\
& + \varepsilon R \int_0^L \{ h(\varepsilon) G(\varepsilon) \kappa(\varepsilon) \frac{\partial \eta^\varepsilon}{\partial z} \frac{\partial \varphi_r}{\partial z} + \frac{h(\varepsilon) E(\varepsilon)}{1 - \sigma^2} \frac{\eta^\varepsilon}{\varepsilon^2 R^2} \varphi_r \} \Big|_{r=\varepsilon R} dz \\
& = - \int_0^{\varepsilon R} A(t) \varphi_z \Big|_{z=L} r dr \quad \forall \varphi = \varphi_r \bar{e}_r + \varphi_z \bar{e}_z \in V^\varepsilon
\end{aligned} \tag{4.3}$$

with

$$\mathbf{v}_r^\varepsilon = \frac{\partial \eta^\varepsilon}{\partial t} \quad \text{on } \Sigma_\varepsilon \times \mathbf{R}_+ \quad (4.4)$$

$$\mathbf{v}_z^\varepsilon = 0 \quad \text{on } \Sigma_\varepsilon \times \mathbf{R}_+, \quad (4.5)$$

and initial conditions

$$\eta^\varepsilon = \frac{\partial \eta^\varepsilon}{\partial t} = 0 \quad \text{on } \Sigma_\varepsilon \times \{0\}. \quad (4.6)$$

We shall consider the pressure drop $A(t)$ across the tube's cross-section as very important. The oscillations of the membrane are due to this pressure drop. These oscillations occur at different time scale than the characteristic physical time. We shall introduce a new time scale $\tilde{t} = \omega^\varepsilon t$ (ω^ε , the characteristic frequency has dimension sec^{-1}).

This time-scale is used to accommodate elastic waves of long wavelength of frequency ω^ε due to fluid velocity which is greater than displacement velocity. We note that pressure drop is a function of \tilde{t} . A suitable choice of ω^ε is required in order to capture the elastic response of the membrane to the oscillations in the pressure drop between the inlet and the outlet boundary. Since this frequency is inversely proportional to fluid viscosity, we have

$$\omega^\varepsilon = \zeta / \mu, \quad \zeta = \text{constant}.$$

Since we consider each fixed $\varepsilon > 0$, we substitute $\zeta = \varepsilon^2$, and we have

$$\omega^\varepsilon = \frac{\varepsilon^2}{\mu} \quad (4.7)$$

This is in line with the assumption (3.47), since this characteristic frequency must adhere to the membrane's wall thickness and Young's modulus of elasticity.

4.1.2 Rescaled problem and asymptotic expansion

Our goal is to consider the FSI problem as $\varepsilon \rightarrow 0$. This would not have been before deriving the energy and *a priori* estimates for the system (Suncica *et al* (2002, 2005)). To start with,

we introduce the nondimensional independent variables $\tilde{r} = \varepsilon r$ and $\tilde{t} = \frac{\varepsilon^2}{\mu} t$, then

$$\begin{aligned}\Omega_\varepsilon &\rightarrow \Omega_1 \\ v^\varepsilon &\rightarrow v(\varepsilon) \\ v^\varepsilon &= v_r^\varepsilon \bar{e}_r + v_z^\varepsilon \bar{e}_z \rightarrow v(\varepsilon) = v(\varepsilon)_r \bar{e}_r + v(\varepsilon)_z \bar{e}_z\end{aligned}$$

Substitute the new values in equations (3.30),(3.31),(3.32) to get the following:

$$\frac{\mu}{\varepsilon^2} \frac{\partial v(\varepsilon)_r}{\partial t} - \frac{\mu}{\varepsilon^2} \left(\frac{\partial^2 v(\varepsilon)_r}{\partial r^2} + \varepsilon^2 \frac{\partial^2 v(\varepsilon)_r}{\partial z^2} + \frac{1}{r} \frac{\partial v(\varepsilon)_r}{\partial r} - \frac{v(\varepsilon)_r}{r^2} \right) + \frac{1}{\varepsilon} \frac{\partial p(\varepsilon)}{\partial r} = 0 \quad \text{in } \times\mathbf{R}_+ \quad (4.8)$$

$$\frac{\mu}{\varepsilon^2} \frac{\partial v(\varepsilon)_z}{\partial t} - \frac{\mu}{\varepsilon^2} \left(\frac{\partial^2 v(\varepsilon)_z}{\partial r^2} + \varepsilon^2 \frac{\partial^2 v(\varepsilon)_z}{\partial z^2} + \frac{1}{r} \frac{\partial v(\varepsilon)_z}{\partial r} \right) + \frac{\partial p(\varepsilon)}{\partial z} = 0 \quad \text{in } \times\mathbf{R}_+ \quad (4.9)$$

$$\frac{1}{\varepsilon} \frac{\partial v(\varepsilon)_r}{\partial r} + \frac{\partial v(\varepsilon)_z}{\partial z} + \frac{1}{\varepsilon} \frac{v(\varepsilon)_r}{r} = 0 \quad \text{in } \times\mathbf{R}_+ \quad (4.10)$$

The quantities specified on the lateral boundary Σ are invariant under the scaling, and so

$$\frac{\mu}{\varepsilon^2} v(\varepsilon)_r = \frac{\partial \eta^\varepsilon}{\partial t}, \quad \frac{\mu}{\varepsilon^2} v(\varepsilon)_z = \frac{\partial s^\varepsilon}{\partial t} = 0 \quad \text{since the axial displacement } s^\varepsilon \equiv 0.$$

The equation of radial force is

$$F_r = -\frac{h(\varepsilon)E(\varepsilon)}{1-\sigma^2} \left(\frac{\sigma}{\varepsilon R} \frac{\partial s^\varepsilon}{\partial z} + \frac{\eta^\varepsilon}{\varepsilon^2 R^2} \right) + h(\varepsilon)G(\varepsilon)\kappa \left(\varepsilon \frac{\partial^2 \eta^\varepsilon}{\partial z^2} \right) - \rho_\omega h(\varepsilon) \frac{\varepsilon^4}{\mu^2} \frac{\partial^2 \eta^\varepsilon}{\partial t^2} \quad (4.11)$$

In the sense of the continuity equations and the lateral boundary conditions we get

$$\begin{aligned}v(\varepsilon)_r &= \frac{\varepsilon^2}{\mu} \frac{\partial \eta^\varepsilon}{\partial t}, \\ &\text{on } \times\mathbf{R}_+ \quad (4.12)\end{aligned}$$

$$v(\varepsilon)_z = 0 \quad (4.13)$$

$$-F_r = p(\varepsilon) - 2\mu \frac{\partial v(\varepsilon)_r}{\partial r} \quad \text{on } \times\mathbb{R}_+ \quad (4.14)$$

If $\varphi = \varphi_r \bar{e}_r + \varphi_z \bar{e}_z$ then

$$D_\varepsilon(\varphi) = \begin{pmatrix} \frac{\partial \varphi_r}{\partial r} & 0 & \frac{1}{2} \left(\frac{\partial \varphi_r}{\partial z} + \frac{\partial \varphi_z}{\partial r} \right) \\ 0 & \frac{\varphi_r}{r} & 0 \\ \frac{1}{2} \left(\frac{\partial \varphi_r}{\partial z} + \frac{\partial \varphi_z}{\partial r} \right) & 0 & \frac{\partial \varphi_z}{\partial z} \end{pmatrix}$$

The initial condition reads:

$$\eta^\varepsilon = \frac{\partial \eta^\varepsilon}{\partial t} = 0 \quad \text{on } \times\{0\} \quad (4.15)$$

with the boundary data:

$$v(\varepsilon)_r = 0 \quad \text{and} \quad p(\varepsilon) = 0 \quad \text{on} \quad (\partial\Omega \cap \{z=0\}) \times \mathbb{R}_+ \quad (4.16)$$

$$v(\varepsilon)_r = 0 \quad \text{and} \quad p(\varepsilon) = A(t) \quad \text{on} \quad (\partial\Omega \cap \{z=L\}) \times \mathbb{R}_+ \quad (4.17)$$

$$\eta^\varepsilon = 0 \quad \text{for} \quad z=0, \quad \eta^\varepsilon = 0 \quad \text{for} \quad z=L \quad \text{and} \quad \forall t \in \mathbb{R}_+ \quad (4.18)$$

4.1.3 Weak Formulation

Let V^\boxplus be a test function space and let V be a solution space. We define as follows:

Definition 4.3 The space $V^\boxplus \subset H^1(\Omega_\varepsilon)^3$ consists of axially symmetric functions φ such that $\varphi_r|_\Sigma, \varphi_z|_\Sigma \in H^1(0,L)$, $\varphi_r(0,r) = \varphi_r(L,r) = 0$, $\varphi_z(L,R) = 0$ for $r \leq R$ and $\text{div} \varphi = 0$ in Ω

Definition 4.4 The space V^\boxtimes consists of all functions $(w_r, w_z, d_r, d_z) \in H^1((0,T); V^\boxplus) \times (H^1((0,L) \times (0,T))^2 \cap H^2((0,T); L^2(0,L))^2)$ such that

$$1. \quad \frac{1}{\varepsilon} \frac{\partial w_r}{\partial r} + \frac{\partial w_z}{\partial z} + \frac{1}{\varepsilon} \frac{w_r}{r} = 0 \quad \text{in} \quad \times\mathbb{R}_+$$

$$2. \quad (r)^{-1} w_r \in L^2((0,T) \times \Omega)$$

$$3. d_r(t,0) = d_z(t,L) = d_r(t,L) = 0 \text{ on } R_+$$

$$4. w_r = 0 \text{ on } (\partial\Omega \cap \{z=0\}) \times R_+$$

$$5. w_r = 0 \text{ on } (\partial\Omega \cap \{z=L\}) \times R_+$$

$$6. w_r = \frac{\varepsilon^2}{\mu} \frac{\partial d_r}{\partial t} \text{ and } w_z = \frac{\varepsilon^2}{\mu} \frac{\partial d_z}{\partial t} \text{ on } \Sigma_\varepsilon \times R_+.$$

We rewrite the variational formulation (equation (4.3)) in rescaled variables; by multiplying it by $\Psi(t)$ and upon integrating on $\Omega \times (0, T)$ we get the variational formulation of the rescaled problem

$$\begin{aligned} & \frac{\rho \varepsilon^2}{\mu} \int_0^T \int_0^L \int_0^R \frac{\partial v(\varepsilon)}{\partial t} \varphi(r, z) \psi(t) r dr dz dt + 2\mu \int_0^T \int_0^L \int_0^R \{D_\varepsilon(v(\varepsilon)) : D_\varepsilon(\varphi(r, z))\} \psi(t) r dr dz dt \\ & + R \int_0^T \int_0^L \left\{ h(\varepsilon) G(\varepsilon) \kappa(\varepsilon) \frac{\partial \eta^\varepsilon}{\partial z} \frac{\partial \varphi_r}{\partial z} + \frac{h(\varepsilon) E(\varepsilon)}{1 - \sigma^2} \frac{\eta^\varepsilon}{\varepsilon^2 R^2} \varphi_r \right\} \Big|_{r=R} \varphi(t) dz dt \\ & + R \rho_\omega h(\varepsilon) \frac{\varepsilon^4}{\mu^2} \int_0^T \frac{d^2 \psi(t)}{dt^2} \left(\int_0^L \eta^\varepsilon \varphi_r \Big|_{r=R} dz \right) dt \\ & = - \int_0^T \int_0^R A(t) \varphi_z r dr dt \end{aligned} \tag{4.19}$$

4.1.4 Energy estimates after rescaling

In order to determine the asymptotic expansions we need the energy estimate of the rescaled problem just like we needed for the whole problem. For the radial velocity we employ the estimate by Suncica *et al* (2005):

$$\left(\left\| \frac{1}{\varepsilon} \frac{v(\varepsilon)_r}{r} \right\| + \left\| \frac{1}{\varepsilon} \frac{\partial v(\varepsilon)_r}{\partial r} \right\| + \left\| \frac{\partial v(\varepsilon)_z}{\partial z} \right\| \right)_{L^2(\Omega \times (0, T))} \leq C \frac{\varepsilon^2}{\mu} \|A\|_v, \tag{4.20}$$

which is the only equation that estimates $v(\varepsilon)_r$ and thus $v(\varepsilon)_r$ satisfies

$$\|v(\varepsilon)_r\|_{L^2(\Omega \times (0,T))} \leq C \frac{\varepsilon^3}{\mu} \|A\|_v$$

The following lemma shall supply important estimates that will be used in getting the reduced equations:

Lemma 1: The solution $(v(\mathbb{Q})_r, v(\mathbb{Q})_z, p(\mathbb{Q}), \mathbb{Q}^{\mathbb{Q}})$ of the rescaled problem satisfies the following estimates

$$\|v(\varepsilon)_r\|_{L^2(\Omega \times (0,T))} \leq C \frac{\varepsilon^3}{\mu} \|A\|_v \quad (4.21)$$

$$\|v(\varepsilon)_z\|_{L^2(\Omega \times (0,T))} \leq C \frac{\varepsilon^2}{\mu} \|A\|_v \quad (4.22)$$

$$\|v(\varepsilon)_r\|_{L^2(\Omega \times (0,T))} \leq C \frac{\varepsilon^2}{\mu} \|A\|_v \quad (4.23)$$

$$\|p(\varepsilon)\|_{L^2(\Omega \times (0,T))} \leq C \|A\|_v \quad (4.24)$$

$$\|v(\varepsilon)_r\|_{L^2(\Omega \times (0,T))} \leq C \varepsilon \|A\|_v \quad (4.25)$$

4.1.5 Asymptotic Expansions

Now we have uniform estimates for $(v(\mathbb{Q})_r, v(\mathbb{Q})_z, p(\mathbb{Q}), \mathbb{Q}^{\mathbb{Q}})$, which are valid for their time derivatives. We represent this vector by $\mathbf{X}^\varepsilon = (v(\mathbb{Q})_r, v(\mathbb{Q})_z, p(\mathbb{Q}), \mathbb{Q}^{\mathbb{Q}})$. We define the asymptotic expansion for \mathbf{X}^ε .

Asymptotic Expansion I

$$v(z, r, t; \varepsilon) = \frac{\varepsilon^2}{\mu} \sum_{i \geq 0} \varepsilon^i v^i(z, r, t) \quad (4.26)$$

$$p(z, r, t; \varepsilon) = \sum_{i \geq 0} \varepsilon^i p^i(z, r, t) \quad (4.27)$$

$$\eta^\varepsilon(z, t) = \varepsilon \sum_{i \geq 0} \varepsilon^i \eta^i(z, t) \quad (4.28)$$

We also have the following:

Asymptotic Expansion II

$$v_r(z, r, t; \varepsilon) = \frac{\varepsilon^3}{\mu} \sum_{i \geq 0} \varepsilon^i v^i(z, r, t) \quad (4.29)$$

$$v_z(z, r, t; \varepsilon) = \frac{\varepsilon^2}{\mu} \sum_{i \geq 0} \varepsilon^i v^i(z, r, t) \quad (4.30)$$

$$p(z, r, t; \varepsilon) = \sum_{i \geq 0} \varepsilon^i p^i(z, r, t) \quad (4.31)$$

$$\eta^\varepsilon(z, t) = \varepsilon \sum_{i \geq 0} \varepsilon^i \eta^i(z, t) \quad (4.32)$$

4.1.6 Justification of asymptotic expansion

Analytic solutions of PDEs of the type under review are, in most cases, nowhere near. In cases that are not amenable to exact solutions, such as the present case, it becomes plausible to seek solutions that approximate the exact solutions. We had conceived of the use of numerical method in solving the problem before us. It would hold well for an approximate solution. In the present case, however, it seems unattractive because of the following reasons:

- There is relative difficulty in the interpretation of solutions; there is incessant varying of parameters to get a clear understanding.
- Difficulties with precision, singularities, stability makes the behavior of numerical method pathological.
- Checking of results will be worrisome.
- The physiological analysis may not be evident from the numerical solution.

When the governing equation is nonlinear and general techniques are not available for exact solution, the asymptotic expansion method becomes attractive. Although asymptotic expansion method is also fraught with the problem of accuracy of solution, we saw it a better option due to the following considerations:

- It does not presuppose convergence of the series involving the parameter of interest; asymptotic series, even when divergent, are practically useful in obtaining good solutions (Subramanian, 2014; see also: www.phys.vt.edu/~ersharpe/spec-fn/app-d.pdf).
- The terms of an asymptotic series usually decrease rapidly at first for sufficiently small parameter ε , say.
- When numerical method gets wobbling, asymptotic approximations may be used as a cushion (See Moshe and Marius (1982)).

To reassure the choice of the method, the problem of accuracy is mitigated by obtaining the energy estimations of the desired variables, as required in the asymptotic expansion. The above was employed in this work. The predilection for the asymptotic approximation method is its readiness to dispense with the stability and convergence – attributes which constitute the hallmark of numerical method.

The next step is to use the expansions **I** and **II** to obtain the reduced equations, and eventually to derive the equation that satisfies pressure.

4.1.7 Reduced problem using Expansion I

We revisit equations (4.8)-(4.10). By using the expansions (4.26) and (4.27) in equation (4.8) we get

$$\begin{aligned}
& \frac{\mu}{\varepsilon^2} \left[\rho \frac{\varepsilon^2}{\mu} \left(\frac{\partial v_r^0}{\partial t} + \varepsilon \frac{\partial v_r^1}{\partial t} + \varepsilon^2 \frac{\partial v_r^2}{\partial t} + \dots \right) - \frac{\varepsilon^2}{\mu} \left(\frac{\partial^2 v_r^0}{\partial r^2} + \varepsilon \frac{\partial^2 v_r^1}{\partial r^2} + \varepsilon^2 \frac{\partial^2 v_r^2}{\partial r^2} + \dots \right) \right. \\
& \quad \left. - \varepsilon^2 \cdot \frac{\varepsilon^2}{\mu} \left(\frac{\partial^2 v_r^0}{\partial z^2} + \varepsilon \frac{\partial^2 v_r^1}{\partial z^2} + \varepsilon^2 \frac{\partial^2 v_r^2}{\partial z^2} + \dots \right) - \frac{1}{r} \frac{\varepsilon^2}{\mu} \left(\frac{\partial v_r^0}{\partial r} + \varepsilon \frac{\partial v_r^1}{\partial r} + \varepsilon^2 \frac{\partial v_r^2}{\partial r} + \dots \right) \right. \\
& \quad \left. + \frac{1}{r^2} \cdot \frac{\varepsilon^2}{\mu} (v_r^0 + \varepsilon v_r^1 + \varepsilon^2 v_r^2 + \dots) \right] + \frac{1}{\varepsilon} \left(\frac{\partial p^0}{\partial r} + \varepsilon \frac{\partial p^1}{\partial r} + \varepsilon^2 \frac{\partial p^2}{\partial r} + \dots \right) = 0
\end{aligned}$$

Collect the powers of

$$\varepsilon^{-1} : \frac{\partial p^0}{\partial r} = 0 \quad (4.33)$$

$$\varepsilon^0 : \rho \frac{\partial v_r^0}{\partial t} - \left(\frac{\partial^2 v_r^0}{\partial r^2} + \frac{1}{r} \frac{\partial v_r^0}{\partial r} - \frac{1}{r^2} v_r^0 \right) + \frac{\partial p^1}{\partial r} = 0 \quad (4.34)$$

$$\varepsilon^1 : \rho \frac{\partial v_r^1}{\partial t} - \left(\frac{\partial^2 v_r^1}{\partial r^2} + \frac{1}{r} \frac{\partial v_r^1}{\partial r} - \frac{1}{r^2} v_r^1 \right) + \frac{\partial p^2}{\partial r} = 0 \quad (4.35)$$

$$\varepsilon^2 : \rho \frac{\partial v_r^2}{\partial t} - \left(\frac{\partial^2 v_r^2}{\partial r^2} + \frac{1}{r} \frac{\partial v_r^2}{\partial r} + \frac{\partial^2 v_r^0}{\partial r^2} - \frac{1}{r^2} v_r^2 \right) + \frac{\partial p^3}{\partial r} = 0 \quad (4.36)$$

Plug in (4.26) and (4.27) in equation (4.9) to get the following:

$$\begin{aligned}
& \frac{\mu}{\varepsilon^2} \left[\rho \frac{\varepsilon^2}{\mu} \left(\frac{\partial v_z^0}{\partial t} + \varepsilon \frac{\partial v_z^1}{\partial t} + \varepsilon^2 \frac{\partial v_z^2}{\partial t} + \dots \right) - \frac{\varepsilon^2}{\mu} \left(\frac{\partial^2 v_z^0}{\partial r^2} + \varepsilon \frac{\partial^2 v_z^1}{\partial r^2} + \varepsilon^2 \frac{\partial^2 v_z^2}{\partial r^2} + \dots \right) \right. \\
& \quad \left. - \varepsilon^2 \cdot \frac{\varepsilon^2}{\mu} \left(\frac{\partial^2 v_z^0}{\partial z^2} + \varepsilon \frac{\partial^2 v_z^1}{\partial z^2} + \varepsilon^2 \frac{\partial^2 v_z^2}{\partial z^2} + \dots \right) - \frac{1}{r} \frac{\varepsilon^2}{\mu} \left(\frac{\partial v_z^0}{\partial r} + \varepsilon \frac{\partial v_z^1}{\partial r} + \varepsilon^2 \frac{\partial v_z^2}{\partial r} + \dots \right) \right. \\
& \quad \left. + \left(\frac{\partial p^0}{\partial z} + \varepsilon \frac{\partial p^1}{\partial z} + \varepsilon^2 \frac{\partial p^2}{\partial z} + \dots \right) \right] = 0.
\end{aligned}$$

Collect the terms of the powers of to get the following:

$$\varepsilon^0 : \rho \frac{\partial v_z^0}{\partial t} - \left(\frac{\partial^2 v_z^0}{\partial r^2} + \frac{1}{r} \frac{\partial v_z^0}{\partial r} \right) + \frac{\partial p^0}{\partial z} = 0 \quad (4.37)$$

$$\varepsilon^1 : \rho \frac{\partial v_z^1}{\partial t} - \left(\frac{\partial^2 v_z^1}{\partial r^2} + \frac{1}{r} \frac{\partial v_z^1}{\partial r} \right) + \frac{\partial p^1}{\partial z} = 0 \quad (4.38)$$

$$\varepsilon^2 : \rho \frac{\partial v_z^2}{\partial t} - \left(\frac{\partial^2 v_z^2}{\partial r^2} + \frac{1}{r} \frac{\partial v_z^2}{\partial r} + \frac{\partial^2 v_z^0}{\partial r^2} \right) + \frac{\partial p^2}{\partial z} = 0 \quad (4.39)$$

We now insert the expansion of $v(\varepsilon)$ in the divergence equation, which yields

$$\begin{aligned} & \frac{\varepsilon^2}{\mu} \left(\frac{\partial v_r^0}{\partial r} + \varepsilon \frac{\partial v_r^1}{\partial r} + \varepsilon^2 \frac{\partial v_r^2}{\partial r} + \dots \right) + \frac{\varepsilon^2}{\mu} \cdot \varepsilon \left(\frac{\partial v_z^0}{\partial z} + \varepsilon \frac{\partial v_z^1}{\partial z} + \varepsilon^2 \frac{\partial v_z^2}{\partial z} + \dots \right) \\ & + \frac{\varepsilon^2}{\mu} \cdot \frac{1}{r} (v_r^0 + \varepsilon v_r^1 + \varepsilon^2 v_r^2 + \dots) = 0 \end{aligned}$$

Collecting the terms of same order we get

$$\varepsilon^0 : \frac{\partial v_r^0}{\partial r} + \frac{1}{r} v_r^0 = 0 \quad (4.40)$$

$$\varepsilon^1 : \frac{\partial v_r^1}{\partial r} + \frac{1}{r} v_r^1 + \frac{\partial v_z^0}{\partial z} = 0 \quad (4.41)$$

$$\varepsilon^2 : \frac{\partial v_r^2}{\partial r} + \frac{1}{r} v_r^2 + \frac{\partial v_z^1}{\partial z} = 0 \quad (4.42)$$

Observe from equation (4.33) that p^0 is independent of r . Use equation (4.40)

$$\frac{\partial v_r^0}{\partial r} + \frac{1}{r} v_r^0 = 0 \Rightarrow \frac{1}{r} \frac{\partial}{\partial r} (r v_r^0) = 0$$

We deduce that v_r^0 is constant, then $v_r^0 = 0$ according to the physical approach of the problem. As we would expect, in the coupled fluid-structure interaction problem for creeping flow, the radial component of velocity is by one order of magnitude smaller than the axial

component. Return to (4.34) and substitute $v_r^0 = 0$ to get $\frac{\partial^2 v_r^0}{\partial z^2} = 0$ in equation (4.36).

Let $p = p^0 + \varepsilon p^1$ and $v_r = v_r^1 + \varepsilon v_r^2$. Combine (4.35) and (4.36) to get

$$\rho \frac{\partial v_r}{\partial t} - \left(\frac{\partial^2 v_r}{\partial r^2} + \frac{1}{r} \frac{\partial v_r}{\partial r} - \frac{1}{r^2} v_r \right) + \frac{\partial p^2}{\partial r} + \frac{\partial p^3}{\partial r} = 0 \quad (4.43)$$

Similarly for $v_z = v_z^0 + \varepsilon v_z^1$ we simplify (4.37) and (4.38) as

$$\rho \frac{\partial v_z}{\partial t} - \left(\frac{\partial^2 v_z}{\partial r^2} + \frac{1}{r} \frac{\partial v_z}{\partial r} \right) + \frac{\partial p}{\partial r} = 0 \quad (4.44)$$

Add (4.41) to ε (4.42) to get

$$\frac{\partial}{\partial r}(r v_r) + \frac{\partial}{\partial z}(r v_z) = 0 \quad (4.45)$$

We therefore summarize the first expansion as: find v_r, v_z and p such that the following is satisfied:

$$\begin{cases} \rho \frac{\partial v_z}{\partial t} - \left(\frac{\partial^2 v_z}{\partial r^2} + \frac{1}{r} \frac{\partial v_z}{\partial r} \right) + \frac{\partial p}{\partial z} = 0 \\ \frac{\partial}{\partial r}(r v_r) + \frac{\partial}{\partial z}(r v_z) = 0 \end{cases} \quad (4.46)$$

4.1.8. Reduced problem using Expansion II

We shall employ the equations (4.29)-(4.31). In a way similar to the method in expansion I, substitute $v_r(z, r, t; \varepsilon)$ in equation (4.8) to get

$$\begin{aligned} & \frac{\mu}{\varepsilon^2} \left[\rho \frac{\varepsilon^2}{\mu} \left(\frac{\partial v_r^0}{\partial t} + \varepsilon \frac{\partial v_r^1}{\partial t} + \varepsilon^2 \frac{\partial v_r^2}{\partial t} + \dots \right) - \frac{\varepsilon^2}{\mu} \left(\frac{\partial^2 v_r^0}{\partial r^2} + \varepsilon \frac{\partial^2 v_r^1}{\partial r^2} + \varepsilon^2 \frac{\partial^2 v_r^2}{\partial r^2} + \dots \right) \right. \\ & \quad \left. - \varepsilon^2 \cdot \frac{\varepsilon^2}{\mu} \left(\frac{\partial^2 v_r^0}{\partial z^2} + \varepsilon \frac{\partial^2 v_r^1}{\partial z^2} + \varepsilon^2 \frac{\partial^2 v_r^2}{\partial z^2} + \dots \right) - \frac{1}{r} \frac{\varepsilon^2}{\mu} \left(\frac{\partial v_r^0}{\partial r} + \varepsilon \frac{\partial v_r^1}{\partial r} + \varepsilon^2 \frac{\partial v_r^2}{\partial r} + \dots \right) \right. \\ & \quad \left. + \frac{1}{r^2} \cdot \frac{\varepsilon^2}{\mu} (v_r^0 + \varepsilon v_r^1 + \varepsilon^2 v_r^2 + \dots) \right] + \frac{1}{\varepsilon} \left(\frac{\partial p^0}{\partial r} + \varepsilon \frac{\partial p^1}{\partial r} + \varepsilon^2 \frac{\partial p^2}{\partial r} + \dots \right) = 0 \end{aligned}$$

Collecting the terms of the same order of ε yields

$$\begin{aligned} \varepsilon^{-1} : \quad & \frac{\partial p^0}{\partial r} = 0 \\ \varepsilon^0 : \quad & \frac{\partial p^1}{\partial r} = 0 \end{aligned} \quad (4.47)$$

$$\varepsilon^1 : \rho \frac{\partial v_r^0}{\partial t} - \left(\frac{\partial^2 v_r^0}{\partial r^2} + \frac{1}{r} \frac{\partial v_r^0}{\partial r} - \frac{1}{r^2} v_r^0 \right) + \frac{\partial p^2}{\partial r} = 0 \quad (4.48)$$

$$\varepsilon^2 : \rho \frac{\partial v_r^1}{\partial t} - \left(\frac{\partial^2 v_r^1}{\partial r^2} + \frac{1}{r} \frac{\partial v_r^1}{\partial r} - \frac{1}{r^2} v_r^1 \right) + \frac{\partial p^3}{\partial r} = 0 \quad (4.49)$$

Put the expansion of $v_r(z,r,t;\varepsilon)$ in equation (4.9) to get

$$\begin{aligned} & \frac{\mu}{\varepsilon^2} \left[\rho \frac{\varepsilon^2}{\mu} \left(\frac{\partial v_z^0}{\partial t} + \varepsilon \frac{\partial v_z^1}{\partial t} + \varepsilon^2 \frac{\partial v_z^2}{\partial t} + \dots \right) - \frac{\varepsilon^2}{\mu} \left(\frac{\partial^2 v_z^0}{\partial r^2} + \varepsilon \frac{\partial^2 v_z^1}{\partial r^2} + \varepsilon^2 \frac{\partial^2 v_z^2}{\partial r^2} + \dots \right) \right. \\ & \quad \left. - \varepsilon^2 \cdot \frac{\varepsilon^2}{\mu} \left(\frac{\partial^2 v_z^0}{\partial z^2} + \varepsilon \frac{\partial^2 v_z^1}{\partial z^2} + \varepsilon^2 \frac{\partial^2 v_z^2}{\partial z^2} + \dots \right) - \frac{1}{r} \frac{\varepsilon^2}{\mu} \left(\frac{\partial v_z^0}{\partial r} + \varepsilon \frac{\partial v_z^1}{\partial r} + \varepsilon^2 \frac{\partial v_z^2}{\partial r} + \dots \right) \right. \\ & \quad \left. + \left(\frac{\partial p^0}{\partial z} + \varepsilon \frac{\partial p^1}{\partial z} + \varepsilon^2 \frac{\partial p^2}{\partial z} + \dots \right) \right] = 0. \end{aligned}$$

Collecting powers of ε :

$$\varepsilon^0 : \rho \frac{\partial v_z^0}{\partial t} - \left(\frac{\partial^2 v_z^0}{\partial r^2} + \frac{1}{r} \frac{\partial v_z^0}{\partial r} \right) + \frac{\partial p^0}{\partial z} = 0 \quad (4.50)$$

$$\varepsilon^1 : \rho \frac{\partial v_z^1}{\partial t} - \left(\frac{\partial^2 v_z^1}{\partial r^2} + \frac{1}{r} \frac{\partial v_z^1}{\partial r} \right) + \frac{\partial p^1}{\partial z} = 0 \quad (4.51)$$

$$\varepsilon^2 : \rho \frac{\partial v_z^2}{\partial t} - \left(\frac{\partial^2 v_z^2}{\partial r^2} + \frac{1}{r} \frac{\partial v_z^2}{\partial r} + \frac{\partial^2 v_z^0}{\partial r^2} \right) + \frac{\partial p^2}{\partial z} = 0 \quad (4.52)$$

Finally we have the divergence equation similar to the one obtained previously

$$\begin{aligned} & \frac{\varepsilon^2}{\mu} \left(\frac{\partial v_r^0}{\partial r} + \varepsilon \frac{\partial v_r^1}{\partial r} + \varepsilon^2 \frac{\partial v_r^2}{\partial r} + \dots \right) + \frac{\varepsilon^2}{\mu} \cdot \varepsilon \left(\frac{\partial v_z^0}{\partial z} + \varepsilon \frac{\partial v_z^1}{\partial z} + \varepsilon^2 \frac{\partial v_z^2}{\partial z} + \dots \right) \\ & \quad + \frac{\varepsilon^2}{\mu} \cdot \frac{1}{r} (v_r^0 + \varepsilon v_r^1 + \varepsilon^2 v_r^2 + \dots) = 0 \end{aligned}$$

Collect terms

$$\varepsilon^0 : \frac{\partial v_r^0}{\partial r} + \frac{1}{r} v_r^0 = 0$$

$$\begin{aligned}\varepsilon^1 : \frac{\partial v_r^1}{\partial r} + \frac{1}{r} v_r^1 + \frac{\partial v_z^0}{\partial z} &= 0 \\ \varepsilon^2 : \frac{\partial v_r^2}{\partial r} + \frac{1}{r} v_r^2 + \frac{\partial v_z^1}{\partial z} &= 0\end{aligned}$$

We note again that $p^0 = p^0(z, t)$ and $p^1 = p^1(z, t)$. From (4.50 and (4.51)

$$\begin{aligned}\rho \frac{\partial v_z}{\partial t} + \frac{\partial p}{\partial z} &= \frac{\partial^2 v_z^0}{\partial r^2} + \frac{\partial^2 v_z^1}{\partial r^2} + \frac{1}{r} \frac{\partial v_z^0}{\partial r} + \frac{1}{r} \frac{\partial v_z^1}{\partial r} \\ &= \frac{\partial^2 v_z}{\partial r^2} + \frac{1}{r} \frac{\partial v_z}{\partial r} \\ &= \frac{1}{r} \frac{\partial}{\partial r} \left(r \frac{\partial v_z}{\partial r} \right)\end{aligned}$$

Hence

$$\rho \frac{\partial v_z}{\partial t} - \frac{1}{r} \frac{\partial}{\partial r} \left(r \frac{\partial v_z}{\partial r} \right) + \frac{\partial p}{\partial z} = 0 \quad (4.53)$$

We have, as in expansion I

$$\frac{\partial}{\partial r} (r v_r) + \frac{\partial}{\partial z} (r v_z) = 0$$

We now collect the important equations:

$$\begin{cases} \rho \frac{\partial v_z}{\partial t} - \left(\frac{\partial^2 v_z}{\partial r^2} + \frac{1}{r} \frac{\partial v_z}{\partial r} \right) + \frac{\partial p}{\partial z} = 0 \\ \frac{\partial}{\partial r} (r v_r) + \frac{\partial}{\partial z} (r v_z) = 0 \end{cases}$$

The above is the same result as in expansion (I). Let $\eta = \eta^0 + \varepsilon \eta^1$. Plug (4.29) (4.30) and (4.31) into (3.46) and (4.14) to get

$$\begin{aligned}F_r &= \frac{-h(\varepsilon)E(\varepsilon)}{(1-\sigma^2)\varepsilon R^2} (\eta^0 + \varepsilon \eta^1 + \dots) + h(\varepsilon)G(\varepsilon)\kappa(\varepsilon)\varepsilon \frac{\partial^2}{\partial z^2} (\eta^0 + \varepsilon \eta^1 + \dots) - \rho_w h(\varepsilon) \frac{\varepsilon^4}{\mu^2} \varepsilon \frac{\partial^2}{\partial t^2} (\eta^0 + \varepsilon \eta^1 + \dots) \\ F_r &= -(p^0 + \varepsilon p^1 + \dots) + 2\mu \frac{1}{\varepsilon} \frac{\partial}{\partial r} \left(\frac{\varepsilon^2}{\mu^2} (\varepsilon v_r^1 + \varepsilon^2 v_r^2 + \dots) \right)\end{aligned}$$

Apply the assumptions (3.48) and (3.49), and as 0 with $p = p^0 + \varepsilon p^1$ and $\eta = \eta^0 + \varepsilon \eta^1$ to get

$$F_r = \frac{-E_0}{(1-\sigma^2)R^2} \eta + G_0 \frac{\partial^2}{\partial z} \eta$$

$$F_r = -p$$

Hence

$$p(z, t) = \frac{E_0}{R^2(1-\sigma^2)} \eta - G_0 \frac{\partial^2 \eta}{\partial z^2} + O(\varepsilon^2) \quad (4.54)$$

The equation (4.54) is the effective pressure. We now consider a situation when the coefficient containing shear modulus is negligible. Then

$$p = \frac{E_0}{R^2(1-\sigma^2)} \eta \quad (4.55)$$

We note that

$$p(0, t) = 0, p(L, t) = A(t)$$

$$p(z, 0) = 0 \text{ in } (0, L)$$

From Laplace's law (see Olufsen *et al* (1999)) the quantity η satisfies,

$$\eta \equiv \frac{R-r}{R} = \left(1 - \frac{r}{R}\right)$$

Since $A(t) = \pi r^2$, we get $r = \sqrt{A(t)/\pi}$ and thus $R = \sqrt{A/\pi}$. Hence

$$p = \frac{E_0}{R^2(1-\sigma^2)} \left(1 - \frac{r}{R}\right)$$

On assumption of material incompressibility, we have $\sigma = 1/2$ (Olufsen (1998), Quarteroni *et al* (2000)). Hence,

$$p = \frac{4E_0}{3R^2} \eta = \frac{4E_0}{3R} \left(1 - \sqrt{\frac{A(t)}{A}} + O\left(\frac{\eta}{R}\right)\right) \quad (4.56)$$

where $A = A(x, t)$ denotes the cross-sectional area at (t, x) and $A(0)$ is the undisturbed cross-sectional area at x , which corresponds to the zero pressure. The above is the pressure equation we have sought. We note that if $A \in C_0^\infty(0, +\infty)$, then $p \in C_0^\infty([0, L] \times [0, T])$. This expression for pressure holds good when the shear modulus is negligible. When it is non-negligible, an initial boundary-value problem may be developed, whose solution is outside the scope of this work.

4.2.0 Nonlinear arterial pulse model

Our goal here is to introduce a model which consists of the sum of a nonlinear superposition of forward solitary waves and a two-element windkessel model. In the first place, we shall present an asymptotic expansion of a quasi one-dimensional model of pressure and flow. We note that for small time and small space scales, boundary layer appears and the windkessel model no longer holds. The conception of boundary layer with a correction of motion of the fluid that a KdV equation satisfies represents the wave phenomena in a rather fast fashion when compared to the windkessel effect.

With our assumption of an elastic artery and incompressible fluid flow, we have the governing Navier-Stokes equations (Crepeau and Sorine (2006)),

$$A_T + Q_Z = 0 \quad (4.57)$$

$$Q_T + \left(\frac{Q^2}{A} \right) + \frac{A}{\rho} P_Z + \nu \frac{Q}{A} = 0 \quad (4.58)$$

where $A(T, Z) = \pi R^2(T, Z)$ is the cross-sectional area of the vessel, $Q(T, Z)$ is the blood flow volume and $P(T, Z)$ is the blood pressure, T and Z being temporal and spatial dimensions respectively; ρ is the blood density, ν is a coefficient of the blood viscosity, and the quantities A_T , P_Z and Q_Z are gradients associated with their respective subscripts. So long as

boundary layer effects are notable, it is imperative that viscosity effect be considered. The works of Wen-Shan *et al* (1997), Fu and ILøchev (2010) considered the fluid as inviscid. The former contended that viscous effects are confined mainly to the boundary layers whose thickness is much less than the vessel radius. It should, however, be borne in mind that fluids undergo internal friction, especially when a fast-moving layer flows past a slow-moving layer.

The motion of the arterial wall satisfies (Yomosa, 1987),

$$\frac{\alpha_w h_o R_o}{A_o} A_{TT} = (P - P_e) - \frac{h_o}{R_o} \sigma_s, \quad (4.59)$$

where α_w is the wall density, P_e is the pressure outside the tube, h_o is the mean thickness of the wall, R_o is the mean radius and σ_s is the extending stress in the tangential direction.

Since A_{TT} is small, $\frac{\alpha_w h_o R_o}{A_o} A_{TT}$ is neglected. Since the wall is elastic, the local compliance of

the vessel is such th

$$\sigma_s = \frac{E \Delta A}{2 A_o} \quad (4.60)$$

where $\Delta A = A - A_o$, where A_o is the cross-sectional area at rest, and E is the coefficient of elasticity. We rewrite the system (4.57) – (4.60) in non-dimensional variables. Let

$$Z = lz, \quad T = \frac{l}{c_o} t \quad (4.61)$$

where l is a typical wavelength of the wave propagated in the tube, c_o is defined as usual. Let

the ratio $\varepsilon = \left(\frac{R_o}{L}\right)^{2/5} \ll 1$ ((Suncica *et al*, (2005))). We rescale pressure, flow and cross-

sectional area thus:

$$P - P_o = \rho c_o^2 p, \quad Q = A_o c_o q, \quad A = A_o(l + a), \quad (4.62)$$

where A_o and P_o denote the constant cross-sectional area and the pressure at rest, ($P_o = P_e$, the external pressure), $Q_o = 0$. We get

$$a_t + q_z = 0 \quad (4.63)$$

$$q_t + \left(\frac{q^2}{1+a} \right)_z + (1+a)p_z = \frac{-v}{A_0 c_0} \frac{q}{1+a} \quad (4.64)$$

$$\frac{\alpha_w h_o R_o}{\rho l^2} a_{tt} + a = p \quad (4.65)$$

By hypothesis,

$$\frac{\alpha_w h_o R_o}{\rho l^2} = \frac{\alpha_w}{\rho} \frac{h_o}{R_o} \frac{R_o^2}{l^2} = 0(\varepsilon^5) = \alpha^5. \quad (4.66)$$

Thus,

$$a_t + q_z = 0 \quad (4.67)$$

$$q_t + \left(\frac{q^2}{1+a} \right)_z + (1+a)p_z = -\wp \frac{q}{1+a}, \quad (4.68)$$

$$(where \wp = \frac{v}{A_0 c_0})$$

$$\alpha \varepsilon^5 a_{tt} + a = p \quad (4.69)$$

We express the solutions as an asymptotic expansion in terms of ε , thus

$$\left. \begin{aligned} a(t, z) &= \sum_{k \geq 1} \varepsilon^k a^k \left(\frac{t-z}{\varepsilon^2}, \frac{z}{\varepsilon}, t, z \right) \\ p(t, z) &= \sum_{k \geq 1} \varepsilon^k p^k \left(\frac{t-z}{\varepsilon^2}, \frac{z}{\varepsilon}, t, z \right) \\ q(t, z) &= \sum_{k \geq 1} \varepsilon^k q^k \left(\frac{t-z}{\varepsilon^2}, \frac{z}{\varepsilon}, t, z \right) \end{aligned} \right\} \quad (4.70)$$

We perform some change of variable as follows:

$$\tau_1 = \frac{t-z}{\varepsilon^2}, \eta_1 = \frac{z}{\varepsilon}, \tau_2 = t, \eta_2 = z \quad (4.71)$$

In the case above, we are considering forward-moving (left to right) wave. The equations

(4.70) and (4.71) become, at the second order of ε

$$\varepsilon \left[a_{\tau_1}^1 - q_{\tau_1}^1 \right] + \varepsilon^2 \left[a_{\tau_1}^1 + q_{\eta_1}^1 - q_{\tau_1}^2 \right] = 0 \quad (4.72)$$

$$\varepsilon \left[q_{\tau_1}^1 - p_{\tau_1}^1 \right] + \varepsilon^2 \left[q_{\tau_1}^2 - 2q^1 q_{\tau_1}^1 + p_{\eta_1}^1 - p_{\tau_1}^2 - a^1 p_{\tau_1}^1 \right] = 0 \quad (4.73)$$

$$\varepsilon \left[a^1 - p^1 \right] + \varepsilon^2 \left[\alpha a_{\tau_1 \tau_1}^1 + a^2 - p^2 \right] = 0 \quad (4.74)$$

And thus

$$a^1 = q^1 \quad (4.75)$$

$$q^1 = p^1 \quad (4.76)$$

$$2q_{\eta_1}^1 - 3q^1 q_{\tau_1} - \alpha q_{\tau_1, \tau_1, \tau_1}^1 = 0 \quad (4.77)$$

In fast times, and in a boundary layer, p^1 is a solution of the KdV equation. In initial variables, we have the following KdV equation for blood pressure, $P'(T, Z) = \left(A_o c_o p^1 \left(\frac{coT - Z}{l\varepsilon^2}, \frac{Z}{l\varepsilon} \right) \right)$, using (4.75) ó (4.77)

$$P'_Z + d_o P'_T + d_1 P' P'_T + d_2 P'_{TTT} = 0 \quad (4.78)$$

with

$$d_o = \frac{1}{c_o}, d_1 = \frac{-3}{2} \frac{1}{A_o c_o^2}, d_2 = \frac{-\alpha_w h_o R_o}{2\rho c_o^3}.$$

The space evolution equation (4.78) describes rather fast traveling waves. After their evanescence across the compartment, a slow varying flow that is akin to parabolic flow is observable. Such flow can be approximated by a windkessel model.

Let $P' = P_s$ be a soliton solution, then we put (4.78) in the form

$$\frac{\partial P_s}{\partial z} + (d_o + d_1 P_s) \frac{\partial P_s}{\partial t} + d_2 \frac{\partial^3 P_s}{\partial t^3} = 0 \quad (4.79)$$

Note that d_i ($i = 0, 1, 2$) characterize the arterial wall, $d_0 + d_1 P_s$ being pressure dependent velocity and $\frac{\partial^3 P_s}{\partial t^3}$ is the dispersion term which is not at the origin of solitons. In what follows, we shall put (4.79) as a canonical KdV equation. To achieve this we perform the following transformation:

$$\Gamma = t - d_0 z, \bar{z} = d_2 z \text{ and } u = \frac{d_1}{6d_2} P_s \quad (4.80)$$

Substituting (4.80) in (4.79) we get the canonical form of the KdV equation:

$$u_{\bar{z}} + 6uu_{\Gamma} + u_{\Gamma\Gamma\Gamma} = 0 \quad (4.81)$$

We have demonstrated two models in this chapter: (i) fluid interaction with the elastic wall (fluid-wall coupling), (ii) nonlinear arterial pulse wave. In the next chapter we shall solve the problems posed by the above mode

4.2.1 Methods of solution of non-linear wave model problem

We need an understanding of an interesting issue in non-linear dispersive wave problems of *solitons*. We see it crucial that a succinct explanation of solitons be made here in the light of its nature as a kind of solution to non-linear wave problem.

Soliton theory is one that is at variance with *chaos theory*. The latter explains that both partial differential equations (PDEs) and ordinary differential equations (ODEs) arising from dynamical structures exhibit some behaviour, allowing some deterministic systems to be exponentially unpredictable for increasing quantity of time. On the other hand, soliton theory furnishes many important cases of non-linear systems that behave in a stable, quasi-linear manner. For instance, chaos can be seen from turbulence in fluids; and arrhythmic writhing of a human heart in moments before death though the patient's cardiac situation might have yielded to clinical diagnosis (from stability to instability). *Soliton* can be seen in nonlinear

pulse wave whose memory effects describe stable peaking and steepening phenomena. We now ask, what is a *soliton*?

Definition 4.5 (Drazin and Johnson (1989), (Zabusky and Porter (2010)))

A soliton (or solitary wave solution) is a solution to any wave equation that preserves the following properties:

- (i) *Retains its shape (initial profile) for all time;*
- (ii) *Is localized (asymptotically constant at $\pm \infty$ or obeys periodicity condition imposed on the original equation);*
- (iii) *Can pass through other solitons and retain size and shape.*

Some non-linear equations permit or dismiss the possibility of solitary wave solutions. In some cases many localized solitons tend to scatter off one another irreversibly. Non-linear PDEs which have soliton-solutions belong to a generic class for which their initial value problem can be solved by means of *inverse scattering transform* method. During solution process new non-linear modes ó generalized Fourier modes may be identified, which are soliton components of the solution, and in addition modes that are purely dispersive,(as in the nonlinear Schrödinger's (NLS) equation), and therefore often called radiation. Solitons admit, at most, a phase change after interaction. It is therefore, possible to ðaddö (in a well defined manner) two soliton solutions to obtain a third soliton, hence achieving a non-linear *superposition principle* akin to linear equations.

Why much interest in soliton? Our interest is to solve non-linear wave problem emerging from arterial pressure pulse. We have seen that the PPW model equations in the previous section transformed to the well known long shallow-water wave Korteweg-de Vries (KdV) equation (Griffitt and Schiesser (2009)). The KdV equation admits non-dispersive soliton solutions. This non-dispersive nature arises not due to the absence of dispersion, but only

because they are balanced by non-linearity in the system (Lomdahl (1984)). Thus, a salient property of the KdV equation is the mutual counter-balancing effect of dispersion and non-linearity which permit wave solutions that propagate without changing form. (Solitons are considered a choice of base functions to analyze arterial blood pressure (ABP).

Invaluable details on solitons were presented by Lamb (1980), Drazin and Johnson (1989), Munteanu and Donescu (2004).

In what follows we shall derive arterial pressure pulse wave equation using a quasi-one dimensional model. Our choice of one dimension is motivated by clinical demands that pressure be measured at discrete points in one dimension (Olufsen, 1998). Moreover, we conceive of a case in which deformation is purely one-dimensional. In this work, we propose a decomposition of the pressure into a traveling wave representing the fast transmission phenomena during the systolic phase and a windkessel term representing slow transmission phenomena during diastolic phase. Parker and Tyberg (2002) applied a similar method in representing ventricular arterial coupling. We, however, present the choice of a forward traveling solitary wave that model the peaking and steepening PW phenomena. We justify this choice on grounds that peaking and steepening are the essential characteristics of PWs, and thus any model that captures them is enough to describe PP phenomena. For any given systolic phase, only 2 or 3 colliding (interacting) solitons are a sufficient descriptor of the pulse wave phenomenon (Laleg *et al*, (2006)).

4.2.2 The *Tanh* (hyperbolic tangent) method of solution

Several researches are ongoing for investigating solution techniques of general non-linear PDEs. Our approach shall be the *tanh* method (Malfliet, (1992, 2004)

Our task in this section is to construct one soliton solution (1SS) and two soliton solution (2SS) of the equation (3.91). These solutions, which have bell-shaped *sech* profile, are enough to describe the *peaking* and *steepening* phenomena that characterize arterial pulse wave (Laleg *et al* (2006)).

We note that these solutions cannot be approximated by plane wave solution; instead they require exponentially decaying solutions of the form $e^{\pm k(x, t)}$. Conventional solutions are asymptotically zero at large distances (Wazwaz, (2002)). Let equation (3.91) be in the form

$$u_{tt} + auu_{\Gamma} + bu_{n\Gamma} = 0 \quad (4.57)$$

where a and b (> 0) are parameters, $n\Gamma$ is the n th order derivative with respect to Γ . In (4.57) above, the third quantity at the left hand side represents a dispersive effect. We give a brief description of the method below. Suppose

$$u_t = G(u, u_x, u_{2x}, \dots) \quad (4.58)$$

We wish to know if the equation admits exact traveling wave solutions, and how to compute them. In the first place the independent variables t and x are combined into a new variable, $\xi = k(x - Vt)$, which defines the traveling frame of reference, $k > 0$ being the wave number and V the velocity of wave. We replace the variable $u(x, t)$ by $u(\xi)$. Thus the equation (3.91) are transformed into

$$-kV \frac{dU}{d\xi} = G(U, k \frac{dU}{d\xi}, k^2 \frac{d^2U}{d\xi^2}, \dots) \quad (4.59)$$

We are now to deal with ODEs instead of PDEs. We then seek exact solution of the ODEs in *tanh* form. Otherwise an approximate solution may be sought. Introduce a new variable $Y = \tanh \xi$ into the ODE. Now the coefficient of the ODE in $u(\xi) = F(Y)$ solely depends on Y , because $\frac{d}{d\xi}$ and subsequent derivatives in (4.59) are replaced by $(1 - Y^2) \frac{d}{dY}$.

We seek solution as finite power series in Y in the form

$$F(Y) = \sum_{n=0}^N a_n Y^n. \quad (4.60)$$

Such solution consists of solitary (bell-shaped) wave and shock (kink-shaped) wave. We

consider our equation (4.57), which transforms into

$$-kV \frac{dU}{d\xi} + U \frac{dU}{d\xi} + bk^3 \frac{d^3U}{d\xi^3} = 0 \quad (4.61)$$

Introduce $Y = \tanh(\xi)$ and thus replace the above equation by

$$\begin{aligned} & -kV(1-Y^2) \frac{dF(Y)}{dY} + kF(Y)(1-Y^2) \frac{dF(Y)}{dY} \\ & + bk^3(1-Y^2) \frac{d}{dY} \left\{ (1-Y^2) \frac{d}{dY} \left((1-Y^2) \frac{dF(Y)}{dY} \right) \right\} = 0 \end{aligned} \quad (4.62)$$

From equation (4.60) we get

$$\frac{dF(Y)}{dY} = \sum_{n=0}^N na_n Y^{n-1}, \quad \frac{d}{dY} \left(\frac{dF(Y)}{dY} \right) = \sum_{n=0}^N n(n-1)a_n Y^{n-2}$$

Substitute as required in equation (4.62) to get (with the range of summation \acute{o} assumed known).

$$\begin{aligned} & kV \left[\sum na_n Y^{n+1} - \sum na_n Y^{n-1} \right] - k \left[\sum \sum na_n^2 Y^{2n+1} - \sum \sum na_n^2 Y^{2n-1} \right] \\ & + bk^3 \left[\sum n(n-1)a_n Y^{n-3} - \sum n(3n^2 - 3n + 2)a_n Y^{n-1} + \sum n(2n^2 + n + 2)a_n Y^{n+1} \right] \\ & - \sum n(n+2)a_n Y^{n+3} = 0 \end{aligned} \quad (4.63)$$

We note a salient aspect of this method: the terms of the series must terminate, and thus we do not expect recurrent relations, typical of infinite series solutions. After due algebraic details we have arrived at the equation (4.63). We equate the highest two powers of $n = N$ to get $2N + 1 = N + 3$ i.e. $N = 2$. With this, equation (4.60) reads

$$F(Y) = a_0 + a_1 Y + a_2 Y^2 \quad (4.64)$$

Substitute (4.64) into (4.62), noting that

$$\frac{dF(Y)}{dY} = F'(Y) = a_1 + 2a_2Y.$$

With this we get

$$\begin{aligned} & -kV[(1-Y^2)(a_1 + 2a_2Y)] + k[(a_0 + a_1Y + a_2Y^2)(1-Y^2)(a_1 + 2a_2Y)] \\ & + bk^3[(1-Y^2)(6a_1 - 16a_2Y + 6a_1Y^2 + 24a_2Y^3)] = 0. \end{aligned}$$

The expanded form yields

$$\begin{aligned} & -kV(a_1 + 2a_2Y - a_1Y^2 - 2a_2Y^3) + k[(a_0a_1 + (a_1^2 + 2a_0a_2)Y + (3a_1a_2 - a_0a_1)Y^2 \\ & + (2a_2^2 - a_1^2 - 2a_0a_2)Y^3 - 3a_1a_2Y^4 - 2a_2^2Y^5] \\ & + bk^3[-2a_1 - 16a_2Y + 8a_1Y^2 + 40a_2Y^3 - 6a_1Y^4 - 24a_2Y^5] = 0 \quad (4.65) \end{aligned}$$

For the series to vanish, the coefficients of the powers of Y must vanish identically. Thus we equate the coefficient of each of the powers of Y to zero.

In doing so we find that the coefficients that are enough to yield a desired result are those of Y^2 and Y^5 , which read respectively,

$$a_1k[V + 3a_2 - a_0 + 8bk^2] = 0 \quad (4.67)$$

$$-2a_2k[a_2 + 12bk^2] = 0, \quad (4.68)$$

With this, $a_1 = 0$, $[V + 3a_2 - a_0 + 8bk^2] \neq 0$ in equation (4.67), $a_2 = 0$ or $a_2 = -12bk^2$ in equation (4.68).

If $a_1 = a_2 = 0$, then $V = a_0 - 8bk^2$ in (4.67); but if $a_2 = -12bk^2$ we get $V = a_0 + 28bk^2$. It is therefore permissible to use $a_2 = -12bk^2$ so that equation (4.64) does not collapse to a constant since a_1 is equal to zero. With this we have, using equation (4.64)

$$F(Y) = a_0 - 12bk^2Y^2 \quad (4.69)$$

Suppose the solution vanishes for $\xi \rightarrow \infty (Y \rightarrow 1)$, we get

$$F(Y) = 12bk^2(1 - Y^2) \quad \text{with } V = 4bk^2 \quad (4.70)$$

Using the original variables, we get

$$u(x, t) = 12bk^2 \operatorname{sech}^2 k(x - Vt). \quad (4.71)$$

This is a solitary wave in a bell-shape, as shown by Figure 4.2 below.

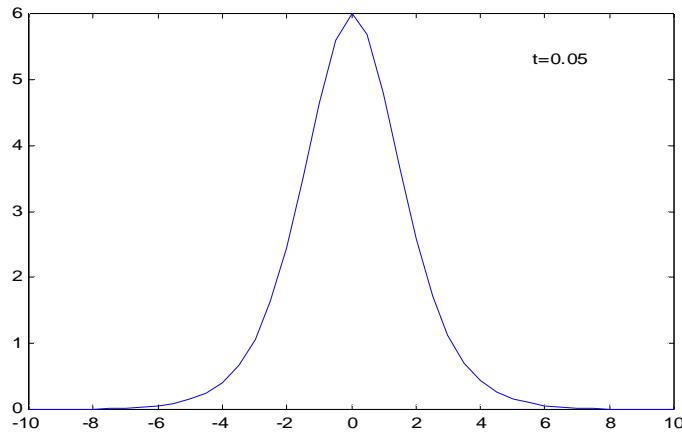


Fig 4.2 Solitary wave

A variety of methods, such as, tanh-sech method, extended tanh method, hyperbolic function method, etc. may be engaged in finding an exact solitary wave solution of nonlinear PDEs.

The main issue is the relative ease with which multi-solitons can be generated from ISS.

In achieving this purpose, we shall involve the bilinear method. The method is applied in the next section.

4.3.0 Bilinear Method

The bilinear method due to Hirota (1980) provides an elegant direct technique for constructing exact solutions to many non-linear PDEs. So long as the bilinear form is obtained, an algorithmic procedure follows. Most incredibly, not more than calculus and algebra is required. In application, the bilinear method requires:

- (i) *A clear change of dependent variable*
- (ii) *Introduction of a novel differential operator*
- (iii) *A perturbation expansion to solve the emerging bilinear equation.*

Let $f(x)$ and $g(x)$ be some ordered pair of functions. We write the Hirota differential operator D_x defined on the $f(x)$ and $g(x)$

$$D_x (f \cdot g) = (\partial_{x_1} - \partial_{x_2}) f(x_1) g(x_2) \Big|_{x_1=x_2=x} \quad (4.72)$$

In general

$$D_x^m D_t^n (f \cdot g) = (\partial_{x_1} - \partial_{x_2})^m (\partial_{t_1} - \partial_{t_2})^n f(x_1, t_1) g(x_2, t_2) \Big|_{\substack{x_1=x_2=x \\ t_1=t_2=t}}, \quad (4.73)$$

where m and n are non-negative integers. There is linearity in both arguments of the differential operator, and thus it is called a *bilinear operator*. The bilinear operators in (4.72) and (4.73) have the following properties:

$$D_x^m (f \cdot 1) = \frac{\partial^m f}{\partial x^m} \quad (4.74)$$

$$D_x^m (f \cdot g) = (-1)^m D_x^m (g \cdot f) \quad (4.75)$$

$$D_x^m (f \cdot f) = 0, \text{ for } m \text{ odd} \quad (4.76)$$

$$D_x^m D_t^n (e^{k_1 x - \omega_1 t} \cdot e^{k_2 x - \omega_2 t}) = (k_1 - k_2)^m (-\omega_1 + \omega_2)^n e^{(k_1+k_2)x - (\omega_1+\omega_2)t} \quad (4.77)$$

Let $P(D_x, D_t)$ be a polynomial in D_x and D_t . Then, from (4.74) and (4.77) we progress as follows: Let (as indeed it is)

$$(e^{k_1 x - \omega_1 t} \cdot e^{k_2 x - \omega_2 t}) = (e^{(k_1+k_2)x - (\omega_1+\omega_2)t} \cdot 1) \quad (4.77a)$$

From (4.74) we have

$$\begin{aligned} P(D_x, D_t) (e^{(k_1+k_2)x - (\omega_1+\omega_2)t} \cdot 1) &= P(D_x, D_t) (f \cdot 1) \\ &= P(k_1 + k_2, -\omega_1 - \omega_2) P(D_x, D_t) e^{(k_1+k_2)x - (\omega_1+\omega_2)t} \end{aligned}$$

We, therefore have the result,

$$P(D_x D_t)(e^{k_1 x - \omega_1 t} \cdot e^{k_2 x - \omega_2 t}) = \frac{P(k_1 - k_2, -\omega_1 + \omega_2)}{P(k_1 + k_2, -\omega_1 - \omega_2)} P(D_x, D_t)(e^{(k_1 + k_2)x - (\omega_1 + \omega_2)t} \cdot 1) \quad (4.78)$$

In what follows we develop a bilinearized form of the KdV equation so that it would be amenable to the bilinear method of finding soliton solutions. Once more, consider the KdV equation (3.91) in the form

$$u_{xxx} + 6uu_x + u_t = 0 \quad (4.79)$$

(Subsequently we may use the form Δ_{nx} , where n is the (numeric) n th order partial derivative of the variable Δ , as the case may be, w.r.t x)

We seek a bilinear form. To do this we carry out the dependent variable transformation

$$u = 2 \frac{\partial^2}{\partial x^2} \log f = 2 \left(\frac{ff_{xx} - f_x^2}{f^2} \right) \quad (4.80)$$

With this, equation (4.79) becomes

$$2(\log f)_{xxt} + 3\partial_x(u^2) + u_{3x} = 0 \quad (4.81)$$

Integrating once with respect to x to get

$$2(\log f)_{xt} + 3u^2 + u_{2x} = 0 \quad (4.82)$$

We therefore calculate the relevant quantities as follows:

$$u^2 = 4 \left(\frac{f_x}{f} \right)^4 + 4 \left(\frac{f_{xx}}{f} \right)^2 - 8 \frac{f_x^2 f_{xx}}{f^3} \quad (4.83)$$

$$u_{2x} = -12 \left(\frac{f_x}{f} \right)^4 + 24 \left(\frac{f_x^2 f_{2x}}{f^3} \right) - 6 \left(\frac{f_{2x}}{f} \right)^2 - 8 \frac{f_x f_{3x}}{f^2} + 2 \frac{f_{4x}}{f} \quad (4.84)$$

$$2(\log f)_{xt} = -2 \left(\frac{f_x f_t}{f^2} - \frac{f_{xt}}{f} \right) \quad (4.85)$$

Substitute (4.83) - (4.85) in (4.82), and perform the necessary algebra and get

$$ff_{xt} - f_x f_t + ff_{4x} - 4f_x f_{3x} + 3f_{2x}^2 = 0 \quad (4.86)$$

The above is a quadratic equation in f_{2x} . We are now set to put the KdVe in a bilinear form, using the Hirota D-operator defined by

$$D_x^m f \cdot g = (\partial x_1 - \partial x_2)^m f(x_1)g(x_2) \Big|_{x_1=x_2=x} \quad (4.87)$$

Consider the two relations below:

$$D_x D_t f \cdot f = 2(f_{tx} f - f f_{tx}) \quad (4.88)$$

$$D_x^4 f \cdot f = 2(ff_{4x} - 4f_x f_{3x} + 3f_{xx}^2) \quad (4.89)$$

Add (4.88) to (4.89) and compare the result to the KdVe (4.86). In doing so we arrive at the bilinear form

$$D_x (D_t + D_x^3) f \cdot f = 0 \equiv B(f \cdot f) \quad (4.90)$$

where B abbreviates the bilinear operator for the KdVe. We have, therefore derived a bilinear equation that represents, in every wise, the KdVe.

4.3.1 Solitons by bilinear method

Our bilinear form (4.90) enables us to construct soliton solutions for the KdVe. Consider a class of bilinear equations of the form

$$P(D_x, D_t, \dots) f f \stackrel{\text{def}}{=} D_x (D_t + D_x^3) f \cdot f = 0 \equiv B(f \cdot f) \quad (4.91)$$

where P is a polynomial in the Hirota partial derivations D . We assume (as we should) that P is even (the D -operator is asymmetric and so the odd terms cancel). We start with the zero-soliton solution ((OSS) or the vacuum). The KdV equation has a trivial solution $u \equiv 0$. We therefore require the corresponding f . From (4.80) we see that $f = e^{e^{2\alpha(t)x + \vartheta(t)}}$ is suitable for equation (4.79). To see this, substitute the given value of f into the first equation of (4.80), and obtain the solution $u = 0$. We are free to choose $f = 1$ as an OSS. It solves (4.91) so long as

$$P(0, 0, \dots) = 0 \quad (4.92)$$

The next activity is to obtain multi-soliton solutions by finite perturbation expansions around the vacuum $F = 1$. We seek a series solution

$$f = 1 + \sum_{n=1}^{\infty} v^n f_n, \quad (4.93)$$

for some unknown functions $f_1(x,t), f_2(x,t), \dots$, where ν is a formal expansion parameter.

Substituting (4.93) into (4.90) and equating to zero the powers of ν yield

$$O(\nu^0) : B(1 \cdot 1) = 0 \quad (4.94)$$

$$O(\nu^1) : B(1 \cdot f_1 + f_1 \cdot 1) = 0 \quad (4.95)$$

$$O(\nu^2) : B(1 \cdot f_2 + f_1 \cdot f_1 + f_2 \cdot 1) = 0 \quad (4.96)$$

$$O(\nu^3) : B(1 \cdot f_3 + f_1 \cdot f_2 + f_2 \cdot f_1 + f_3 \cdot 1) = 0 \quad (4.97)$$

$$O(\nu^4) : B(1 \cdot f_4 + f_1 \cdot f_3 + f_2 \cdot f_2 + f_3 \cdot f_1 + f_4 \cdot 1) = 0 \quad (4.98)$$

$$O(\nu^n) : B\left(\sum_{j=0}^n f_j \cdot f_{n-j}\right) = 0, \text{ with } f_0 = 1 \quad (4.99)$$

For our KdV equation, the operator B is defined in (4.90). Since the KdV equation admits N soliton solutions (Drazin and Johnson (1989)), equation (4.93) will terminate at $n = N < \infty$, (this is an essential feature of Hirota method a case where there exists a finite number of terms of the series as seen in (4.93), provided f_i is the sum of precisely N simple exponential terms. We now obtain ISS ($N = 1$) from

$$f_1 = \exp \theta = \exp (kx - \omega t + \delta)$$

where k, ω and δ are constants. The dispersion law

$$\omega = k^3 \quad (4.100)$$

is determined by (4.95). Equation (4.96) permits us to set $f_2 = 0$, and in effect we can take $f_i = 0$ for $i > 2$. Let $\varepsilon = 1$, and we get

$$f = 1 + f_1 = 1 + \exp \theta = 1 + \exp (kx - \omega t + \delta).$$

Substitute f in (4.83) with (4.100), and get

$$u(x, t) = 2 \frac{\partial^2 \log f(x, t)}{\partial x^2} = 2 \left(\frac{f f_{2x} - f_x^2}{f^2} \right)$$

For a 1SS we write

$$u(x, t) = 2 \frac{\partial^2 \log(1 + \exp(kx - \omega t + \delta))}{\partial x^2} = \frac{2k^2 e^{kx - \omega t + \delta}}{(1 + e^{kx - \omega t + \delta})^2} = \frac{2k^2 \exp(\zeta)}{(1 + \exp(\zeta))^2}, \quad (4.100a)$$

where $\chi = kx - \omega t + \delta$. The last expression of equations (100a) takes the form of

Padé approximant (Curry (2008)), the rational function G/F, which describes the function,

$$u(x, t) = \frac{k^2}{2} \operatorname{sech}^2\left(\frac{\zeta}{2}\right)$$

Substitute $\zeta = kx - \omega t + \delta$ and get

$$u(x, t) = \frac{1}{2} k^2 \operatorname{sech}^2 \frac{1}{2} (kx - k^3 t + \delta)$$

Let $k = 2K$; we get

$$u(x, t) = 2K^2 \operatorname{sech}^2(Kx - 4K^3 t + \delta/2) \quad (4.101)$$

The above is a pulse shaped solitary wave solution of the KdV equation, and it compares to the solution (4.71).

In what follows we shall construct a 2SS ($N = 2$) in order to represent the wave peaking and steepening phenomena. The construction of the 2SS can help in producing $N (> 2)$ solutions.

Consider the 1SS (4.101) and, for simplicity, write $k = K = 1$, $\delta = 0$. With these we get

$$u(x, t) = 2 \operatorname{sech}^2(x - 4t) = 4 \frac{\partial}{\partial x} \left(\frac{e^{2x-8t}}{1 + e^{2x-8t}} \right) = 2 \frac{\partial^2}{\partial x^2} \log(1 + e^{2x-8t}) \quad (4.102)$$

We may, for notational convenience, write

$$B[f, g] = D_x (D_t + D_x^3) f \cdot g,$$

and obtain that for $f = 1 + e^{2x-8t}$

$$\begin{aligned} B[f, f] &= B[1 + e^{2x-8t}, 1 + e^{2x-8t}] \\ &= B[1, 1] + B[1, e^{2x-8t}] + B[e^{2x-8t}, 1] + B[e^{2x-8t}, e^{2x-8t}] = 0 \end{aligned} \quad (4.103)$$

The above equation (4.103) is a solution to (4.90). We need only to generalize this solution to cater for N -soliton solutions. We had assumed that f possesses an asymptotic expansion about

the parameter ν (see 4.93), through which an infinite sequence of equations on the components of the expansion can be obtained, and write,

$$f = 1 + \sum_{n=1}^{\infty} \nu^n f_n(x, t) \quad (4.104)$$

When the above is substituted into (4.90), and upon collecting the powers of ν we get (see equations (4.94)-(4.99)),

$$\begin{aligned} & B[1,1] + \nu(B[1, f_1] + B[f_1, 1]) + \nu^2(B[1, f_2] + B[f_1, f_1] + B[f_2, f_1]) + \dots \\ & + \nu^r \left(\sum_{m=0}^r B[f_m, f_{r-m}] \right) + \dots = 0 \end{aligned} \quad (4.105)$$

This expression (4.105) reduces to a series of equations, requiring each term with common power of ε to vanish. Using equations (4.88) and (4.89) we have the equation for f_1 reduce to

$$\left(\frac{\partial}{\partial t} + \frac{\partial^3}{\partial x^3} \right) f_1 = 0, \quad (4.106)$$

Introduce the following notation:

$$\tilde{D} = \left(\frac{\partial}{\partial t} + \frac{\partial^3}{\partial x^3} \right), \quad D = \tilde{D} \frac{\partial}{\partial x}.$$

Then we get the first few equations from (4.105) read,

$$\begin{aligned} \tilde{D}f_1 &= 0 \\ 2Df_2 &= -B[f_1, f_1] \\ 2Df_3 &= -B[f_1, f_2] - B[f_2, f_1] \end{aligned} \quad (4.107a, b, c)$$

Suppose $f_i = \exp(\gamma_i)$ where $\gamma_i = l_i x - l_i^3 t + \beta_i$ for l_i and β_i arbitrary constants, then

$$\tilde{D}f_1 = 0, \quad B[f_1, f_1] = 0, \quad \text{and} \quad \tilde{D}f_2 = 0.$$

On the choice of $f_n = 0$, for $n = 2, 3, \dots$ in (4.105) we regain the solitary wave solution. We note the linearity of equation (4.107a). This linearity is very crucial in generating multi-soliton solutions to the KdV equation under our consideration. Assume that

$$f_1 = \exp(\gamma_1) + \exp(\gamma_2) \quad (4.108)$$

By linearity condition, $\tilde{D}f_1 = 0$. From (4.107b) we find that

$$\begin{aligned} 2Df_2 &= -B[f_1, f_1] \\ &= -B[\exp(\gamma_1), \exp(\gamma_1)] - B[\exp(\gamma_1), \exp(\gamma_2)] - B[\exp(\gamma_2), \exp(\gamma_1)] \\ &\quad - B[\exp(\gamma_2), \exp(\gamma_2)]. \end{aligned}$$

We note that the non-zero terms contain both γ_1 and γ_2 and thus

$$2Df_2 = -2\{(k_1 - k_2)(k_2^3 - k_1^3) + (k_1 - k_2)^4\} \exp(\gamma_1 + \gamma_2) \quad (4.109)$$

The above equation (4.109) has a solution of the form

$$f_2 = A_2 \exp(\gamma_1 + \gamma_2),$$

Which upon substituting into (4.109) yields

$$A_2 = \left(\frac{k_1 - k_2}{k_1 + k_2} \right)^2$$

Substitute expressions for f_1 and f_2 in equation (4.107c) and find that

$$\begin{aligned} 2Df_3 &= -A_2 B[\exp(\gamma_1), \exp(\gamma_1 + \gamma_2)] - A_2 B[\exp(\gamma_1 + \gamma_2), \exp(\gamma_1)] \\ &\quad - A_2 B[\exp(\gamma_2), \exp(\gamma_1 + \gamma_2)] - A_2 B[\exp(\gamma_1 + \gamma_2), \exp(\gamma_2)] \\ &= -2A_2 \{(-k_2)k_2^3 + (-k_2)^4\} \exp(2\gamma_1 + \gamma_2) \\ &\quad - 2A_2 \{(-k_1)k_1^3 + (-k_1)^4\} \exp(2\gamma_1 + \gamma_2) = 0 \end{aligned}$$

By putting $\varepsilon = 1$ in (4.105) we get an exact two-soliton solution to the KdV equation:

$$f = 1 + \exp(\gamma_1) + \exp(\gamma_2) + \left(\frac{k_1 - k_2}{k_1 + k_2} \right)^2 \exp(\gamma_1 + \gamma_2).$$

Substitute f in (4.80), and choose

$$\begin{aligned} e^{\delta_i} &= \frac{c_i^2}{k_i} e^{k_i x - \omega_i t + \Delta_i} \quad \text{for } i = 1, 2, \\ \tilde{f} &= \frac{1}{4} f e^{\frac{1}{2}(\tilde{\gamma}_1 + \tilde{\gamma}_2)} \quad \text{where } \tilde{f}_i = k_i x - \omega_i t + \Delta_i, \text{ for } i = 1, 2, \end{aligned}$$

we obtain

$$\tilde{u}(x,t) = 2 \frac{\partial^2 \ln \tilde{f}(x,t)}{\partial x^2} = 2 \frac{\partial^2 \ln f(x,t)}{\partial x^2} = u(x,t).$$

Take $A_i^2 = \left(\frac{k_1 + k_2}{k_1 - k_2} \right) k_i$ for $i = 1, 2$, then

$$\tilde{f}(x,t) = \left(\frac{1}{k_1 - k_2} \right) \left(k_1 \cosh \frac{\tilde{\gamma}_1}{2} \cosh \frac{\tilde{\gamma}_2}{2} - k_2 \sinh \frac{\tilde{\gamma}_1}{2} \sinh \frac{\tilde{\gamma}_2}{2} \right).$$

We therefore write

$$\begin{aligned} u(x,t) &= \tilde{u}(x,t) = 2 \frac{\partial^2 \ln \tilde{f}(x,t)}{\partial x^2} \\ &= \left(\frac{k_1^2 - k_2^2}{2} \right) \left(\frac{k_1^2 \cosh^2 \frac{\tilde{\gamma}_1}{2} + k_2^2 \sinh^2 \frac{\tilde{\gamma}_2}{2}}{\left(k_1 \cosh \frac{\tilde{\gamma}_1}{2} - k_2 \sinh \frac{\tilde{\gamma}_2}{2} \right)^2} \right). \end{aligned} \quad (4.110)$$

We can generalize to any exact N-soliton solution just by putting

$$f_1 = \sum_{i=1}^N \exp(\gamma_i) \quad (4.111)$$

then the expansion (4.105) is guaranteed to terminate after the f_N term. The above clearly shows the ability to take soliton solutions and combine them to generate multi-soliton solutions, an elegant feature of integrable systems. As we stated earlier, two soliton solutions are enough to explain our required peaking and steeping wave phenomena in the systolic phase. Each of the solitons refers to a well distinguished peak of the pressure pulse.

In the section that follows we shall employ another method of solution that de-emphasizes perturbation process.

4.4 Systolic and diastolic PW representation

As we indicated earlier, solitons lead to the estimation of the systolic phase. A two-element windkessel model may be needed to cater for the diastolic phase. Much as the solitons can

effectively describe physiological states, we deem it necessary to include the diastolic phase in our solution, in case issues regarding residual flow waves are being considered. However, we do not consider deriving the equations that apply to the windkessel model since they estimate the diastolic phase.

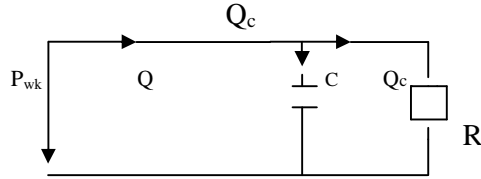


Fig 4.4. 2-element windkessel model of flow phenomena

We denote the windkessel pressure by P_{wk} . The windkessel theory stipulates that the variation of aortic P_{wk} is supplied by the difference between the inflow and outflow and the volumetric change (Wang *et al*, (2002)). The equation governing the above theory in time domain is given by, Wang *et al* (2002)

$$\frac{d}{dt} P_{wk}(t) - \frac{dP_{wk}}{dV_{wk}} \frac{dV_{wk}(t)}{dt} = \frac{Q_{i-o}(t)}{C} \quad (4.112)$$

where $Q_{i-o} = Q_{input} - Q_{output}$, and C is the compliance of the whole arterial tree, assumed to be constant and V_{wk} is the windkessel velocity. By a simple resistive relationship, $Q_0 = \frac{(P_{wt}(t) - P_{\infty})}{R}$, in which case the outflow is assumed to be driven by the difference between P_{wk} and the asymptotic pressure of the diastolic exponential decay (P_{∞}), (see (Shrier *et al* (1993))), where flow from the arteries to veins ceases. Let R_p be the effective resistance of the peripheral system circulation. Substitute Q_0 in terms of P_{wk} and P_{∞} and we have equation (4.112) for P_{wk} in the form

$$\frac{dP_{wk}(t)}{dt} + \frac{P_{wk}(t) - P_{\infty}}{R_p C} = \frac{Q_i}{C} \quad (4.113)$$

The above equation (4.150) has the general solution

$$P_{wk}(t) - P_{\infty} = (P_0 - P_{\infty})e^{-\frac{t}{RC}} + e^{-\frac{t}{R_p C}} \int_{t_0}^t \frac{Q_i(t')}{C} e^{\frac{t'}{R_p C}} dt' \quad (4.114)$$

In the equation (4.113), the quantities R_p , C and P_{∞} have to be supplied from experimental data.

Having been supplied with the solitons and the windkessel pressure P_{wk} we write the arterial blood pressure (ABP) in the form:

$$P(z, t) = \otimes_{j=1}^{\eta} P_{sj}(z, t) + P_{wk}(t), \quad (4.11)$$

where $\otimes_{j=1}^{\eta} P_{sj}(z, t)$ is a wave term given by a non-linear superposition of solitary wave $P_{sj}(z, t)$

CHAPTER FIVE

RESULTS AND DISCUSSIONS

In chapter three we discussed the interaction of blood (fluid) with the arterial wall. It was found that the action of the fluid on the wall consists of a normal pressure, and the accompanying shear which is tangent to the wall. We proceeded to build the fluid-wall interaction model (see section 3.1.2). Both the fluid and the elastic wall form a coupled system at their interface. Thus, at the deformed interface, velocity of the fluid must be equal to the Lagrangean velocity of the membrane. (We had considered the arterial wall as a membrane, in which bending stress is negligible; the artery itself being kept torsion-free). The FSI problem is presented in equations (3.30)-(3.32), together with other adjunct equations. Solutions to the problem were sought in chapter four. By using asymptotic expansion (see equations (4.26)-(4.32)), the pressure equation was obtained. Naturally, the model of arterial pulse wave should take convective terms into account, and thus consider the wave as non-linear. We presented the justifications for non-linearity (section (3.2.0)) against the assumptions of linearity. Our justifications are a bulwark against the non-linear wave model which we expounded hereto.

The assumption of incompressible flow via an elastic arterial wall led to the governing equations (4.57) and (4.58), with the motion of the arterial wall satisfied by (4.59). In arriving at a solution we applied asymptotic expansions about the factor ϵ while considering forward-moving wave (symmetric with) backward-moving wave. A salient aspect of the expansion was the derivation of an equation of pressure in the form of a KdV equation (4.78). This done, we sought a solution (in chapter four). It was found that the resulting KdV equation is amenable to soliton-solutions. Solitons are enough to describe the *peaking* and *steepening*

pulse wave phenomena. Since a two-loop (2SS) completely describes such phenomena, we were satisfied with a 2SS of the wave problem. We combined the *Tanh* (hyperbolic tangent) method and the *bilinear* method in arriving at the canonical KdV equation (4.81). Each of the named methods has its peculiarities. In what follows, we shall visit these peculiarities.

5.1.0 Features of:

(1) Tanh Method

The *tanh* method:

- (i) Reduces the problem to an ordinary differential equation (ODE) which makes solution easily tractable.*
- (ii) Circumvents integration to get a closed-form solution, albeit (most times) at the cost of rigorous algebra.*
- (iii) Does not utilize perturbation expansion.,*

(2) Bilinear method

The bilinear method:

- (i) Has predilection to algebra and calculus.*
- (ii) Reduces the problem to a bilinear form.*
- (iii) Engages perturbation expansion.*
- (iv) is very effective in harnessing the bilinear equation in the construction of multi-soliton solutions.*

We have combined the *tanh* method and the bilinear method in obtaining the solution to our problem; once the PDE is reduced to an ODE and the ODE is reduced to an algebraic process, the *tanh* method of solution yields a feasible result; the bilinear method has an

endearing property of furnishing the required number of soliton solutions with relative ease. We used the *tanh* method in obtaining the 1SS, and extended to the 2SS by means of the bilinear method; the other *n*-soliton solutions are a mere nonlinear superposition of the 1SS.

5.2.0 Physiological Analysis using solitary waveform

Waves convey information regarding the matter in which they propagate. A model of arterial wave propagation widens our knowledge about the working of the cardiovascular system and provides a clue to the diagnosis of pathological conditions, and in effect the outcome of medical interventions may be predicted. From the result of our mathematical study, we extend to the clinical interest. We are here persuaded to bring our discussions to bear on human physiological exigencies. We shall analyze the behavior of the solitons from two standpoints, the *distance effects* and the *time effects*.

The solution of the wave problem given by equation (3.11) describes the -peakingø and -steepeningø phenomena that are typical of solitary waves. Such pulse waves propagated through the arterial bed are an estimator of the systolic phase of blood pressure. A usual phenomenon in wave motion is reflection. Waves are reflected at various arterial sites, which may include, but not limited to, points of bifurcation, areas of changes in arterial geometry, peripheral and terminal regions. However, it is customary to integrate multiple reflected waves as a single wave, which sums with the forward ejected wave and forms the final pattern of the pressure pulse wave.

5.2.1 Distance effect

An issue that is of clinical importance is the return of the reflected waves. This brings to concern the implication of proximity or otherwise of an organ to the heart. Pulse wave was analyzed in relation to the distance travelled. To do this, distance was varied at a fixed time

mark. The understanding of the waveform at various distances occupied by the wave would provide a clue to its relationship with arterial length (wherein stature plays a role) so that a physiological condition may be analyzed. The length of the arterial tree is stature-related. Short stature, for instance, implies a reduction in length of the arterial tree (Smulyan et al., 2001).

5.2.2 Short and tall stature

Who is short and who is tall? The answer to this question could sometimes be determined in relation to sex, age, race and some other factors. There is no confluence of views regarding short and tall stature. Most commonly (Hoyme, 2014):

ó Short Stature: Height < -2SD or <3% for age

ó Tall Stature: Height > +2SD or > 97% for age

Short stature is therefore defined as an adult height that is more than 2 standard deviations below the mean for age and gender, which corresponds to the shortest 2.3% of individuals (Pedicelli et al. (2009)). By standard this includes adult men who are shorter than 163 centimeters (5 ft 4 in) tall and adult women who are shorter than 150 centimeters (4 ft 11 in) tall (Becker (2001)). For the purpose of this work, we shall assume the following:

- (i) The individual person is at least twenty years of age.
- (ii) The individual short person has normal growth variants (familial short stature and/or constitutional short stature).
- (iii) The individual tall person has normal tall (familial) stature
- (iv) The body/mass index (BMI) of the individual person is within normal range.

- (v) Both statures are within same physiological range of health, at least from twenty years of age.

Anthropometry in assessing growth (Hoyme, 2014)

•*Arm span measurement*

- Extend both hands outward (each arm abducted to 90)
- Measure finger tip to Finger tip



Figure 5.0: Arm-span measurement for growth assessment (Hoyme: http://www.sanfordhealth.org/files/0a2b44cd-bd4a-47bd-91fb-842ec062ac0a/Too_Short_or_Too_Tall_Hoyme.pdf)

Normal results

ÉChildren: Arm Span is 1 cm shorter than height

ÉAdolescent: Arm Span is same length as height

ÉAdult: Arm Span exceeds height by more than 5 cm

The graphs (A-F), which represent six 2SS (shown in Figure 5.1) at various distances, reveal much about distance effects on solitons. Each successive increase in distance caused the shorter wave to plummet (see graphs A-F). In graph F the shorter wave was almost encapsulated by the taller one. There is successive diminishing of the wavelength. Consider

the frequency domain in which large mammalian artery's wavelength and arterial length relationship is given by (Berger et al. (1994), Mohammad et al. (2007))

$$\frac{\lambda}{L} = \frac{j\omega}{HR.L\sqrt{j\omega C'(j\omega L' + R')}} = \frac{j\omega}{HR.L\sqrt{j\omega C'\left(j\omega\frac{\rho}{\pi^2} + \frac{8\mu}{\pi^4}\right)}} \approx \frac{\sqrt{\pi^2 / \rho C'}}{HR.L}, \quad (5.1)$$

with L being the length of the arterial segment, C' and R' the respective arterial compliance and resistance per unit length, HR the heart rate, ρ blood density, μ blood viscosity and ω the fundamental frequency. This frequency ω defines the periodicity of the ejecting source (HR). As can be seen from equation (5.1), pulse wavelengths become long relative to the lengths of vessels when heart rate is low, vessel compliances are low, or vessel radii are extremely large. We observe as well that changes in r , HR and C' may increase wavelength. It is observed that pulse wavelength increases with decreased frequency and compliance (Quick et al. (1998)). We deduce from Figure 5.1 (graphs A-F) that there is a progressive thinning of the wavelengths. The thinning of the wavelength as observed at infinite length admits that pulse wave amplification is more pronounced with increased length (Avalio et al. (2009)) This, in effect, suggests that compliance is akin to distance. Short stature, synonymous with reduced arterial length, is known to induce faster heart rate, a short diastolic period and lower arterial compliance (Smulyan et al., 2001).

The extent to which reflected wave travels before the arrival of an oncoming wave is related to the cardiac function. It is physiologically absurd to conjecture a reflection that would get to the root of propagation (i.e the heart) in the event of sustained or minimal LV ejection. Low pulse wave amplification is associated with early return of reflected waves. The following can be inferred:

(a) Pulse pressure and heart rate are essentially distance (height)-related; within physiological state, tall stature is more likely to have lower pulse pressure and heart rate than short stature.

(b) Short statures are likely to experience more shortened return time of reflected waves, and thus lower pulse amplification than tall statures. (This implies that the return of reflected waves to the aorta in early systole even with normal wave velocity would demand more pulsatile effort from the left ventricle (LV) in short statures.)

(c) At an infinitely long distance pulse wavelength gets thinner. The fifth and sixth graphs on Fig.5.1, indicate this. This is in line with the transmission theory (Mohammad et al. (2007)) which supposes finite wavelength.

The progressive thinning of the wavelength, as seen in the figure, is a consequence of wave reflection at a site distal to the propagating site.

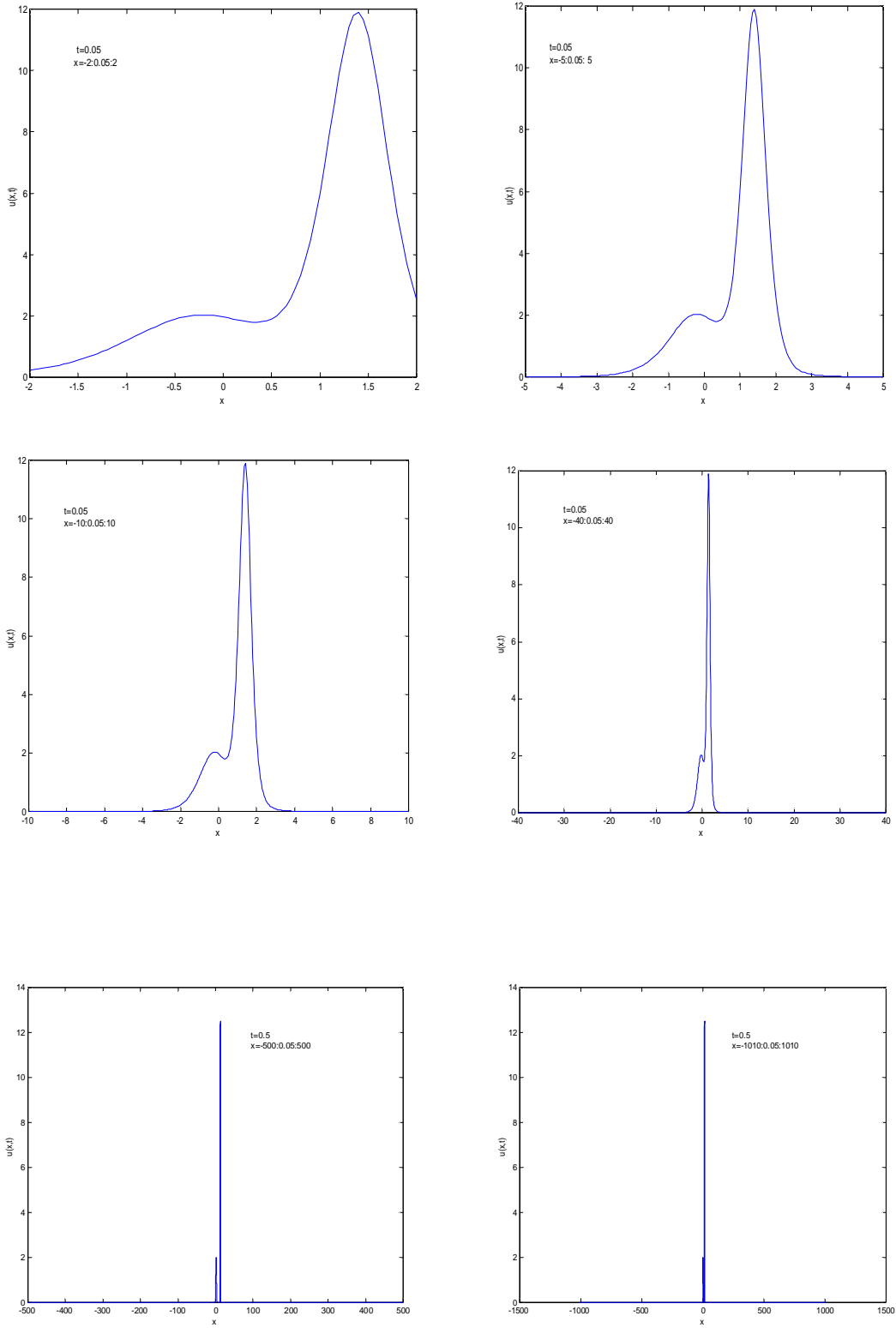


Fig 5.1 2-Soliton Solutions at various distances

Usually, wavelengths become long relative to cardio-vascular parameters such as the length of vessels, low heart rate, low vessels compliance and large vessels radii. The thinning of the wavelength as observed at infinite length suggests that PW amplification is less in tall persons. This is underscored by the fact that slower heart rates (within physiological range) associated with tall stature lessens PW amplification (Mohammad (2007)).

It is noteworthy that the maximum distance to which a reflected wave could reach is the midpoint of the propagating distance. The extent to which reflected wave propagates before the arrival of an oncoming wave must be related to the cardiac function.

5.2.3 Time effects

The understanding of the waveform at various time intervals occupied by the wave would provide a clue to physiological conditions. To this effect, the systolic time interval (STI) and the left ventricular ejection time (LVET) are of interest (Nzerem and Ugorji (2014)). The graphs of Fig. 5.2 represent two soliton solution at various times, at a constant distance ($x = 40$ units). Each LV ejection has an accompanying wave. In each of the graphs A-F of Fig 5.2, the aortic pre-ejection period is the interval of time before the appearance of the taller (tandem) wave. Graph A shows the emergence of a tandem wave (during LV afterload). In Graph B the tandem wave approaches the shorter (precursor) wave. In the real sense, another wave in tandem with the tandem wave had evolved, which moves behind the tandem wave and, expectedly, would overtake it at some time. We had said that two solitons are enough to describe the wave phenomena. Graph D shows the enveloping of the precursor wave by the tandem wave. LVET is the interval from the commencement to the termination of aortic flow. It is associated with LV preload and afterload (Reant *et al.* (2010)).

In wave analysis, it is the time it takes the LV to create a tandem wave that would eventually interact with the precursor wave. This time interval may be obtained by detecting the position of the precursor wave just before the onset of the tandem wave. Within LV preload interval, the tandem wave would have been on the verge of interaction with its precursor. This is seen in Graph B. Physiological LVET must be maintained. Shortened ejection duration is a cardiac liability (Reant et al. (2010)). In event of shortened LVET, there is the tendency of early wave reflection to have a dominant effect on flow than on pressure (O'Rourke and Lei (1997), Westerhorf and O'Rourke (1995)). Graph F shows that a physiological tandem wave must displace a precursor wave unscathed before its eventual evanescence at infinity.

Shortened LVET would generate rather more waves with stunted amplitudes in a relatively short time. On account of this condition, the time taken by the tandem wave to approach and interact with the precursor wave will be too short, thus, resulting in profusion of tandem waves. There must be a balance between pre-ejection period and LVET. Shortened LVET, together with prolonged pre-ejection period, amounts to LV dysfunction. In such circumstances a dicrotic pulse wave that marks an incipient pathology may be observed. The implication is that a subject is likely to present with issues related to systolic heart failure (SHF) (Brutsaert and Gilbert (1993), Federman and Hess (1994). On the other hand, the prolonging of LVET, due to slowed calcium re-uptake (O'Rourke and Pauca (2001)) will cause the early reflected waves to be dominant on pressure than on flow. When this happens, the precursor-tandem wave interaction would be such that the precursor wave is enveloped for a relatively long time.

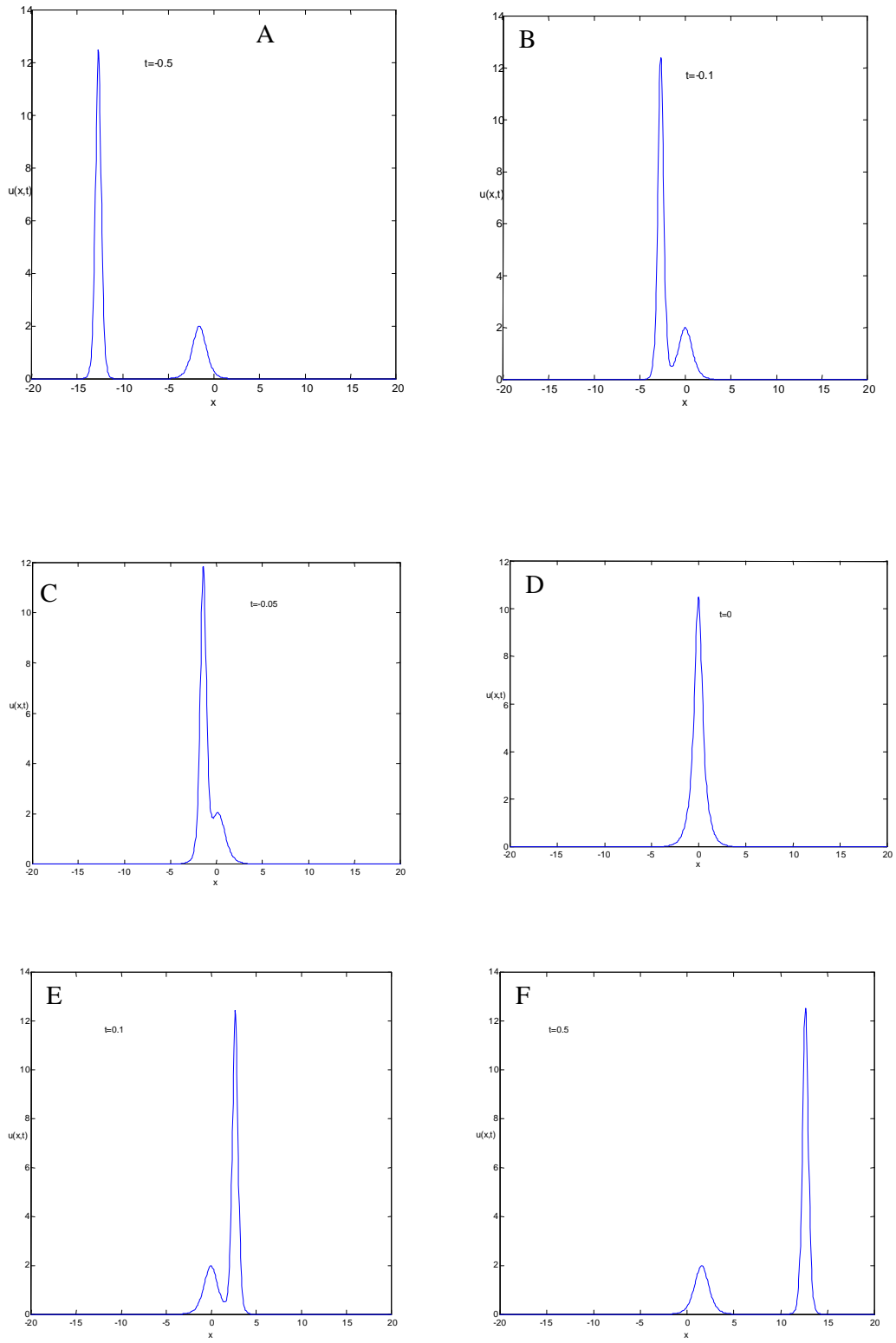


Fig 5.2 2-Soliton Solutions for various time intervals, at different phases of its propagation.

This may account for the perception that there is no second wave in person living with diabetes or atherosclerosis (Keener and Sneyd (1998)). The dominance of early reflected waves on pressure than on flow may predispose a subject to LV hypertrophy (Federman and Hess (1994)).

The following derive from time effects:

(a) Decreased LVET is a risk factor in SHF.

(b) Prolonged LVET predisposes a subject to LV hypertrophy.

5.2.4 Harmonic components of arterial pulse wave

It is possible to decompose arterial pulse waves into many distributed stationary waves associated with harmonic components of the periodic force exerted by the heart (Wang, *et al* (2008)). As depicted by Jan, *et al* (2003) the response of pressure to a harmonic force can be represented by a sum of stationary oscillatory waves, which are eigenmodes of the whole arterial system, characterized by a set of natural frequencies that are related to the eigenvalues and the wave velocity. Pulse wave usually responds to the driving force originating from the heart and the matching condition between the HR and the natural frequencies of the arterial system. The wave amplitude of the corresponding eigenmode is greatly enhanced when the frequency of the input force is close to the one of the natural (fundamental) frequencies. Thus, solitary wave that is in harmony with this condition shows a frequency-matching condition between the heart and the main arterial system. We can decipher, therefore, that any matching with the highest efficiency of power transmission to the arterial tree must reside at the natural frequency, which is the integral multiple of the HR (Wang *et al* (2004)).

5.2.5 Heart-Organ Resonance

Besides the influence of the input pulsatile blood, an organ is influenced by harmonic driving forces. These forces are proportional to the pulse pressure at the connecting site of the local main artery. The relationship between the input force F_i and the peripheral pressure of the organ P_{org} is given by Stacy and Giles (1959) as

$$F_i = \ell_1 \frac{\partial^2 P_{org}}{\partial t^2} + \ell_2 \frac{\partial P_{org}}{\partial t} + \ell_3 P_{org} , \quad (5.2)$$

where ℓ_i ($i=1,2,3$) are constants, and where the first term on the right hand side of equation (5.1) is the inertial force due to the intermediate column of blood: the second term is the frictional effect due to fluid viscosity, and the third term is the elastic coupling due to the distensible property of the vessel. Jan *et al* (2003) suggested that each internal organ can act as a resonator, with its own natural frequency. The main artery provides the needed periodic blood input to the connecting side branches, with its own power needed to transport blood to the organs. It supplies forces at the harmonic frequencies which induces the organ to a forced vibration. The natural frequency of the organ must be near any of the frequencies of the input force in order that a maximum response may be achieved. This is therefore the resonance of the organ with the heart. As we know, the main artery is connected with the organ through a side branch artery. The organ will, therefore, react to the pressure from the main artery as a resonator, which delivers some energy back to the main artery. This is in line with the resonance theory, which stipulates that the heart will resonate with the organs to reduce the resistance of the arterial pulse propagating into the organs (Jan *et al.* (2003), Wang *et al.* (1990)). The pressure force is proportional to the pressure of the organ P_{org} , with the harmonic components attaining a maximum value near the natural frequencies of the particular organ. It was shown (Wang *et a l.* (2004)) that frequency matching of the organ with the harmonic mode of the heart influences pressure content all through to the peripheral arteries. Under a

patho-physiological state, the resonance property of the organ would deviate from its normal value, and thus its natural frequency would be shifted from a particular harmonic component of the force source; moreover, we expect a significant change in the pulse spectrum of the entire artery. This, in effect, reduces the efficiency of blood distribution into a particular organ.

We can decipher some facts from wave amplitude and phase matching about the state of organs. Technically speaking, optimal efficiency is tenable when work is delivered at the fundamental frequency. Each of the organs is assigned a harmonic component of its fundamental frequencies thus: heart (C_0), liver (C_1), kidney (C_2), spleen (C_3), and lung (C_4), (where the $C_i, i=0$ to 4 are the assigned harmonics) (Kuo *et al* (2004), Chin-Ming *et al* (2010), Wang *et al* (2012)). Typically diminishing pulse wave amplitude is in line with increasing frequency. Most arterial pulse energy reside on the frequency range 0-10 Hz. The amplitude of each component may be used to compute the amount of oscillatory power that resides at the frequency.

We may appreciate how solitons can give clues to organ problems! Taking normal organs as a benchmark, measure the amplitudes of the solitons for some n -number (statistically $n \times 30$) of healthy organs. Get a suitable range of amplitudes, and then compare this with the amplitudes of solitary waves to organs in incipient pathological conditions. This method is valid for all the individual organs of the body. It is noteworthy that pulse waves have quite large wavelengths. This property offers the benefit of determining the resonance condition of related organs, and thus reads off the health condition of the organ in question.

5.2.6 Hypertension and vaso-active agents

Besides giving information about the functioning of organs, solitary waves are a good indicator of normotensive or hypertensive states. Atherosclerosis and diabetes are cases in

which there is the absence of the second wave (Keener and Sneyd (1998)). Increasing systolic pressure elevates arterial wall circumferential stress and predisposes to atherosclerotic plaque generation. The atherosclerotic plaque generation can be implicated in the disappearing of the second wave.

One of the risk factors of diastolic heart failure is (untreated) hypertension. It may result in LV *hypertrophy*, and in effect the diastolic left ventricular dysfunction (DLVD). In the radial artery, a decrease in amplitude of the secondary systolic wave, even with maintenance of the initial peak indicates decrease in ascending aortic and LV pressure (O'Rourke and Pauca (2001)). This decrease in pulse wave amplitude in the brachial artery is a marker of abnormality of the LV systolic pressure.

In patients with cardiac failure, diabetes mellitus, nephropathy, in the grey area of systolic 130-140 mmHg, the interpretation of the arterial pulse helps in deciding when and how aggressively to treat. In treatment itself peripheral vasodilatation is to be maintained from fall in mean pressure, wave reflection from fall in augmented pressure (in patients without heart failure), and beneficial effect of a β -adrenoceptor blocking drug from increase in diastolic period as well as decrease in heart rate (O'Rourke *et al* (2001)).

Besides, the work done by Wang *et al* (2010) is of the position that C_4 may be used as a specific index of hypertension as well as for the evaluation of the efficacy of hypertension therapy. In essence, the harmonic frequency and amplitude of solitary waves about the lungs can furnish details about the damaging effects of hypertension, and as well provide us with details about the efficacy or otherwise of vasoactive agents.

The physio-pathology induced by hypertension is palpable in cardiac function. In course of the disease, cardiac output is raised, while total peripheral resistance (TPR) is normal. This trend is reversible over time. The rise in TPR explains the high amplitude of early reflected

waves, which in effect causes the amplitude of the forward waves to plummet, with attendant high harmonic frequency component which is associated with low efficiency (Wu and Kovacs, (2006)). The wave amplitude and the associated harmonic component of the kidney (C_2) will certainly elucidate the state of the kidney in event of the TPR-cardiac output trend stated. Thus, the inability of the kidneys to excrete sodium resulting from natriuretic factors such as arterial natriuretic factors which are secreted to promote salt excretion will have the effect of increasing total peripheral resistance. There is the possibility that resistance vessel structural adaptation in hypertension may be closely related to pulse pressure than to other blood pressure parameters. Studies show that the widening of PP is seen as a consequence of a loss of compliance in the large conduit arteries and increased wave reflections from the periphery and less to increased resistance in peripheral arteries (Safar (1993)). It is most likely to be evident in, and prognostic of, cardio-vascular abnormality. In the course of exercise PP may increase as much as 100mmHg in normal subjects, due to increased stroke volume. The total peripheral resistance drops during exercise. PP is considered abnormally low if it is less than 25% of the systolic value. If left ventricular stroke volume drops, PP value narrows significantly. Traumatic condition may lower PP. This case suggests significant blood loss, as insufficient preload reduces cardiac output. In congestive heart failure (CHF), PP may be 25mmHg or less.

5.2.7 Dying Process

A sure means of drawing conclusion about impending death (arising from a disease) is a detail supplied by the pulse spectrum. Variations in the harmonics of pulse waves must explain the failure of various organs in the process of dying. It is expected that any, or all, of the concerned organ(s) would have the wave's frequency component reside at a harmonic that is higher than the specific harmonic of the organ. In general, specific frequency above

the 0-10Hz range means that the internal organs are damaged or that functional disorder exists. In event of this, the pulse wave amplitude about the concerned organ must decrease considerably. This is supported by the *Radial Coupled Resonance Theory*, alongside several experiments (Wang *et al.*, (1990, 1991)). Monitoring systolic and diastolic blood pressure is good, but it is not sufficient to predict a terminal or end-stage condition. The work carried out by Kuo *et al.* (2004, 2005, 2006) showed that the drop in diastolic blood pressure, even at lower than 40 mmHg did not indicate that death was inevitable, although it is an indicator of pathological state. When arterial pressure falls below about 20mmHg, the flow of blood is blocked, whereas the flow of plasma is blocked in arterioles at pressures between 5 and 10 mm Hg (Keener and Sneyd (1998)). So long as the coefficient variation of C_4 magnitude of the pulse wave did not show a marked increase, such drop in BP may rise again and death can be averted. When there is a clear increase in the coefficient of variation of C_4 of pressure pulse wave, this drop in pressure becomes irreversible and death becomes imminent. In the process of dying, all the harmonic components would lose their stability- from the normal frequency components and slowly shifting to abnormal-frequency components.

5.3.0 Summary and Conclusion

In this work we studied hemodynamic pulse waves in fluid-structure interaction. Fluid was used synonymously with blood whereas structure was used synonymously with the artery.

Contrary to seeing the arterial wall as a physical flow boundary, we have treated it, as should be done, as a companion in sustaining the integrity of flow. As would be expected, both the fluid and the artery are always in relative motion, against the background of which equations of motion were developed for each of them. Since relative motion is enhanced, and some contact force exists, we treat the arterial flow as a coupled system.

The pulse waves created due to heart beat was resolved into nonlinear superposition of forward and backward waves. We saw that the nonlinear model so built generated solitons, which are solitary waves that possess the stated properties (see Definition 4.1). Many of such solitons could be generated through finite superposition of solutions; but we were done with two solitons since they are enough to describe the characteristic peaking and steepening phenomena of the arterial pulse wave. In the main, a nonlinear arterial model consists of superposition of forward solitary waves and a two-element windkessel model. While solitons are a good estimator of the systolic phase, the two-element windkessel model caters for the diastolic phase. Therefore, a complete arterial pulse wave is given as the sum of both the solitons and the windkessel model. We therefore posit that contrary to the earlier propositions of the windkessel model as a sustaining descriptor of the complete arterial pulse wave, it could only furnish substantial clue to waves that are generated in the diastolic phase.

Granted that solitons were generated from our nonlinear model, we ask: Can solitons be employed to analyze the physiological state of animated life, of humans especially? The answer is, to all reasonableness, yes. If they cannot, then our effort would just become a mere beautiful construction which may be niggardly of applications. Arterial pulse and flow are physiological, and thus any mathematical touch on them must meet applicability. Against this background, we considered the physiological relevance of our model. We analyzed the results obtained from the solitary solutions and the harmonic components of the pulse waves so generated. It was seen that the harmonic components of pulse waves can be applied to analyze the patho-physiological state and the resonance condition of the internal organs. Most of all, we saw that *stature* and *LVET* could independently predict cardio-vascular state. Specifically, each of them can be implicated in cardio-vascular events. The result is in line with the cohort study carried out by Smulyan *et al.* (1998). They achieved similar results by means of linear and stepwise multiple regression analysis. In the said study, short stature was

found to be associated faster heart rates, shortened return times for reflected waves and increased augmentation of the primary systolic pulse. These factors each account for increase in the stroke and work time of the left ventricle and reduction of the diastolic time and pressure available for coronary filling. This supports a physiologic explanation for the increased risk of cardiovascular disease in short people.

Assuredly, analysis of pulse waves is substantial in offering details on organ pathogenesis. So long as the harmonic component of any organ is known, any coefficient variation from such component is a marked indication of organ anomaly, and should be treated as such. We therefore desire that pulse waves together with their harmonic components be accorded adequate recognition in medical practice, as it is essential in cardio-vascular physiology and internal medicine.

5.4.0 Recommendation(s) for further studies

The artery is treated here as a membrane, which presupposes the absence of bending stress. Indeed, we are in search of a treatment that caters for bending stress.

References

- [1] Abbaoui K and Cherruault. **New ideas for proving convergence of decomposition methods**. Comput. Maths. Appl., 29(7):103-108,1995
- [2] Almanasreh H. **Blood Flow Modelling in Compliant Arteries; Deriving effective equations using asymptotic analysis methods**. M.Sc Thesis,Chalmers University of Technology (2007).
- [3] Atabek HB, **Wave propagation through a viscous fluid contained in a tethered initially stressed,orthotropic elastic tube**, Biophys.J.8:626-649,1968.
- [4] Avolio A P. ,Van Bortel, L M., Boutouyrie P, Cockcroft J R., McEniery C M., Protogerou A D. Roman M J., Safar ME., Segers P.,SmulyanH, **Role of Pulse Pressure Amplification in Arterial Hypertension: Seventh International Workshop on Structure and Function of the Vascular System, Hypertension**.Vol. 54, doi: 10.1161/ HYPERTENSIONAHA.109.134379 (2009).
- [5] Babin , A. and Figotin A.,**Linear superposition in nonlinear wave dynamics**, Rev. Math. Phys. 18, 971 (2006), DOI: 10.1142/S0129055X06002851
- [6] Barbu V,Grujic Z, Lasiecka N, and Tuffaha A, **Smoothness of weak solutions to a non-linear fluid-structure interaction model**. Indiana Univ.Math.,J. 57:1173-1207 ,2008
- [7] Bakirtas I and Demiray H.**Amplitude modulation of nonlinear waves in a fluid-filled tapered elastic tube**.Appl.Math and Comput.154; 747-767,2004.
- [8] Becker, K.L., ed. (2001). **Growth and Development in the Normal Infant and Child**, Table 7.1. Principles and Practice of Endocrinology and Metabolism (3 ed.). Philadelphia, Pa.: Lippincott, Williams & Wilkins. p. 69.
- [9] Berger DS, Li JKJ., Laskey WK and,Noordergraaf .A, **Repeated reflection of waves in the systemic arterial system**. Am. Physiol.Soc., 269-281,1993.
- [10] Berger DS, Li JK, Noordergraaf A. **Differential effects of wave reflections and peripheral resistance on aortic blood pressure: a model-based study**. Am J Physiol Heart Circ Physiol 266 H16266H1642, (1994).

- [11] Boulakia M., **Existence of weak solutions for the motion of an elastic structure in an incompressible viscous fluid**, CR.Acader,1336, 985-990,2003.
- [12] Boutouyrie P, Dominique P, Tropeanu A-I, Lalour B , Carezzi F, Zidi M Jeunemaitre X Laurent S., **Compressibility of the carotid artery in patients with pseudoaxanthoma elasticum**. Hypertension 38:1181-1184, 2001.
- [13] Brutsaert DL, S.U Gilbert T.H. Systemic and Diastolic Failure: Pathophysiology and therapeutic information. J Am Coll Cardiol,22:318-325,1993.
- [14] Canic S, Kim EH., **Mathematical analysis of the quasi-linear effects in a hyperbolic model of blood flow through compliant axi-symmetric vessels**, Math. Methods, Appl.Sc , 2006
- [15] Canic S.,**Blood flow through compliant vessels after endovascular repair: Wall deformation induced by the discontinuous wall properties**, Comput. Vis
- [16] Canic,S.,Mekelic,A.,Lamponi D and Tambaca J, **Self –consistent Effective Equations Modeling Blood Flow in Medium- to-Large Compliant Arteries**. Multiscale Modeling and Simulation 3(2005), 559-596.
- [17] Carew TE, Ramesh NV, Patel DT, **Compressibility of the arterial wall**, Circ. Res. ,23:61-68, 1968.
- [18] Chin-Ming Huang, Ching-Chuan Wei^{*}, Yin-Tzu Liao, Hsien-Cheh Chang¹, Shung-Te Kao and Tsai-Chung Li, **Developing the Effective Method of Spectral Harmonic Energy Ratio to Analyze the Arterial Pulse Spectrum eCAM**, doi:10.1093/ecam/neq054,2010
- [19] Choung CJ and Fung YC, **Compressibility and constitutive equation of arterial wall in radial compression experiments**, J.Biomech. 17:35-40,1984
- [20] Ciarlet PG, Lods V., **Asymptotic analysis of linearly elastic shells,1.Justification of membrane shell equations**, Arc.Rational Mech. Anal. 136:119-161,1996.
- [21] Crepeau E and Sorine M, **A reduced model of pulsatile flow in an arterial compartment,Chaos ,Solids and Fractiles** (Article in Press),2006.
- [22] Curry JM, **Solitons solution of integrable systems and Hirotha's method**, The Havard college of Mathematics Review 2.1, 2008.

- [23] Darne B, Girerd X, Safar M, Cambien F Guire L. **Pulsatile versus steady component of blood pressure: A cross-sectional analysis and a prospective analysis on cardio-vascular mortality** Hypertension 13: 392-18, 1989.
- [24] Delfour MC, Zolesco J-P, **Differential equations for linear shells: Comparism between intrinsic and classical models**, CRM-2298, 1995.
- [25] Demiray H., **Large deformation analysis of some basic problems in biophysics**, Bull.Math.Biol.38; 701-711, 1976.
- [26] Drazin PG, and Johnson RS (1989), **Solitons: an introduction** Cambridge University Press.
- [27] Dudley R. (1989), **Real Analysis and Probability**. Wadsworth, Brooks and Cole.
- [28] A.D.A.M [In] Dugdale D.C. (2010) MedlinePlus, www.nlm.nih.gov/medlineplus/ency/imagepages/19192.htm
- [29] Fan, YY <http://www.yuanyifan.com/2011/09/18/biorhythm-a-biologically-inspired-audio-visual-installation-2010/>
- [30] Federmann M, and Hess OM. **Differentiation between systolic and diastolic dysfunction**, Eur Heart J.15 (Suppl D);2-6,1994.
- [31] Fu YB, and Ilchev AT, **Solitary waves in fluid-filled elastic tubes: Existence, Persistence and the role of axial displacement**, IMA Journal of Appl. Maths.75:257-268, 2010.
- [32] Fung YC (1996), **Biomechanics (2nd ed)**, Circulat
- [33] Fung YC, **Biomechanics: Mechanical properties of living tissues.**, Springer-Verlag, NY., 1993.
- [34] Fung YC., **Biodynamics: Circuation**, Springer óverlag, NY, 1981
- [35] Griffiths GW and Schiesser WE, **Linear and non-linear waves**, Scholarpdia,4(7): 4308,2009.
- [36] Hai-Chao H , David NKU and Raymond PV, **Arterial wall adaptation under elongated longitudinal stretch in organ culture**, Ann. Biomed Eng. Vol.31:403-411,2003. Becker R. C. Acad Sc.Paris 258:5144-5147,1994.
- [37] Henry Theil <http://schipul.com/quotes/1034/>, (12/6/2012)
- [38] Hirotha R., **Solitons**. In Topics in Physics 17 (Bullough RK, Caudery PI, eds). Springer-Verlag Berlin, 157-176, 1980.

- [39] Hoyme H.E., **Too Short or Too Tall: When to Expect a Genetic Syndrome**
http://www.sanfordhealth.org/files/0a2b44cd-bd4a-47bd-91fb-842ec062ac0a/Too_Short_or_Too_Tall_Hoyme.pdf [online], Retrieved, 10-03-2014
- [40] Jan,MY,Hsin H,Hsu TL,Wang Wk,and Wang YYL. **The physical conditions of different organs are reflected in the pressure pulse spectrum of the peripheral artery specifically.** J. Cardiovasc Eng., 3:21-29, 2003
- [41] Jeffrey A and Kawahara T (1981), **Asymptotic Methods in Nonlinear wave theory**, Pitman, Boston
- [42] John R.J, (1975) **Introduction to tensor analysis**, Longman Group Ltd,London
- [43] Kang,IS. **A Microscopic Study on the Rheological Properties of Human Blood in Low Concentration Limit.**Korea-Australia Rheology Journal.2002; 14:77-86.
- [44] Kavouklis CN, Hyung TA, Shashkov M., **Level Set method for incompressible two-phase flow, in modeling and analysis**, Los Alamso Nat. Library (<http://math.lan.gov/>),26 july,2011.
- [45] Kechris AS, (1995) **Classical descriptive set theory**, Vol.156, Springer-Verlag.
- [46] Keener J and Sneyd J.(1998), **Mathematical Physiology**, Springer-Verlag,NY
- [47] Ku, DN. **Blood Flow in Arteries.**Annual Review of Fluid mech.2000; 32:347-382
- [48] Kukavia I., Tuffaha A, Ziane M., **Strong solutions to a non-linear fluid-structure interaction system**, J. Diff.Eqns., 247:1452-1478, 2009
- [49] Kukavica I,Tuffaha A ,Ziane M., **Strong solutions for fluid- structure interaction system: Advances in differential equations**, Vol:15(3-4),231-254,2010.
- [50] Kuo YC, Chui TY,Jan MY, Bau JG,Li SP, Wang WK and Wang YYL. **Losing harmonic stability of arterial pulse in terminally ill patients.**Blood Press Monit.2004 Oct;9(5):255-8.
- [51] Kuo YC, Lo SH, andWang WK. **Harmonic variations of arterial pulse during dying process in rats.** <http://www.dtic.mil/cgi-bin> ,Retrieved 6July,2012.
- [52] Kuo YC, Lo SH,Chaso PT Hsiu H, Wang WK and WangYYL.**Raising harmonic variation of arterial pulse in dying rats.** Am.J Chin. Med.,33:73-85,2005 22.

- [53] Laleg M, Crispeau E and Sorine M, **Arterial pressure modeling by an integrable approximation of Navier-Stokes equation** IN 5th Mathmod Vienna Proceedings, Vol.1, page 337, ARGESIM Report, 2006.
- [54] Laleg T, Crispeau E, Sorine M., **Separation of arterial pressure into solitary waves and windkessel flow**, MCBMS06, IFAC Reims, 2006.
- [55] Lamb (Jr) GL, **Elements of solution theory**, NY, John Wiley and sons, 1980.
- [56] Lawton RW, Greene LC., **A method for in-situ study of aortic elasticity in dog, USA: AMALUS Navy and Air Devt. Center NADC MA-5603**, 1956.
- [57] Lious P-L., **Mathematical topics in fluid mechanics**, Oxford Sc. Pub., 1996.
- [58] Lomdahl PS, **What is a soliton?** [in] **Solitons in Biology**, Los Alamos
- [59] Luchini P, Lupo M, Pozzi A. **Unsteady Stokes flow in a distensible pipe**, Z Angew. Math. Mech. 71:367-378, 1991.
- [60] Ma X, Lee GC, Wu SG, **Numerical simulation for the propagation of nonlinear waves in arteries**, Trans. ASME 114:490-496, 1992.
- [61] Malfliet W., **The tanh method: a tool for solving certain class of nonlinear evolution and wave equations**, J. Comp. Appl. Math 164-165, 529-541, 2004
- [62] Malfliet W. **Solitary wave solutions of nonlinear wave equations**, Am. J. Phys. Vol 60(7), 650-654, 1992.
- [63] Maoyeri M, Zendchbudi G. **Effects of elastic property of the wall on flow characteristics through arterial stenosis**, J. Biomech., 36:525-555, 2003.
- [64] Martin A.J, Pamela ACW, John F.P., Herbert T., John D.S. **Pulse Pressure and Resistance Artery Structure in the Elderly**, Hypertens., 26:301-306, 1995.
- [65] Mbah, GCE and Adagba OH.(a) **Deformation of the wall of an artery with stenosis due to pulsatile flow of blood**. J. Math Sc. Vol. 21, No. 2, 99-109, 2010.
- [66] Mbah, GCE and Adagba OH.(b) **Flow of blood through a constricted capillary**. J. Math Sc. Vol. 21, No. 2, 115-126, 2010.
- [67] McDonald DA, **Blood flow in arteries** (2nd ed.), London, UK: Arnold, 1974.
- [68] Milne-Thomson L.M. (1974), **Theoretical hydrodynamics** (5th ed.), McMillian Press Ltd. Monit., 9:255-258, 2004.

- [70] Mohammad W M, Glen AL, Christopher MQ, **Increase in pulse wavelength causes the systemic arterial tree to degenerate into a classical windkessel**, AJP - Heart August vol. 293(2) H1164-H1171, 2007.
- [71] Monteanu L and Donescu S. (2004), **Introduction to solution theory: Application to Mechanics**. Kluwer Acad. Publishers, Dordrecht. Wang JJ, O'Brien AB, Shrive NG,
- [72] Moshe I. and Marius U., **Improvement of Numerical Solution of Boundary Layer Problem by incorporation of Asymptotic approximation**, Numer. Math. 39, 309-324, 1982.
- [73] Nobile F., **Numerical approximation of fluid-structure interaction problems with application to hemodynamics**, Ph.D Thesis, EPFL, Lausanne, 2001.
- [74] Nwachukwu C.O., Ifidon E.o., **Prolongations and Symmetric Groups of Partial differential equations: The Case of the Generalized K-dV Equations**, Journal of the Nigerian Math Soc., Vol 10, 1991.
- [75] Nzerem, F.E., Alozie, H.N., **The Underlying Physiology of Arterial Pulse Wave Morphology in Spatial Domain**, Applications and Applied Mathematics, Vol. 8, Issue 2, 2013.
- [76] Nzerem F.E., Ugorji H.C., **Arterial Pulse Waveform under the watch of Left Ventricular Ejection time: A physiological outlook**, Mathematical Theory and Modeling, Vol. 4, No. 4, 2014
- [77] Oates C. (2001), **Cardiovascular Haemodynamics and Doppler Waveforms Explained**. Cambridge University Press.
- [78] O'Rourke MF and Lei J. **Separation of systolic from diastolic dysfunction as a cause of cardiac failure by analysis of the arterial pulse wave**. Aust. NZ J. Med. 28:114, 1997.
- [79] O'Rourke MF, Pauca A, Jiang X-J, **Pulse Wave Analysis**. Br J Clin Pharmacol. 2001 June; 51(6): 507-522. doi: 10.1046/j.0306-5251.2001.01400.x
- [80] Olufsen M, Nadim A. **On deriving lumped models for blood flow and pressure in the systemic arteries**. Math. BioSc. Eng.(1):61-80, 2004.
- [81] Olufsen MS, **Modeling the arterial system with reference to an anesthesia simulator**: Tech. report IMFUFA Text 345 Denmark, PhD Thesis, 1998.
- [82] Olufsen MS. **Structured tree outflow condition for blood flow in large systemic arteries**, Am. J. Physiol Heart Circ. Physiol 276:H257-H268, 1999.
- [83] Oscuii HN, Shadpour MT and Ghlich F. **Flow characteristic in elastic arteries using fluid-structure interaction model**, Am. J Appl. Sc. 4(8), 515-524, 2007.

- [84] Panton R.(1996), **Incompressible flow**, NY,John Wiley and Sons.
- [85] Parker KH, and Tyberg JV, **Time domain representation of ventricular arterial coupling as a windkessel and wave system**,Am. J. Physiol Heart Circ Physiol,2002.
- [86] Pedley TJ (.1980), **The fluid mechanics of large Blood vessels**, Cambridge University Press,
- [87] Pedrizzetti G.,Dominichini F,**Fluid flow inside deformable vessels and in the left ventricle [In]** Pedrizzetti G. and Perktold K(2003) **Cardiovascular fluid mechanics**(CISM courses and lectures), Springer Verlag
- [88] Pedrizzetti,G ,Perktold K.(2003),**Cardiovascular fluid mechanics**,(CISM courses and lectures),Springer Verlag NY
- [89] Pedicelli S, Peschiaroli E, Violi E, Cianfarani S (2009). **Controversies in the definition and treatment of idiopathic short stature (ISS)** . J Clin Res Pediatr Endocrinol **1** (3): 105ó15. doi:10.4008/jcrpe.v1i3.53
- [90] Quarteroni A, Tuveri M, Veneziani A.,**Computational vascular fluid dynamics:Problems , models and methods**. Comput.Vis.Sci.,2:163-197,2000.
- [91] Quick CM, Berger DS, Noordergraaf A., **Apparent arterial compliance**. Am J Physiol Heart Circ Physiol 274 H1393óH1403, 1998.
- [92] Rachev A. **A model of arterial adaptations in blood flow**, J. Elast. 61:83-111, 2000
- [93] Rappich G and Perktold K. **Computer Simulation of Convective diffusion process in large arteries**.J.Biomech.,29:207-215,1996.
- [94] Reant, P., Marina, D., Erwan, D., Aude M., Philippe R.,Pierre B., Pierre D.S.,Christophe L., Raymond R., Gilbert H., and Stephane L.(2010). **Systolic time intervals as simple echocardiographic parameters of left ventricular systolic performance: correlation with ejection fraction and longitudinal two-dimensional strain**. European Journal of Echocardiography 11,834ó84doi:10.1093/ejechocard/jeq084
- [95] Reismann H., **Elastic Plates: Theory and Applications**, Wiley,NY.,1988.
- [96] Safar M.E, Levy B.I, Harry SB. **Current perspectives on arterial stiffness and pulse pressure in hypertension and cardio-vascular diseases**. Circulation,107:2863,2003.
- [97] Safar M E, **Hemodynamic Changes in elderly hypertensive patients.**, Am J Hypertens.,1993;20S-23S

- [98] Saloua MA, **Approximation techniques for an unsteady dynamic koiter shell.** J.Appl.Math., Article 1D:24238,2007
- [99] Shibeshi S, Collins W. **The rheology of blood flow in a branched arterial system.** Apl. Rheol.15 (6):398-405, 2005
- [100] Shrier.I, Hussian SMA, Magder S, **Effects of carotid sinus stimulation on resistance and critical closing pressure of the canine hind-limb,** Am Physiol. Heart Circ Physiol., 264:H1560-H1566,1993
- [101] Smulyan H., Asmar R.G, Rudnicki A., London G.M, Safar M.E, **Comparative effects of aging in men and women on the properties of the arterial tree** J. Am Coll. Cardiol. 37(5):1374-1380, 2001. doi:10.1016/S0735-1097(01)01166-4
- [102] Smulyan H., Sylvain J. M., Bruno P.,Guerin A. P., Safar M. E., London G.M., **Influence of Body Height on Pulsatile Arterial Hemodynamic Data** JACC Vol. 31, No. 5,1998:110369,
- [103] Stacy RW and Giles FM. **Computer analysis of arterial properties,** Circ.Res.7:1031-1038, 1959.
- [104] Subramanian R. S., **An Introduction to Asymptotic Expansions**
<http://web2.clarkson.edu/projects/subramanian/ch527/supplem/asympt.pdf> Retrieved [online], 2014-04-02
- [105] Suncica C and Andro M., **Effective equations modeling the flow of a viscous incompressible fluid through a long elastic tube,** C.R. Mecanique, Vol. 330, pp. 661-666, 2002.
- [106] Suncica C, Daniel L, Andro M, and Josip T.,**Self-Consistent Effective Equations Modeling Blood Flow in Medium-to Large Compliant Arteries.** Multiscale modeling and Simulation 3:559-596, 2005
- [107] Surulescu C, **On the time-dependent motion of a viscous incompressible fluid through a tube with compliant walls,** Studia Univ.øBabes-Bolyaiø Mathematic, Vol.L111(4),2008.
- [108] Thiriet M., **Anatomy and Physiology of the Circulatory and Ventilatory Systems,** Springer, 2013.
- [109] U.S. Department of Health and Human Services - National Institutes of Health
en.wikipedia.org/wiki/pulse (5/25/2012)
- [110] Vaughn A (2011) **Blood pressure chart,Normal pressure range** www.vaughns-1-pagers.com

- [111] Wada S and Karino T. **Theoretical Study on Flow-Dependent Contraction Polarization of low density lipoproteins at the luminal surface of a straight artery.** *Biorheol*,36:207-223,1999
- [112] Wang JJ, O'Brien A.B, Shrive N.G, Parker KH and Tyberg JV. **Time-domain representation of ventricular-arterial coupling as a windkessel and wave system.** *Am.J Physiol Heart Circ Physiol*,2002.
- [113] Wang LYY, Chang SL, Wn YE, Hsu TL, Wang WK: **Resonance-The missing phenomenon in hemodynamics.** *Circ Res*.69:246-249,1991.
- [114] Wang SH, Hsu TL and Jan MY **Effects of captopril on specific harmonic indexes of the peripheral pressure pulse waveform,** *Proc.The 4th Int. Conference of Bioinform. And Biomed Eng.*,2010
- [115] Wang WK, Lo YY, Chieng Y, Wang LYY, Hsu TL: **Resonance of organs with the heart,** in Young WJ(ed):*Biomed Eng., an International Symposium.* New York, Hemisphere Publishing Corp.259-297,1990.
- [116] Wang YYL, Sze WK, Bau JG, Wang SH, Jan MY, Hsu TL and Wang WK. **The ventricular –arterial coupling system can be analyzed by the eigenvalue modes of the whole arterial system,** *Appl.Phys. Lett.*92, 153901, 2008.
- [117] Wang YYL, Jan MY, Shyu CS, Chiang CA and Wang WK. **The natural frequencies of the arterial system and their relation to the heart rate,** *IEEE Trans.Biomed. Eng.*,51:193-195,2004.
- [118] Wang WK, Bau JG, Hsu TL, Wang YL **Influence of Spleen Meridian Herbs on the Harmonic Spectrum of the Arterial Pulse**
http://findarticles.com/p/articles/mi_m0HKP/is_2_28/ai_65774107/?tag=content(5June,201)
- [119] Warriner RK, Johnston KW and Cobbold RS., **A visco-elastic model of arterial wall motion in pulsatile flow: Implications of Doppler ultrasound clutter assessment,** *Physiol., Meas.*, 29:157-179, 2008.
- [120] Wazwaz AM, **Tanh-Coth method combined with the Riccati equations for solving the KDV equation,** *Arab J. of Math. And math.Sc.* Vol.1(1),27-34,2007.
- [121] Wazwaz AM(2002), **Partial differential equations: Method and applications,** Balkema Publishers, The Netherlands.
- Wen-Shan D, Wang B-R and Wei RJ, **Reflection and transmission of nonlinear blood waves due to arterial branching,** *Physical Review E,* Vol.55(2), 1997.
- [122] Westerhorff N., Sipkema P, Van denBos GC and Elzinga G., **Forward and backward waves in the arterial system,** *Cardiovascular.Res.*6, 648-656,1972.
- [123] Westerhorff N, O'Rourke MF. **The hemodynamic basis for the development of left ventricular failure in systolic hypertension.** *J.Hypertens,* 13:943-952, 1995

[124] Wu Y, and Kovacs SJ, **Frequency-based analysis of the early rapid filling pressure-flow relation elucidates diastolic efficiency mechanisms**, Am.J.PhysiolHeart Circ. Physiol, 291:H2949,2006.

[125] Yomosa S. **Solitary waves in large blood vessels**. J Phys Soc Jpn,56:506-520,1987

[126] Zabusky NJ, Porter MA, **Soliton**, Scholarpedia, 5(8):2086, 2010.

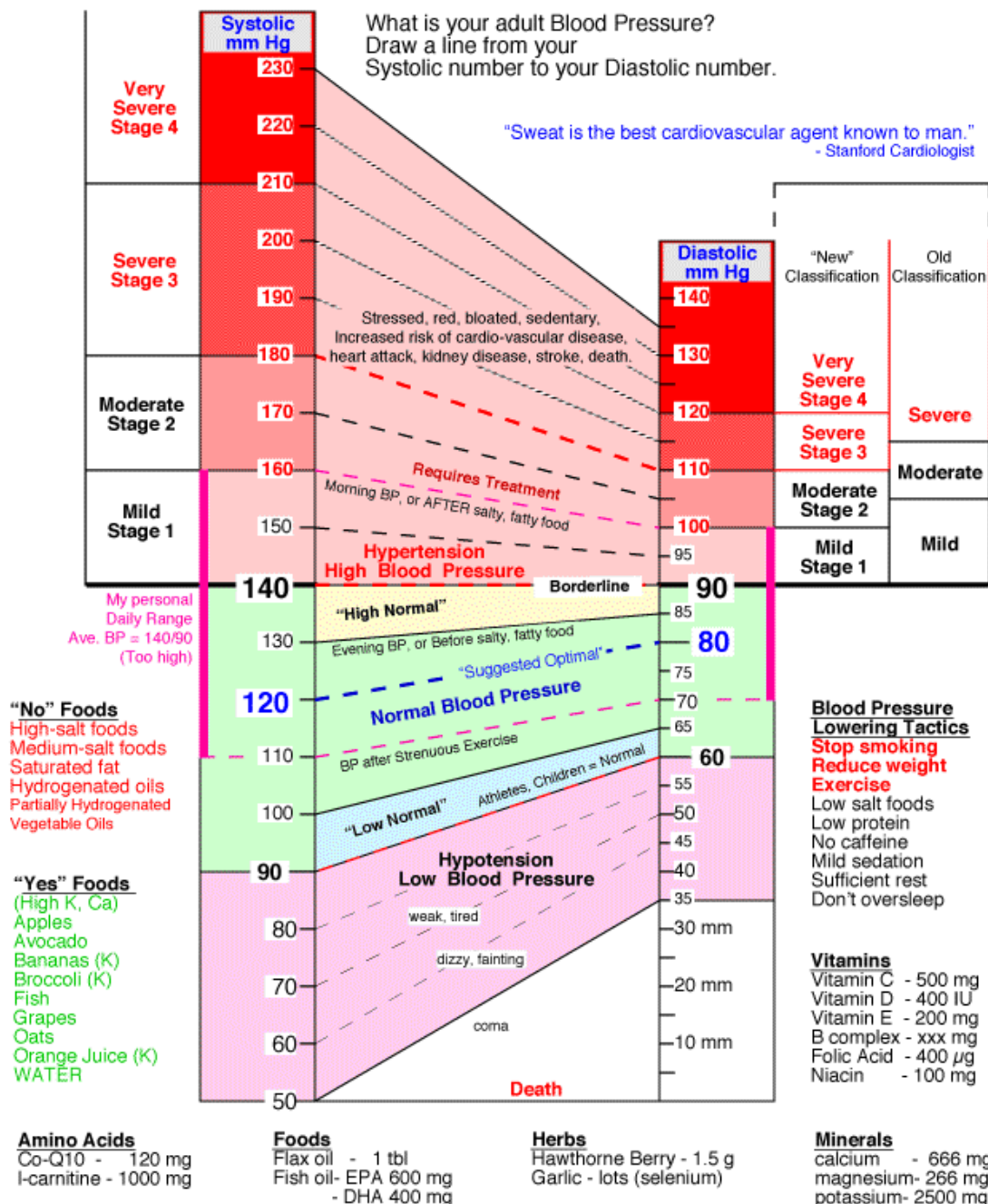
[127] ZangX, Zuazua E.,**Asymptotic behavior of hyperbolic-parabolic coupled system arising in fluid-structure interaction**, Int, Series of Num. Math., Vol.154:445-45

Appendix A: *Blood pressure chart:Vaughn (2011)*

Vaughn-1-Page68.com

MedicalSummaries

Blood Pressure Chart



These are the personal thoughts of the author - nothing is implied, promised or guaranteed - no advice is intended.

Fname: md-11.blood-pressure.18

Appendix B: List of figures and tables

<i>Figure</i>	<i>Page</i>
<i>Fig.1.1</i> Human arterial system.	3
<i>Fig 1.2</i> Photomicrograph of the cross section of an artery showing the tunica intima,tunica media, and tunica externa.	5
<i>Fig1.3</i> Formed elements of blood	6
<i>Fig1.4</i> Arterial pulse points	9
<i>Fig 3.1</i> Idealized cubical fluid region	22
<i>Fig 3.2</i> Unit normal to the vessel wall	26
<i>Fig 3.3</i> Idealized spherical particle	28
<i>Fig 3.4</i> Action of fluid on the wall	29
<i>Fig 3.5</i> Reference domain diagram	30
<i>Fig 3.6</i> Wall displacement	35
<i>Fig 4.2</i> Solitary wave	72
<i>Fig 4.3.</i> 2-element windkessel model of flow phenomena	81
<i>Figure 5.0.</i> Arm-span measurement for growth assessment	87
<i>Fig 5.1</i> 2-Soliton Solutions at various distances	90
<i>Fig.5.2</i> 2-Soliton Solutions for various time intervals, at different phases of its propagation.	93
Tables	
<i>Table 1.1</i> The 43 human main arteries and related function	4
<i>Table 1.2</i> Normal pulse rates at rest, in beats per minute	8

Appendix C: **Publications**

Nzerem, F.E and Alozie H N, The underlying physiology of arterial pulse wave morphology in spatial domain, Appl. Appl.Math . Vol. 8, issue 2, 2013, pp. 495 ó 505

Nzerem F. E. and Ugorji H C, Arterial pulse waveform under the watch of left ventricular ejection time: a physiological outlook, Mathematical Theory and Modeling, vol.4, no.4, 2014 pp 119-128.

Nzerem F. E., On expressive construction of solitons from physiological wave phenomena Pure and Applied Mathematics Journal 2014; 3(3): 70-77 doi: 10.11648/j.pamj.20140303.13